

# Tectonic and magmatic processes along the transform margin of southern Africa

## Dissertation

zur Erlangung des Doktorgrades der Naturwissenschaften im Fachbereich  
Geowissenschaften (FB 5) der Universität Bremen

von

Nicole Parsiegla

Bremerhaven, 2008



# Table of contents

<b><u>Zusammenfassung.....</u></b>	<b><u>1</u></b>
<b><u>Abstract.....</u></b>	<b><u>5</u></b>
<b><u>1 Introduction.....</u></b>	<b><u>7</u></b>
1.1 Motivation and aims of this thesis .....	7
1.2 Structure of the thesis .....	9
<b><u>2 Large Igneous Provinces .....</u></b>	<b><u>13</u></b>
2.1 The formation of Large Igneous Provinces.....	13
2.2 Large Igneous Provinces and climate.....	15
<b><u>3 Geology and tectonic background.....</u></b>	<b><u>17</u></b>
3.1 Geological overview of southern Africa and its offshore basins .....	17
3.2 Continental margins of southern Africa.....	22
<b><u>4 Geoscientific concepts.....</u></b>	<b><u>25</u></b>
4.1 Crustal stretching .....	25
4.2 Processes at transform faults .....	26
<b><u>5 The Agulhas Plateau: Structure and evolution of a Large Igneous Province .....</u></b>	<b><u>29</u></b>
Abstract .....	29
Keywords.....	29
5.1 Introduction .....	30
5.2 Geological and tectonic background.....	32
5.3 Data acquisition and processing.....	33
5.4 Modelling.....	37
5.5 Crustal type and structure.....	44
5.6 The Agulhas Plateau LIP in a plate-tectonic context .....	48
5.7 Consequences of crustal generation .....	50
5.8 Conclusions.....	55
Acknowledgements .....	56
<b><u>6 Deep crustal structure of the sheared South African continental margin: first results of the Agulhas-Karoo Geoscience Transect .....</u></b>	<b><u>57</u></b>
Abstract .....	57
Keywords.....	58
6.1 Introduction .....	58

6.2	Tectonic framework.....	59
6.3	Seismic data acquisition .....	62
6.4	Data processing .....	62
6.5	Data and modelling .....	63
6.6	Velocity-depth structure from the Agulhas Bank to the Agulhas Passage .....	67
6.7	Model quality .....	70
6.8	Discussion .....	72
6.9	Conclusion .....	77
	Acknowledgements .....	78

**7 Crustal structure of the southern margin of the African continent:  
Results from geophysical experiments..... 79**

	Abstract .....	79
7.1	Introduction .....	79
7.2	Profile setting .....	81
7.3	Seismic data acquisition .....	84
7.4	Wide-angle seismic data processing .....	85
7.5	Results .....	89
7.6	Discussion.....	94
7.7	Summary.....	101
	Acknowledgements .....	102

**8 The southern African continental margin – dynamic processes of a  
transform margin..... 103**

	Abstract .....	103
	Keywords.....	104
8.1	Introduction .....	104
8.2	Geological and tectonic background.....	106
8.3	Seismic data acquisition, processing, and modelling .....	109
8.4	Seismic refraction and wide-angle reflection results and implications.....	113
8.5	Crustal stretching and tectonic processes along/across the southern African margin ....	116
8.6	Geodynamic evolution of the margin .....	123
8.7	Conclusions.....	125
	Acknowledgements: .....	126

**9 Conclusions and Outlook ..... 127**

9.1	Conclusions.....	127
9.2	Outlook.....	129

**10 References ..... 131**

**11 Acknowledgements ..... 151**

**12 Erklärung..... 153**

### Zusammenfassung

Als der Superkontinent Gondwana zerbrach, formten gigantische Scherprozesse Afrikas südlichen Kontinentalrand. Sie wirkten entlang einer mehr als 1000 km langen Transformstörung. Ihre Spur – die Agulhas-Falkland-Bruchzone – erstreckt sich heutzutage vom Falklandplateau bis zum südöstlichen Kontinentalrand Afrikas. Die Erforschung der Prozesse, welche die Entstehung einer derart langen Transformstörung auslösten und während ihrer aktiven Phase wirksam waren, ist notwendig, um zu verstehen, wie sich dieser gescherte Kontinentalrand entwickelte. Afrikas südlicher Kontinentalrand ist nicht nur eines der besten Beispiele, um die schmalen Kontinentoceanübergangszonen, die Marginalrücken-, Bruchzonen- und Beckenstrukturen, die mit Transformrändern in Verbindung gebracht werden, zu untersuchen. Er bietet auch die einmalige Möglichkeit zu beleuchten, wie die magmatischen Prozesse abliefen, die zur Bildung einer großen Eruptivprovinz an einem gescherten Kontinentalrand führten. In dieser Doktorarbeit verwende ich refraktionsseismische, reflexionsseismische Daten und plattentektonische Rekonstruktionen, um den Aufbau und die Dynamik dieses Kontinentalrandes zu untersuchen. Diese Methoden sind hierfür hervorragend geeignet, weil sie Geschwindigkeitstiefenmodelle und somit Aussagen über die gegenwärtige Struktur des Kontinentalrandes liefern. Eine zeitliche Einordnung und Plattengeometrien werden mithilfe der plattenkinematischen Rekonstruktion erreicht.

Die Agulhas-Falkland-Bruchzone stellt die südliche Begrenzung des Outeniquabeckens und Diazrückens dar. Durch Analyse der Dehnungsfaktoren im Outeniquabecken konnte gezeigt werden, dass dessen Entstehung in zwei Phasen stattfand. Im frühen Jura dominierten intrakontinentale Dehnungsprozesse die beginnende Entstehung dieses Beckens und fanden viel eher statt als die ersten frühkretazische Blattverschiebungen entlang der Agulhas-Falkland-Transformstörung. Durch Bewegungen entlang der Transformstörung wurde die Kruste in den südlichen Teilen des Beckens während einer zweiten Phase weiter gedehnt.

Eine bisher unbekannte Niedergeschwindigkeitszone im Geschwindigkeitstiefenmodell unter dem Outeniquabecken wurde als metasedimentäres Becken interpretiert. Es ist möglich, dass der Diazrücken während einer Transpressionsphase oder durch thermische Prozesse verursacht durch einen vorbeiziehenden Spreizungsrücken aus diesem

## Zusammenfassung

metasedimentären Becken herausgehoben wurde. In beiden Fällen kann die Entstehung des Diazrückens mit dem Scherprozess in Verbindung gebracht werden. Die Phasen der aktiven Blattverschiebungen entlang des südafrikanischen Kontinentalrandes klangen in der späten Kreide ab, als der Spreizungsrücken weiter westlich lag. Diese Arbeit jedoch liefert Hinweise darauf, dass der Kontinentalrand in der Episode nach der Scherung nicht wie bisher gedacht, völlig inaktiv war. Anhand tieferreichender Störungen in den Sedimenten konnte gezeigt werden, dass die Agulhas-Falkland-Bruchzone immer noch eine krustale oder sogar lithospärische Schwächezone sein könnte. Das bedeutet für das von Plumeaktivität gepägte südliche Afrika, dass die Hebung wahrscheinlich durch subvertikale Bewegungen entlang der Bruchzone begünstigt wurde. Die sich daraus ergebende anomale Erhöhung der Topographie wird häufig dem afrikanischen Superplume zugeschrieben.

Die seismischen und plattentektonischen Untersuchungen dieser Arbeit liefern wichtige Hinweise, dass Plumeaktivität und das Wechselspiel zwischen dem Bouvetplume und dem Bouvettripelpunkt zur Entstehung des Agulhasplateaus führten. Sie zeigen, dass das Agulhasplateau aus verdickter ozeanischer Kruste besteht und als große Eruptivprovinz entstand. Durch die Modellierung und Inversion der refraktionsseismischen Daten konnte ein mächtiger Hochgeschwindigkeitskörper im unteren Bereich des Plateaus in der Unterkruste aufgelöst werden. Zusammen mit den reflexionsseismischen Daten konnten auch Hinweise darauf gefunden werden, dass Lavaströme den oberen Teil des Plateaus bilden. Beide Beobachtungen stimmen mit dem typischen Aufbau von großen Eruptivprovinzen überein. Aus plattentektonischen Rekonstruktionen dieser Arbeit zeigte sich, dass das Agulhasplateau zusammen mit der Nordost-Georgia-Schwelle und der Maudschwelle als ein Teil einer riesigen Eruptivprovinz entstand, die zwischen 100 und 94 Ma ausbrach. Bereits in der Endphase der Entstehung begann die Eruptivprovinz entlang der Rücken des Bouvettripelpunktes zu zerbrechen. Während der Eruption wurden große Mengen Kohlenstoffdioxid freigesetzt, von denen bisher ein möglicher Einfluss auf das Klima angenommen wurde. Allerdings konnte hier gezeigt werden, dass der Kohlenstoffdioxidausstoß zu gering war, um einen signifikanten Einfluss auf das Klima zu haben.

Die hier präsentierten Ergebnisse liefern mit der Untersuchung der Krustenstruktur in der Agulhasregion wichtige Erkenntnisse über das komplexe Zusammenspiel zwischen der Hebung des südlichen Afrikas, der Plumeaktivität und Plattenbewegung, sowie erste quantitative Aussagen über die

## Zusammenfassung

Klimarelevanz großer Eruptivprovinzen in Bezug auf ihren Kohlenstoffdioxid-eintrag in die Atmosphäre.



## Abstract

Giant shear processes shaped Africa's southern margin during the break-up of the supercontinent Gondwana. They acted along a more than 1000 km long transform fault, whose remnant structure – the Agulhas-Falkland Fracture Zone – stretches today from the Falkland Plateau to the southeastern margin of Africa. A study of the processes which initiated such a long-offset transform fault and acted during their active phase is essential to understand how this sheared margin developed. Africa's southern margin is not only one of the best examples to study the sharp continent-ocean-transition zones, the marginal ridge, fracture zone, and basin structures usually associated with transform margins, but it provides the unique opportunity to study how excessive magmatic processes acted which formed a Large Igneous Province at a sheared margin. In this thesis, I use seismic refraction, seismic reflection data and plate-tectonic reconstructions to investigate the structure and dynamics of this margin. These are ideal methods as they lead to high-quality velocity-depth models showing the present-day structure across the margin and provide timing and geometries by means of plate kinematics.

The Agulhas-Falkland Fracture Zone bounds the Outeniqua Basin and the Diaz Marginal Ridge to the south. The early formation of Outeniqua Basin is a result of an intra-continental stretching episode in Jurassic times which acted well before the strike-slip motions along the Agulhas-Falkland Transform occurred in the Early Cretaceous. The transform itself has caused crustal thinning in the southern parts of this basin in a second stretching episode.

Beneath this sedimentary basin, an as-yet unknown region with relatively low velocities was discovered and interpreted as a pre-break-up metasedimentary basin. It is possible that the Diaz Marginal Ridge was uplifted from this basin in a transpressional episode or is a result of thermal uplift due to a passing spreading ridge. In either case the formation of the Diaz Marginal Ridge is linked with the shear process itself. The active shear episode of the southern African margin ceased in late Cretaceous times when the spreading ridge passed to the west. In this thesis evidence was provided that the margin was not inactive in this post-shear phase as previously thought. Deep faults in the sediments show that the Agulhas-Falkland Fracture Zone may still be a zone of crustal or even lithospheric weakness. This means for southern Africa – a region, which was and still is affected by plume activity – that uplift is possibly

## Abstract

accommodated by sub-vertical motion at the fracture zone. The resultant anomalously high topography is often attributed to the African superplume.

The seismic and plate-tectonic investigations of this thesis showed that plume activity and interactions between the Bouvet plume and Bouvet triple junction were responsible for the evolution of the Agulhas Plateau. They indicate that the Agulhas Plateau consists of overthickened oceanic crust and formed as a Large Igneous Province (LIP). Seismic refraction modelling revealed a thick high-velocity lower crustal body at the base of the plateau and evidenced together with seismic reflection records that extensive volcanic flows build the cover of the plateau. Both of these observations are consistent with the typical structure of oceanic LIPs. Plate-tectonic reconstructions of this thesis showed that the Agulhas Plateau developed together with Northeast Georgia Rise and Maud Rise as part of a huge LIP which erupted between 100 and 94 Ma. It broke apart along the ridges of the Bouvet triple junction already in the final stages of its emplacement. The large amount of carbon dioxide released during its eruption was suspected to have had an impact on the climate. However, it is shown here that the carbon dioxide emission was not enough to have a significant impact on the climate.

The presented results of the crustal structure of the Agulhas region shed more light on the complex interactions between the uplift of southern Africa, plume activity and plate motion as well as provide first quantitative estimates of the climate impact of LIPs with regard to carbon dioxide emission into the atmosphere.

# 1 Introduction

## 1.1 Motivation and aims of this thesis

Southern Africa and its surroundings represent a rich and distinctive laboratory where earth scientists encounter a great variety of geological settings (Figure 1-1). Billions of years old cratons and mobile belts, remnants of global-scale fold belts, large fracture zones, and different types of Large Igneous Provinces (LIP) constitute the tectonic and magmatic provinces. This unique assemblage of various geological sites provides the opportunity to detail study processes of supercontinental amalgamation, continental break-up and post-break-up development in a single region during the 3.8 billion year geological history of southern Africa.

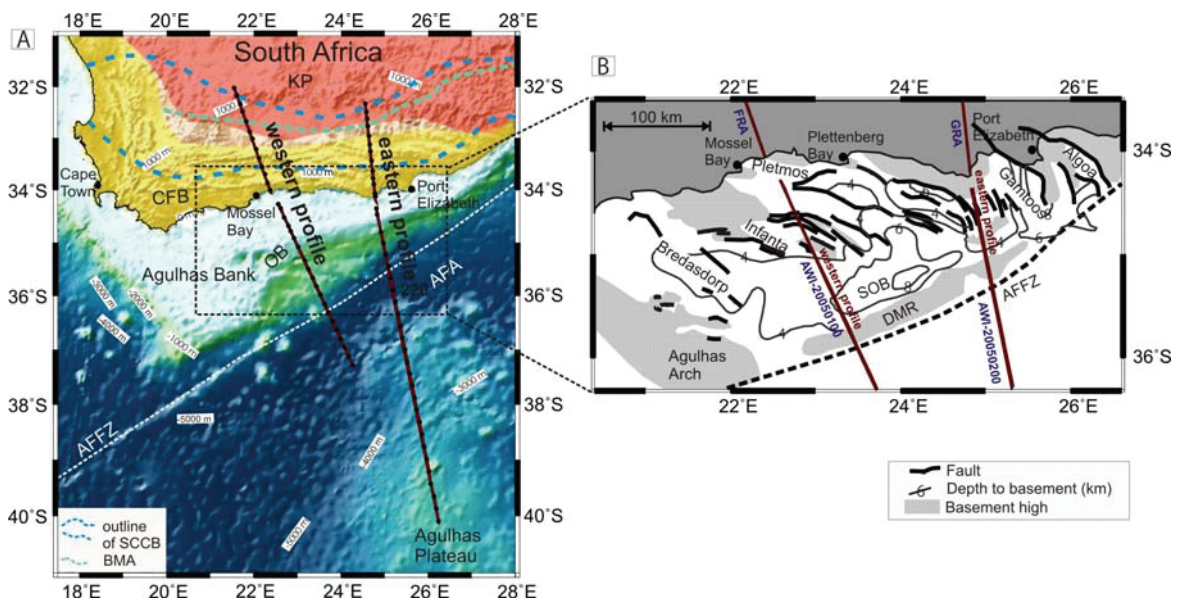


Figure 1-1: A) Overview map showing the position of the two onshore-offshore seismic refraction/reflection profiles of the Agulhas-Karoo Geoscience Transect (brown lines mark the profiles, black dots mark shot locations onshore and ocean bottom seismometer locations offshore). The white dashed line marks the Agulhas-Falkland Fracture Zone (AFFZ). The blue dashed lines show the extent of the Southern Cape Conductivity Belt (SCCB) and the green dashed line the Beattie Magnetic Anomaly (BMA). These are the two major geophysical anomalies in southern Africa. APA = Agulhas Passage, CFB = Cape Fold Belt, KP = Karoo Province, OB = Outeniqua Basin, B) Detail map showing the sub-basins of the Outeniqua Basin and the location of the Diaz Marginal Ridge (DMR). Both profiles consist of an onshore (FRA, GRA) and offshore part (AWI-20050100, AWI-20050200). SOB = Southern Outeniqua Basin.

The *Inkaba yeAfrica* program was initiated as a German-South African co-operation with the aim to investigate these processes in southern Africa [de Wit and Horsfield, 2006]. Being a vital component of *Inkaba yeAfrica* the

## Introduction

Agulhas-Karoo Geoscience Transect (Figure 1-1) is an ambitious venture to reveal the secrets of Africa's southern margin and the two largest geophysical anomalies on the African continent (the Beattie Magnetic Anomaly and the Southern Cape Conductivity Belt, Figure 1-1). In this research co-operation, my thesis constitutes an integral part as it addresses the structure and formation of the continental transform margin and provides new insights into the processes that formed it and its magmatic surroundings. With a better understanding of the structure and tectonic regime, my project provides input for other Inkaba projects which deal with sedimentation processes and the investigation of past catastrophic events.

In order to understand the crustal processes that led to the evolution of the continental break-up related geological features, geophysical methods have been used to provide physical parameters of the deep crust down to the crust-mantle boundary (Mohorovičić discontinuity) and the uppermost mantle. New high quality seismic refraction and reflection data along two profiles crossing the margin (Figure 1-1) were acquired to reveal the deep crustal structure of the southern African margin where large-scale processes have left their distinct marks. A detailed picture of the crustal structure including the continent-ocean transition zone is inevitable to be able to understand the dynamic processes involved in the formation of the basin and fracture configurations of the margin. My thesis contains, for instance, the first characterisation of the basement of the Outeniqua Basin and the extension history of the underlying crust which has important relevance for reconstructing the history of this oil-prone sedimentary basin. This basin is separated from the Agulhas-Falkland Fracture Zone (AFFZ) by the Diaz Marginal Ridge, whose composition as well as the mechanism of its formation were unknown. These details together with the investigation of the Agulhas-Falkland Fracture Zone in terms of its structure, possible re-activation events and its possible role as a zone of lithospheric weakness are major topics of this thesis which can be summarized in the first key question:

**Which processes were involved in the formation of the southern African marginal structures and which role did interactions of shear processes and new crustal formation play?**

Crustal formation in southern Africa's offshore area does not only involve seafloor spreading but it was possibly influenced by the activity of mantle plumes. A large submarine plateau, the Agulhas Plateau, is located south of the AFFZ (Figure 1-1). It has been a matter of debate during the last decades whether this plateau consists of large-scale continental fragments or is a Large Igneous Province of oceanic affinity. As the arguable crustal type of the plateau

## Introduction

represents a key problem for plate-tectonic reconstructions in this region, it is important to bring to light when and how this plateau formed. A formation as an oceanic Large Igneous Province does not only have an impact on plate-tectonic reconstructions of this region, it also introduces an environmental and climate issue into this debate. It is often expected that Large Igneous Provinces have a major influence on the climate during their formation. These unsolved problems lead to the second battery of questions:

**Is the Agulhas Plateau a Large Igneous Province? If yes, what is the source of its magmatism and has the released carbon dioxide climate relevance?**

Both key topics are related in terms of the Gondwana break-up during which the Agulhas-Falkland Fracture Zone was an active transform fault and new seafloor was generated in the Indian Ocean. This link involves the interaction of spreading ridges, triple junctions and plumes, thermal influences across the AFFZ and the still enigmatic origin of the anomalous high elevation of southern Africa. My thesis aims to provide new insights into the dynamic processes and magmatic episodes which shaped southern Africa and their possible relationships.

### **1.2 Structure of the thesis**

Published and submitted manuscripts to peer-reviewed international journals make up the core of my thesis. In the following, I show where co-authors have contributed to the publications. Helpful comments by others than the co-authors are stated in the acknowledgements of the manuscripts themselves. Everything else can be considered as my work. The only exception is the publication in chapter 7, where I served as a co-author and state my contributions. To achieve a continuous line of thoughts, the publications are sorted thematically, rather than chronologically after their submission dates. This gives my thesis the following structure:

Chapter 1 is the introduction, which illustrates the aims and motivation of my thesis. Additionally, this chapter is designed to provide guidance for reading this thesis by describing its structure.

Chapters 2, 3 and 4 provide the earth science background of my thesis. This includes an explanation of Large Igneous Provinces with a definition, their sources and a summary of their possible environmental impact (chapter 2). The

## Introduction

geological history of southern Africa and its offshore basins as well as a short description of its continental margins is the topic of chapter 3. The geoscientific concepts of crustal thinning and processes at transform faults are shortly illustrated in chapter 4.

Chapter 5 consists of the second published manuscript of this thesis:

**Parsiegla, N., Gohl, K. & Uenzelmann-Neben, G., 2008. *The Agulhas Plateau: Structure and evolution of a Large Igneous Province*, *Geophys. J. Int.*, 174, 336-350, doi: 310.1111.j.1365-1246X.2008.03808.x.**

This manuscript deals with the question whether the Agulhas Plateau is a continental fragment or an oceanic plateau. It investigates how and when it formed. We used seismic refraction, seismic reflection and magnetic methods to show that the Agulhas Plateau is an oceanic Large Igneous Province, which formed 100 million years ago together with Maud Rise and North East Georgia Rise. Furthermore, we used information from an additional seismic refraction profile [Gohl and Uenzelmann-Neben, 2001] to calculate the volume of the Agulhas Plateau with emphasis on the part of the volume which was extruded as volcanic flows. This information was applied to calculate the carbon dioxide emission due to the formation of the LIP. It is the first time that such an estimate was calculated for an oceanic Large Igneous Province and it provides a valuable input to the discussion on climate impact of LIP formation in general. Dr. K. Gohl and Dr. G. Uenzelmann-Neben helped with discussions; additionally Dr. G. Uenzelmann-Neben provided three seismic reflection figures. This article was published in 2008.

Chapter 6 comprises the first published manuscript of this thesis:

**Parsiegla, N., Gohl, K. & Uenzelmann-Neben, G., 2007. *Deep crustal structure of the sheared South African continental margin: first results of the Agulhas-Karoo Geoscience Transect*, *S. Afr. J. Geol.*, 110, 393-406, doi:10.2113/gssajg.110.2/3.393.**

In this manuscript, which was published in 2007, we use seismic refraction and seismic reflection data to investigate the deep crustal structure of the southern margin of Africa. We found evidence for renewed tectonic activity at the Agulhas-Falkland Fracture Zone and discussed their possible sources. A previously unknown velocity anomaly beneath the Outeniqua Basin could be identified, which was interpreted as pre-break-up metasedimentary basin. Dr. Karsten Gohl contributed with discussions. Dr. Gabriele Uenzelmann-Neben processed the seismic reflection data, which is shown in three figures and helped with discussions.

In Chapter 7, I present a manuscript which I have co-authored:

## Introduction

*Stankiewicz, J., Parsiegl, N., Ryberg, T., Gohl, K., Weckmann, U., Trumbull, R. & Weber, M., in press. Crustal Structure of the Southern Margin of the African Continent: Results from Geophysical Experiments, J. Geophys. Res.*

Most ideas and modelling presented in this paper are produced by the first author Dr. J. Stankiewicz. In addition, I provided modelling results and contributed to the interpretation of the Agulhas-Karoo Geoscience Transect data. This publication compares the results of seismic refraction modelling with magnetotelluric models to provide a better understanding of the major geophysical anomalies in southern Africa (Figure 1-1). Additionally the differences of sheared margins in contrast to other passive margins are highlighted. As a co-author, I contributed to this paper by providing data and figures of the offshore part. I performed the modelling the offshore part of the velocity-depth model, helped with discussions, added ideas, comments and wrote small sections.

Chapter 8 includes my third submitted manuscript:

*Parsiegl, N., Stankiewicz, J., Gohl, K., Ryberg, T., Uenzelmann-Neben, G., submitted, The southern African continental margin – dynamic processes of a transform margin*

For this study two combined land-sea velocity-depth models were created. From these models, stretching factors across the southern African continental margin were calculated for the first time and led to the identification of two episodes that formed the Outeniqua Basin. These were triggered by intracontinental stretching and motion along the Agulhas-Falkland Fracture Zone. This article presents a new hypothesis on the formation of the Diaz Marginal Ridge and provides a synthesis on the dynamic processes that formed the African's southern continental margin. All co-authors contributed with discussions. Additionally, Dr. G. Uenzelmann-Neben provided the basis for figure 11 and Dr. J. Stankiewicz provided data of the onshore experiment and did part of the modelling job (onshore part of the western profile). The paper was submitted to Geophysics, Geochemistry, Geosystems (G3) in July 2008.

In Chapter 9, I summarize the results and give an outlook of the next research steps which should build on the outcome of my thesis.





## Large Igneous Provinces

hypothesis by Morgan [1971] this concept remains heatedly debated. My thesis is not based on data which could lead to any new arguments against or in favour the plume hypothesis. Therefore, I do not intend to contribute to this discussion. LIPs form when a plume rises, spreads out and decompressional melting thickens the crust from below [e.g. Neal, *et al.*, 1997]. This structure can be identified in velocity-depth models, where it makes up a high-velocity lower crustal body. Such a feature is common for all types of LIPs which include oceanic plateaus, continental flood basalts and volcanic rifted margins (Figure 2-2). From the base of the crust, rising magma intrudes the crust and penetrates it in form of dyke swarms. The crustal type being intruded differs in the divers LIP types. It can be oceanic (Figure 2-2a), continental (Figure 2-2b) or continental to transitional (Figure 2-2c). When reaching the top of the crust vast volumes of lava spread over the surface. The extrusion occurs under subaerial conditions during the emplacement of continental flood basalts, but can be either subaerial or submarine when forming oceanic plateaus, and is usually submarine at volcanic margins.

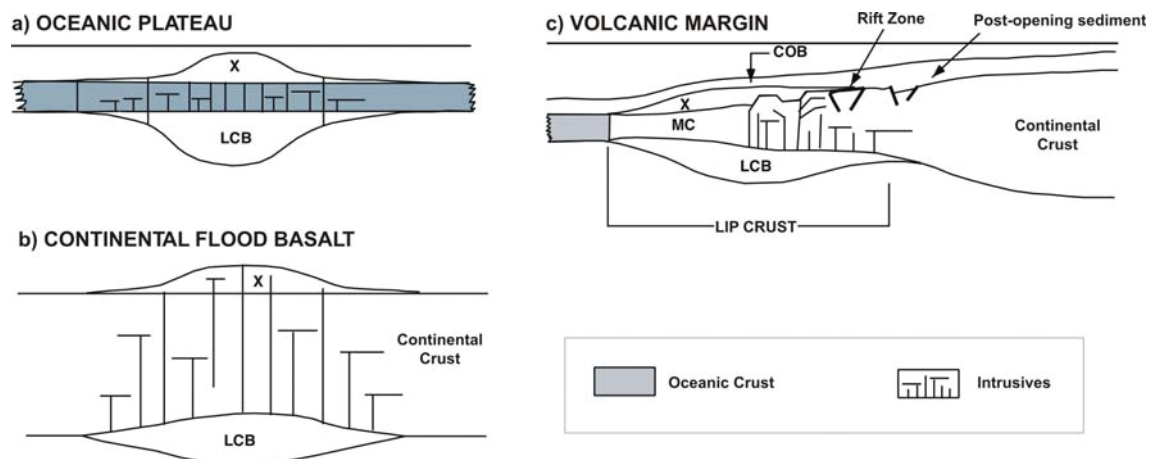


Figure 2-2: Summary of the different types of Large Igneous Provinces modified after Eldholm and Coffin [2000]. COB = continent-ocean boundary, LCB = Lower Crustal Body, MC = middle crust, and X = extrusive cover.

All of the three types of LIPs (Figure 2-2) are found in Southern Africa (Figure 2-1) and had a great impact of the evolution of its landscapes. The Agulhas Plateau (Figure 2-1, Figure 2-2a) is suspected to be a plateau of oceanic origin [Gohl and Uenzelmann-Neben, 2001; Uenzelmann-Neben, *et al.*, 1999]. Its crustal nature and development will be addressed in more detail in chapter 5. The vast Entendeka and Karoo continental flood basalts (Figure 2-2b) frame the western and eastern margins of southern Africa and were emplaced before the Gondwana break-up in this region. The western continental margin is a Large Igneous Province itself comprising huge

## Large Igneous Provinces

magmatically underplated zones and seaward dipping reflectors, representing basalt flows (Figure 2-2c). The locations of most hot spots which influenced southern Africa by forming these LIPs are now far away from the African continent. However, southern Africa is still anomalously elevated [Nyblade and Robinson, 1994]. Recently results of mantle tomography have shown that this region is underlain by a low velocity region [e.g. Ni and Helmberger, 2003; Simmons, et al., 2007]. Commonly this low-velocity zone is attributed to the presence of a superplume which is suspected to be the source of this uplift.

### 2.2 Large Igneous Provinces and climate

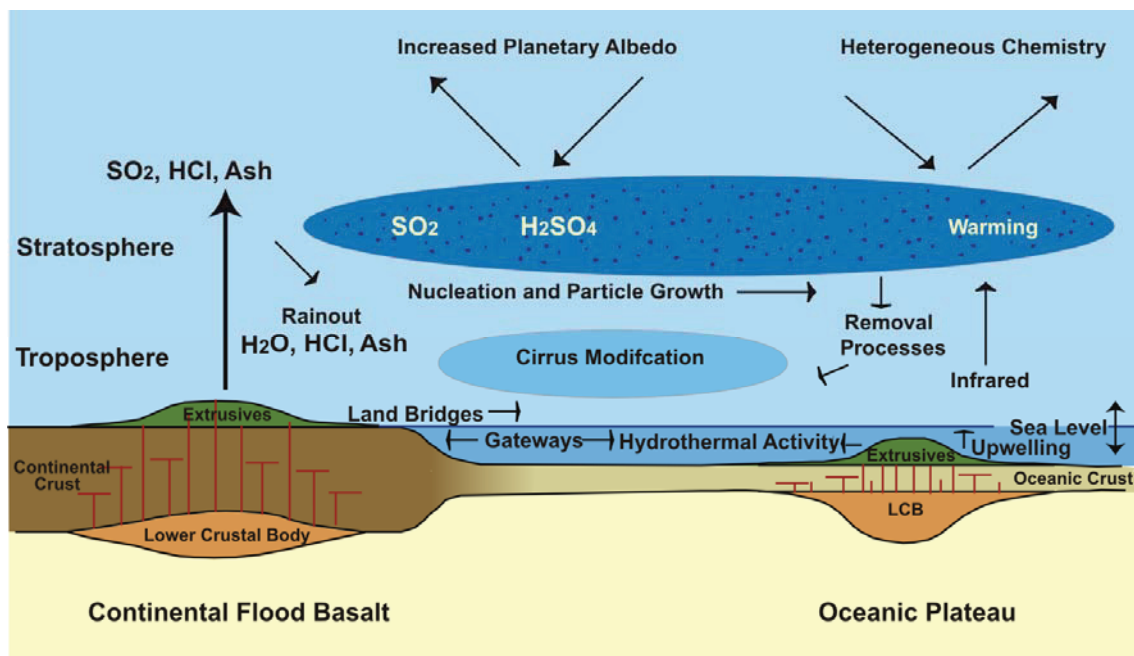


Figure 2-3: Compilation of the potential effects of a LIP formation modified after Coffin et al. [2006].

A possible link of the formation of Large Igneous Provinces with environmental/climate changes and mass extinctions is of general interest because such a connection would be capable to contribute to the solution of the questions how major climate changes are driven and what triggers mass extinctions. As a cause-and-effect chain such a relationship has been investigated during the last years (Figure 2-3) [Coffin, et al., 2006; Coffin and Eldholm, 1994; e.g. Eldholm and Thomas, 1993; Kerr, 2005; Self, et al., 2005; Wignall, 2005] but less attention has been paid to verify if the heat production is capable to fundamentally change environmental conditions in the oceans and whether the gas production represents a major factor.

## Large Igneous Provinces

Possible environmental effects of LIP eruptions are various (Figure 2-3). Here, I give a short overview. Volcanic ashes and aerosols produced during the eruption of a Large Igneous Province can backscatter solar radiation which would have a short-term cooling effect. Gases such as carbon dioxide, sulphur dioxide and nitrous oxides as well as water vapour are released from the extruded lava into the atmosphere and can cause climate cooling (SO<sub>2</sub>) or heating (CO<sub>2</sub>, water vapour). Further environmental impact is likely, if magma is intruded into carbon-rich sedimentary layers or gas hydrates and releases additional CO<sub>2</sub> or methane. In oceanic settings sulphur and carbon dioxides can cause water acidification and influence the marine ecosystem. At the same time, oxygen may be removed from the water due to the thermal impact of the extruding lava causing anoxic conditions which may lead to the extinction of species.

The displacement of water by rock can cause a local rise of the sea level. This and the formation of a new barrier (i.e. the oceanic plateau itself) may result in a change of ocean currents due to a modified water current gateway setting.

Most of these relations have only been proposed but were not tested in terms of quantitative assessment. In Chapter 5 the question is addressed how much carbon dioxide was released during the formation of the Agulhas Plateau Large Igneous Province.

### 3 Geology and tectonic background

#### 3.1 Geological overview of southern Africa and its offshore basins

The geological history of southern Africa covers a period of 3.8 Ga during which some of the oldest cratons on Earth formed and collided [e.g. O'Reilly, 2001; Tankard, et al., 1982], Large Igneous Provinces were emplaced [e.g. Duncan, et al., 1997; Parsiegla, et al., 2008], and sheared [e.g. Parsiegla, et al., 2007; Scrutton, 1976] and rifted continental margins evolved during the break-up of the supercontinent Gondwana [e.g. Bauer, et al., 2000]. This chapter gives a very condensed overview of this complex history.

The Kaapvaal and Zimbabwe cratons (Figure 3-1) developed in the Archean [e.g. Tankard, et al., 1982]. During the early Proterozoic these continental cores were buried beneath a sedimentary cover and magma intrusions formed the Bushveld Complex (Figure 3-1). Africa was repeatedly involved in supercontinent assembly and break-up processes. After the break-up of the supercontinent Rodinia, the supercontinent Gondwana started to amalgamate.

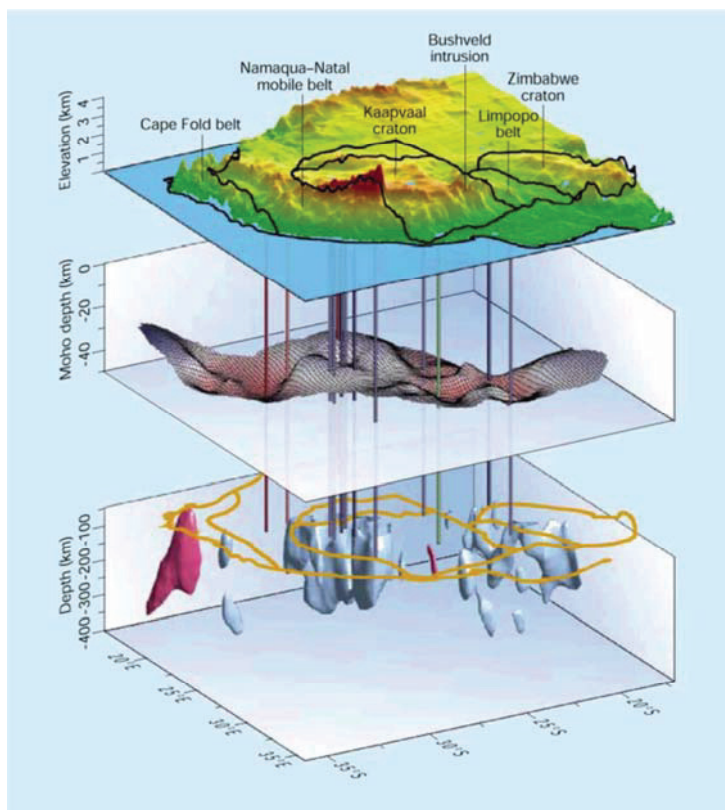


Figure 3-1: Map summarizing the topographic and deep crustal features of southern Africa [O'Reilly, 2001]. Top: surface topography and the main geological boundaries (black lines). Middle: topography of the crust-mantle boundary (Mohorovičić discontinuity). Bottom: cratonic cores show high seismic velocities (blue) and low seismic velocities (red) characterize the upper mantle beneath the Cape Fold Belt.

## Geology and tectonic background

Gondwana formed between 800 and 530 Ma during a series of collision events (East Africa, Brasiliano, and Kuunga Orogeny, Figure 3-2) of earlier supercontinent fragments [Meert and van der Voo, 1996].

### 3.1.1 The Gondwana Era

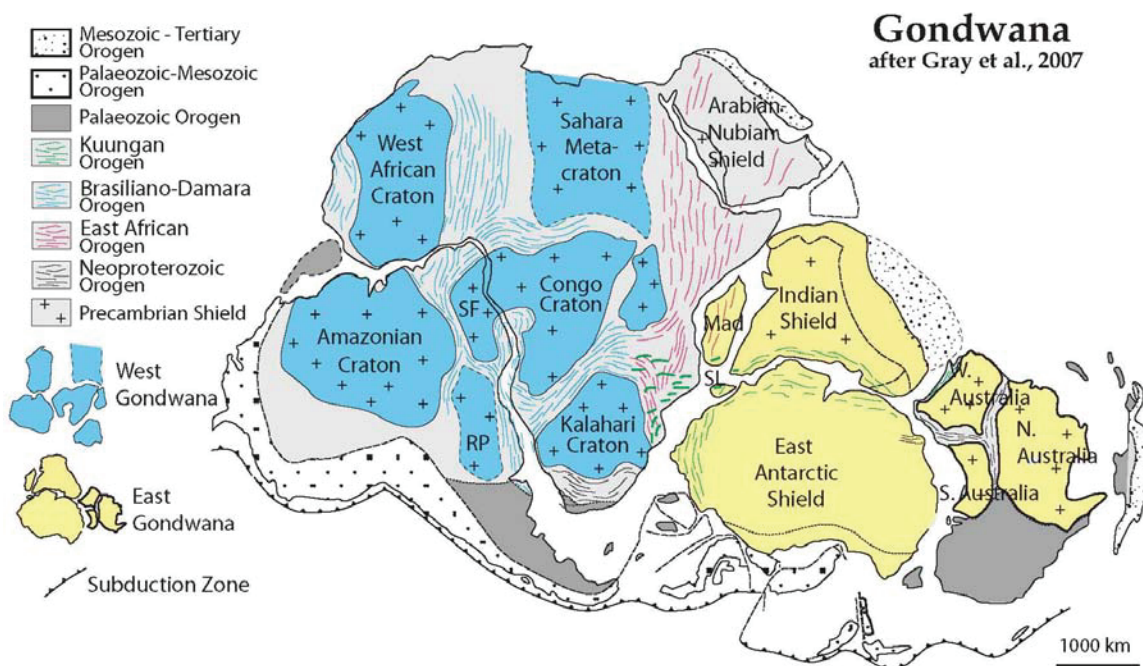


Figure 3-2: Map of Gondwana after its amalgamation (~530 Ma) showing its cratonic cores and the orogens during which supercontinental fragments were combined [modified after Gray, et al., 2008]. The Kalahari craton consists of the Kaapvaal craton, the Zimbabwe craton, and the Limpopo belt (Figure 3-1).

Gondwana consisted of the present-day continents of Africa, South America, Antarctica, Australia and smaller fragments (Figure 3-2). For southern Africa three plate-tectonic episodes are of great importance: the formation of the Cape Fold Belt as an orogen within the supercontinent, intracontinental extension causing the formation of today's offshore basins, and continental break-up resulting in its present-day continental margins.

At 530 Ma Gondwana can be considered to have fully assembled [Meert and van der Voo, 1996]. This episode of collision is followed by a period of uplift and erosion in southern Africa, which resulted in a southward dipping platform [Hälbich, 1993]. There, the Cape Supergroup (Figure 3-3) was deposited between 450 and 300 Ma [Hälbich, 1993]. These rocks consist of clastic sediments, which were deposited during transgression and regression cycles

## Geology and tectonic background

[e.g. *Tankard, et al., 1982*]. The Cape Supergroup strata were deformed during four deformation pulses at 278, 256, 248, and 230 Ma during the Cape Orogeny [*Hälbich, 1993*]. The Cape Fold Belt and its foreland basin – the Karoo Basin (Figure 3-3) – are the products of this orogeny. The mechanism of the Cape Orogeny is not completely understood, yet. Many authors are in favour of a flat plate subduction [e.g. *Dalziel, et al., 2000; de Wit and Ransome, 1992; Lock, 1980*] but there are also hypotheses about a collision origin [*Pankhurst, et al., 2006*] or a transpressional scenario [*Johnston, 2000*]. During its formation the Cape Fold Belt was part of the Gondwananide orogen, which was dispersed during Gondwana break-up into the Sierra de la Ventana (eastern Argentina), the Ellsworth and Pensacola Mountains (Antarctica), the Cape Fold Belt (South Africa) and parts of the Falkland Islands ([e.g. *Dalziel, 2007; Dalziel, et al., 2000*], Figure 3-4, Figure 3-5).

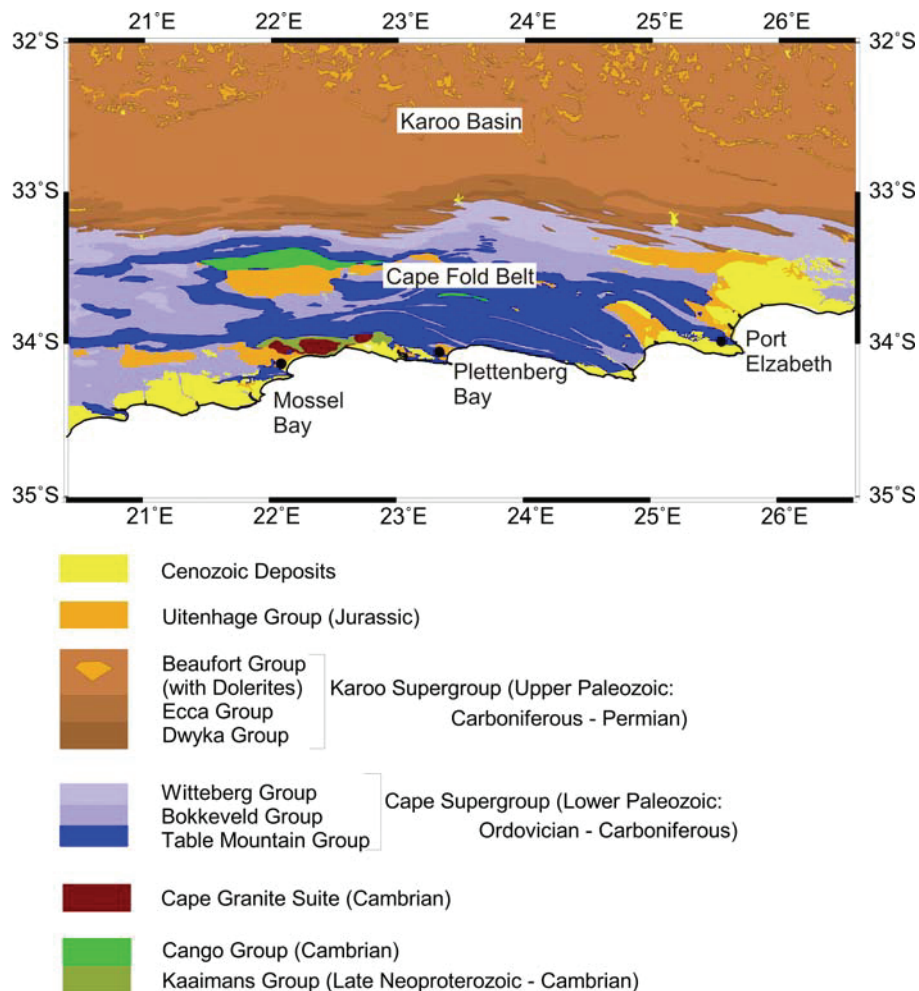


Figure 3-3: Geological map of southern Africa with geological information from the Africa Earth Observatory Network (AEON) data base [de Wit and Stankiewicz, 2006].

## Geology and tectonic background

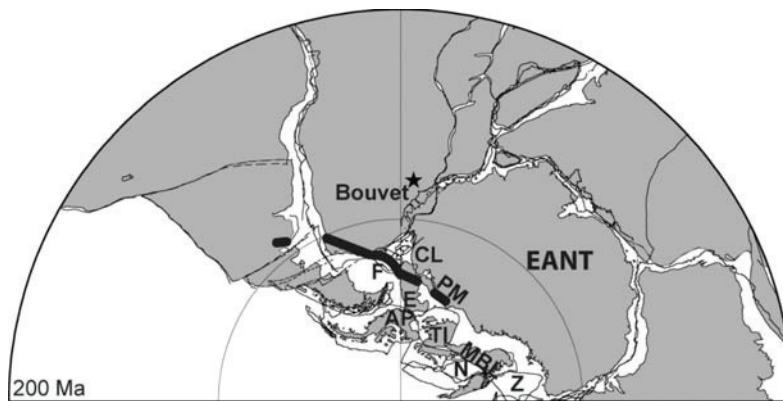


Figure 3-4: Late Triassic reconstruction of Gondwana [Dalziel, 2007]. The reconstructed position of the Gondwanide Fold Belt is marked with a thick black line. The star illustrates the location of the Bouvet hotspot at this time. AP = Antarctic Peninsula, CL = Coats Land, E = Ellsworth-Whitmore, EANT = East Antarctic craton, F = Falkland Islands, MB, NZ = New Zealand, TI = Thurston Island-Eights coast.

North of the Cape Fold Belt the Karoo Basin is located (Figure 3-3). This foreland basin was formed due to folding and thrusting during the Cape Orogeny (280-235 Ma, [Hälbich, 1993]). In the Karoo Basin sediments were deposited from Late Carboniferous and Early Jurassic times forming the Karoo supergroup (Figure 3-3) [Cole, 1992]. These strata were intruded by basaltic lavas during the emplacement of the Karoo Large Igneous Province (183 ± 1 Ma, [Duncan, et al., 1997], Figure 3-5). This event is often interpreted as a precursor of the beginning of the break-up between East and West Gondwana [e.g. Dalziel, et al., 2000].

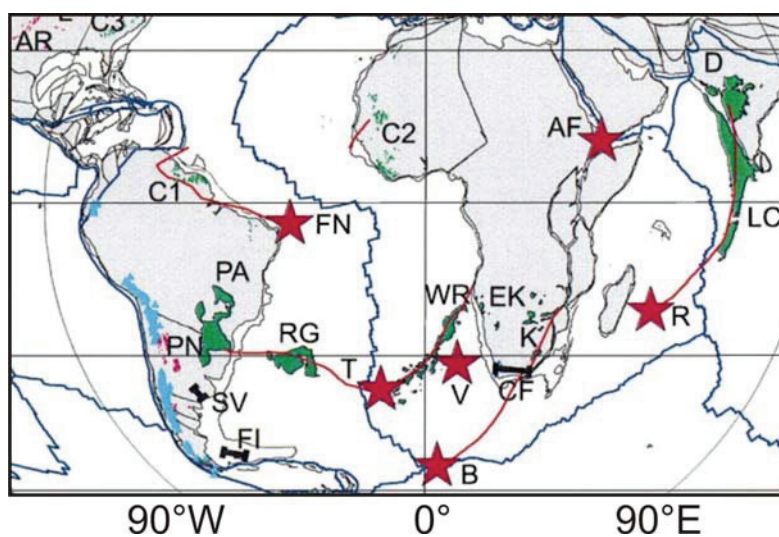


Figure 3-5: Map of the present day Earth [modified after Dalziel, et al., 2000] showing the fractions of the of the Gondwanide fold belt in Africa and South America (CF = Cape Fold Belt; FI = Falkland Islands, SV = Sierra de la Ventana, black bars), selected hotspots (AF = Afar, B = Bouvet, FN = Fernando da Noronha, R = Reunion, T = Tristan da Cunha, V = Vema sea mount, red stars), hotspot tracks (red lines), selected LIPs (C1-C3 = Central Atlantic Magmatic Province, D = Deccan, EK = Etendeka, K = Karoo, LC = Laccadive Ridge, PA = Parana, RG = Rio Grande Rise, WR = Wavis Ridge, green), and active volcanic zones in the Andes (blue).

bars), selected hotspots (AF = Afar, B = Bouvet, FN = Fernando da Noronha, R = Reunion, T = Tristan da Cunha, V = Vema sea mount, red stars), hotspot tracks (red lines), selected LIPs (C1-C3 = Central Atlantic Magmatic Province, D = Deccan, EK = Etendeka, K = Karoo, LC = Laccadive Ridge, PA = Parana, RG = Rio Grande Rise, WR = Wavis Ridge, green), and active volcanic zones in the Andes (blue).

### 3.1.2 The Post-Gondwana era

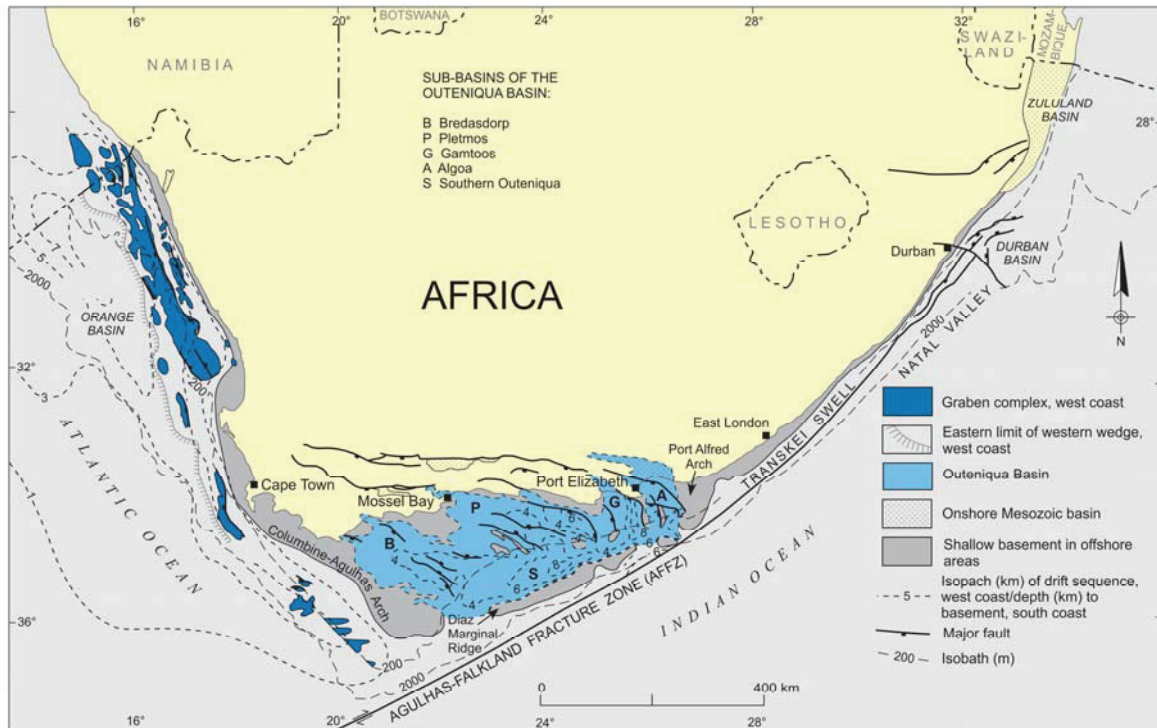


Figure 3-6: Map of the southern African offshore basins modified after Broad et al. [2006]. The Algoa Basin (A), the Bredasdorp Basin (B), the Gamtoos Basin (G), Pletmos Basin (P), and Southern Outeniqua Basin (S) are collectively called the Outeniqua Basin.

The end of the Gondwana era was marked by first intracontinental stretching and the beginning of the break-up at ~167 Ma with rifting in the Mozambique and Somali basins [König and Jokat, 2006]. Different scenarios for continental break-up in this region are possible. Most common are plume-related break-up scenarios [Dalziel, et al., 2000], but some studies showed that plumes can pre-date continental break-up by more than 20 million years [Jokat, et al., 2003; Storey, 1995]. An alternative to the mantle plume model could be the mechanism of supercontinent insulation [Anderson, 1982]. In this hypothesis, the break-up of continents is initiated by the excess heat, thermal expansion and partial melting which is the result when large parts of the mantle are insulated by a overlying continent for more than  $10^8$  years [Anderson, 1982]. Detailed mantle tomography studies as carried out in the last years [Burke and Torsvik, 2004; Li and Van der Hilst, 2008; Montinelli, et al., 2006] provide a great potential to obtain clues about the actual mechanisms which cause continental break-up.

## Geology and tectonic background

Rifting processes which started to form the Outeniqua Basin offshore southern Africa are connected with the early break-up process of Gondwana [e.g. *McMillan, et al.*, 1997]. The Outeniqua Basin is located between the southern African coast and the Agulhas-Falkland Fracture Zone (Figure 3-6). It consists of six sub-basins, these are the shallow Bredasdorp, Infanta, Pletmos, Gamtoos, and Algoa basins, as well as the deep Southern Outeniqua Basin (Figure 3-6). The sedimentary structures of the northern basins are well investigated mostly by hydrocarbon exploration surveys [e.g. *Broad, et al.*, 2006; *McMillan, et al.*, 1997]. The Southern Outeniqua Basin is more than two kilometres deep making it as yet unattractive for hydrocarbon exploration. Therefore, almost no seismic and drill data exist. Two publications of this thesis (chapter 6, 8) address issues concerning these basins which are still poorly understood. They include the deep crustal structure of the Outeniqua Basin and crustal stretching processes.

### **3.2 Continental margins of southern Africa**

Passive continental margins surround southern Africa (Figure 3-6). The formation of these margins dates back to the Late Jurassic - Early Cretaceous when Gondwana broke up.

The western continental margin of southern Africa is a volcanic rifted continental margin with massive underplating and sequences of seaward dipping reflectors [*Bauer, et al.*, 2000; *Hirsch, et al.*, 2008]. It represents an extensively studied and well understood type of margin [e.g. *Bauer, et al.*, 2000; *Eldholm and Grue*, 1994; *Eldholm and Thomas*, 1993; *Gladczenko, et al.*, 1997b; *Hirsch, et al.*, 2008; *Voss and Jokat*, 2007] in contrast to the southern margin. The western margin developed during the Early Cretaceous break-up between Africa and South America. Rifting initiated the formation of the sedimentary basins offshore (Figure 3-6). *Gladczenko* [1997b] attributed the magmatic activity at this margin to the Tristan da Cunha hotspot (Figure 3-5).

The south to southeastern continental margin represents a sheared continental margin which is bounded by the Agulhas-Falkland Fracture Zone. Transform margins are characterized by much smaller continent-ocean transition zones (~50 km) than other passive margins. This means that the distinct temperature and material differences between continental and oceanic crust occur within a short distance, which has a great impact on the basin formation processes at the continental margin and its structure. Additionally,

## Geology and tectonic background

these margins with long-offset transforms experience compressional and extensional forces which are superimposed to the shear forces. This makes the basin formation processes much more complex than in rifted margin basins. Often these long-offset transforms represent deep seated features which make them long lasting and their fracture zones may be re-activated.

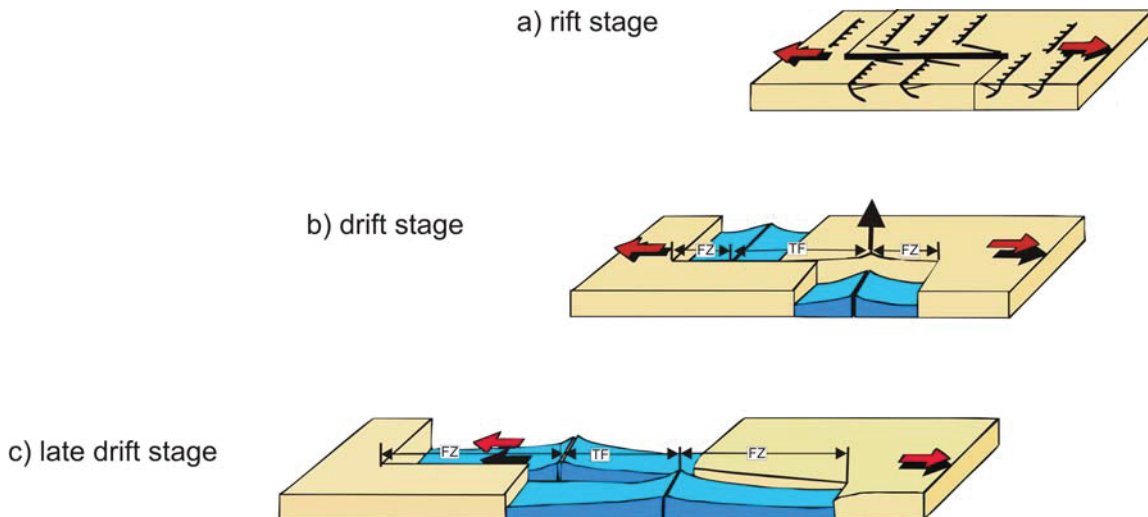


Figure 3-7: Sketch of the development of a sheared continental margin modified after Lorenzo [1997]. a) Rift stage, b) during the early drift stage young oceanic crust slides past old continental crust, c) in the late drift stage, the margin becomes inactive. Red arrows illustrate the plate motion, black arrows show thermal uplift. TF = transform fault, FZ = fracture zone.

Typical features of sheared margins are found at the southern African margin. These are e.g. large-scale fracture zones, marginal ridges and deep sedimentary basins. The formation of the southern African transform margin started with a rift stage in the Early Cretaceous (Figure 3-7a). Right lateral motion along Agulhas-Falkland transform fault and rifting are the major processes during this period. The formation of the transform itself is relatively unknown, as it is not yet established whether this transform exploited a pre-existing zone of weakness or formed entirely in the Cretaceous. During the second stage of this margin - the drift stage - (Figure 3-7b) the young, hot oceanic crust, which had developed south of the African continent, slides past the old, cold continental crust of Africa. This temperature difference can possibly cause thermal uplift as observed at other sheared margins e.g. the transform margin south of the Ivory Coast [Lorenzo, 1997]. When the spreading ridge had passed the African continent, the sheared margin reached the post-shear stage (Figure 3-7c). Although this general picture about the formation of the margin can be drawn, details about its evolution were unknown before the

## Geology and tectonic background

results of Chapters 6 and 8 were published. This work sheds light on the complex two-phase opening history of the Outeniqua Basin and explains the existence of the Diaz Marginal Ridge.

## 4 Geoscientific concepts

### 4.1 Crustal stretching

The main processes associated with the formation of sedimentary basins are block faulting and subsidence [e.g. *McKenzie*, 1978]. Estimations of crustal stretching using the strike and dip of the faults are often inaccurate due to the curved nature of listric faults which are observed in many sedimentary basins. Therefore, a better method of deriving the crustal extension in sedimentary basins is provided by direct determination of the crustal thickness of the stretched crust using seismic refraction velocity-depth models.

Crustal stretching can be quantitatively described in terms of the stretching factor  $\beta$ . The stretching factor is calculated as follows:

$$\beta = \frac{b_{unstreched}}{b_{stretched}}$$

where  $b_{unstreched}$  is the thickness of the crust (or lithosphere) before stretching and  $b_{stretched}$  is the thickness after stretching [*McKenzie*, 1978] (Figure 4-1).

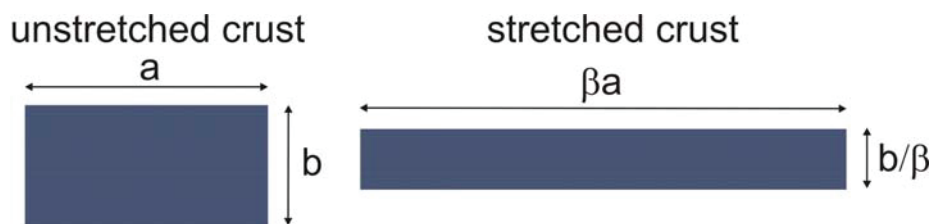


Figure 4-1: Illustration of the meaning of the stretching factor  $\beta$  [modified after *McKenzie*, 1978]

While the thickness of the stretched crust can be directly derived from seismic refraction measurements, the thickness of the unextended crust is usually more difficult to access unless unstretched crust with a similar basement geology is available in the vicinity. This fortunate situation could be exploited in Chapter 8 where the crustal extension in the Southern Outeniqua, Gamtoos and Pletmoos Basins was calculated and provides the first estimate of this kind in the Outeniqua Basin. The knowledge of the stretching factors of these basins provided a tool to distinguish between different phases of crustal extension and to understand in which parts of the basin these episodes had a significant impact. An understanding of the phases of crustal stretching is important

because they provide a quantitative measure of the rifting processes within the basin. When the beta factor approaches  $\sim 4$  [Allen and Allen, 1990], oceanic crust starts to form in between the fragments of continental crust. In the case of the Outeniqua Basin, this process was terminated well before that time and crustal thinning was followed by passive thermal subsidence.

### **4.2 Processes at transform faults**

Transform faults are plate boundaries which undergo strike-slip motion [e.g. Fowler, 1990]. Types of transforms are defined by the nature of the crust opposed across the transform (ocean-ocean, continent-continent, ocean-continent) or the structures that are liked by the transform i.e. ridge-ridge, ridge-trench, and trench-trench transforms [e.g. Woodcock, 1986].

As differences in temperature, lithospheric thickness, rate of subsidence and (in the case of ocean-continent transforms) crustal type exist across the transform, a variety of processes are triggered [e.g. Kastens, 1987]. These include shear heating and convection from the younger, hotter to the older, cooler plate with possible thermal expansion of the old plate and contraction of the young plate [e.g. Kastens, 1987]. At the ridge-transform intersection an increased distance from the magmatic supplies and accelerated cooling of oceanic crust when opposed to cooler crust (cold edge effect) causes an alteration of the spreading process in the vicinity of the transform fault. This modified spreading process leads to a deviation of the crustal structure from "normal" oceanic crust in terms of thickness and velocity structure [e.g. White, et al., 1984]. At ocean-ocean transforms, the resultant oceanic crust is thinner, layer 3 (the gabbro layer) is often absent and the average crustal velocities are lower than in normal oceanic crust [White, et al., 1984]. During the formation of normal oceanic crust, the interaction between water and magma occurs mainly at the surface forming pillow lavas. In contrast to this, the existence of the transform fault transfers the water to deeper levels causing serpentinization of the mafic crust and therefore the reduced crustal velocities. At continent-ocean transforms the cold edge effect causes anomalously thin oceanic crust without a layer 3 [Sage, et al., 1997].

Shear processes acting at large-scale transforms are often not simple strike-slip motions but often involve an orthogonal or oblique component of crustal shortening or stretching [e.g. Dewey, et al., 1998]. These transpressional or transtensional processes can be caused by a change in the pole of rotation for example [e.g. Kastens, 1987]. In transpressional regimes, crustal shortening

## Geoscientific concepts

orthogonal to the shear motion often causes crustal uplift which can lead to the development of a ridge which is parallel to the transform fault (Figure 4-2a). This process is one possibility for the development of a marginal ridge. Other possibilities are flexural uplift due to the erosion of sediments and thermal processes. Thermal uplift of a marginal ridge can be caused when continental crust is opposed to oceanic crust and a convection cell transfers heat from the hot oceanic crust to the cold continental crust (Figure 4-2b). This situation is enhanced when the spreading ridge itself passes the continental margin because the temperature difference between continental and oceanic crust is highest.

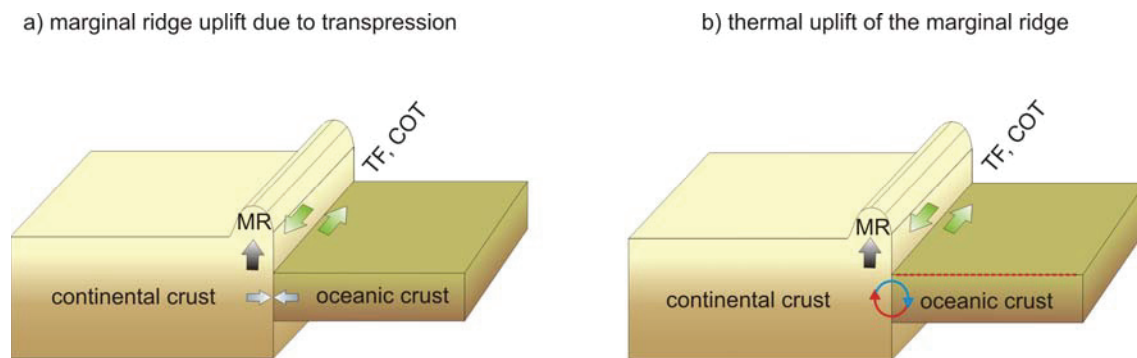


Figure 4-2: Simplified illustration of the mechanisms which are suspected to cause the uplift of a marginal ridge (MR). The figure is not to scale, the extent of the continent-ocean transition zone (COT) and the structure of the transform fault (TF) are not shown but their position is marked. Green arrows show the strike-slip direction. a) The motion along the transform fault does not occur in a simple strike-slip manner but a component of crustal shortening orthogonal to the shear direction exists (blue arrows). This transpressional regime causes the uplift of the marginal ridge. b) The uplift (gray arrow) of the marginal ridge is a result of the temperature difference of old continental crust and new oceanic crust. Heat transfer in terms of a convection cell (red-blue circle, red = hot, blue = cold) leads to this thermal uplift. The red dashed line indicates the position of the spreading ridge.



## 5 The Agulhas Plateau: Structure and evolution of a Large Igneous Province

Parsiegla, N., Gohl, K., Uenzelmann-Neben, G.

### ***Abstract***

Large Igneous Provinces (LIP) are of great interest due to their role in crustal generation, magmatic processes and environmental impact. The Agulhas Plateau in the southwest Indian Ocean off South Africa has played a controversial role in this discussion due to unclear evidence for its continental or oceanic crustal affinity. With new geophysical data from seismic refraction and reflection profiling, we are able to present improved evidence for its crustal structure and composition. The velocity-depth model reveals a mean crustal thickness of 20 km with a maximum of 24 km, where three major units can be identified in the crust. In our seismic reflection records, evidence for volcanic flows on the Agulhas Plateau can be observed. The middle crust is thickened by magmatic intrusions. The up to 10 km thick lower crustal body is characterized by high seismic velocities of 7.0 to 7.6 km/s. The velocity-depth distribution suggests that the plateau consists of overthickened oceanic crust similar to other oceanic LIPs such as the Ontong-Java Plateau or the northern Kerguelen Plateau. The total volume of the Agulhas Plateau was estimated to be  $4 \times 10^6$  km<sup>3</sup> of which about ten percent consists of extruded igneous material. We use this information to obtain a first estimate on carbon dioxide and sulphur dioxide emission caused by degassing from this material. The Agulhas Plateau was formed as part of a larger LIP consisting of the Agulhas Plateau itself, Northeast Georgia Rise and Maud Rise. The formation time of this LIP can be estimated between 100 and 94 ( $\pm 5$ ) Ma.

### ***Keywords***

South Africa, oceanic plateau, seismic reflection, seismic refraction, velocity-depth model, excessive magmatism

## 5.1 Introduction

Large Igneous Provinces (LIP) are voluminous emplacements of extrusive and intrusive rocks [e.g. *Coffin and Eldholm*, 1994]. Continental flood basalts, oceanic basin flood basalts, oceanic plateaus, volcanic rifted margins, and aseismic ridges make up the various types of LIPs [e.g. *Coffin, et al.*, 2006]. Causes and consequences of LIP formation are still poorly understood and include a great variety of aspects including geodynamic, thermodynamic, geochemical, and petrologic issues. Of particular interest are interactions between LIP emplacement and continental break-up and rifting, discussions about their sources, and LIPs as a mechanism for heat release. LIPs provide a possibility to investigate petrologic and geochemical properties of the mantle. Growing interest has been attracted to climate and environmental consequences of LIP formation during the last years [e.g. *Saunders*, 2005; *Wignall*, 2005].

The Agulhas Plateau is an oceanic plateau south of South Africa in the SW Indian Ocean (Figure 5-1). *Scrutton* [1973] suggested a composition of oceanic crust from an abandoned spreading centre. Other authors identify the northern Agulhas Plateau with its rough topography to consist of thickened oceanic crust [*Barrett*, 1977] whereas the southern plateau is argued to be composed of continental fragments [*Tucholke et al.*, 1981, *Angevine and Turcotte*, 1983]. Studies by *Uenzelmann-Neben et al.* [1999] and *Gohl and Uenzelmann-Neben* [2001] were based on seismic reflection and refraction data on the southern Agulhas Plateau and identify the plateau as an oceanic LIP. They derived a crustal thickness of 25 km with high seismic velocities of 7.0-7.6 km/s for the lower part of the crust.

Those controversial results on the oceanic or continental origin of this plateau justified the collection of additional geophysical data across the plateau's central and northern part. Improved evidence for either continental or oceanic affinity would have consequences for the role the plateau played in the regional supercontinental assembly and break-up. If the plateau consists of continental fragments, their origin and correlation to conjugate continental platforms have to be investigated in order to solve their fit into the jigsaw of plate-kinematic reconstructions. If the plateau is an oceanic LIP, questions regarding the time of its formation and consequences of the excessive magmatic emplacement have to be addressed.

The Agulhas Plateau: Structure and evolution of a Large Igneous Province

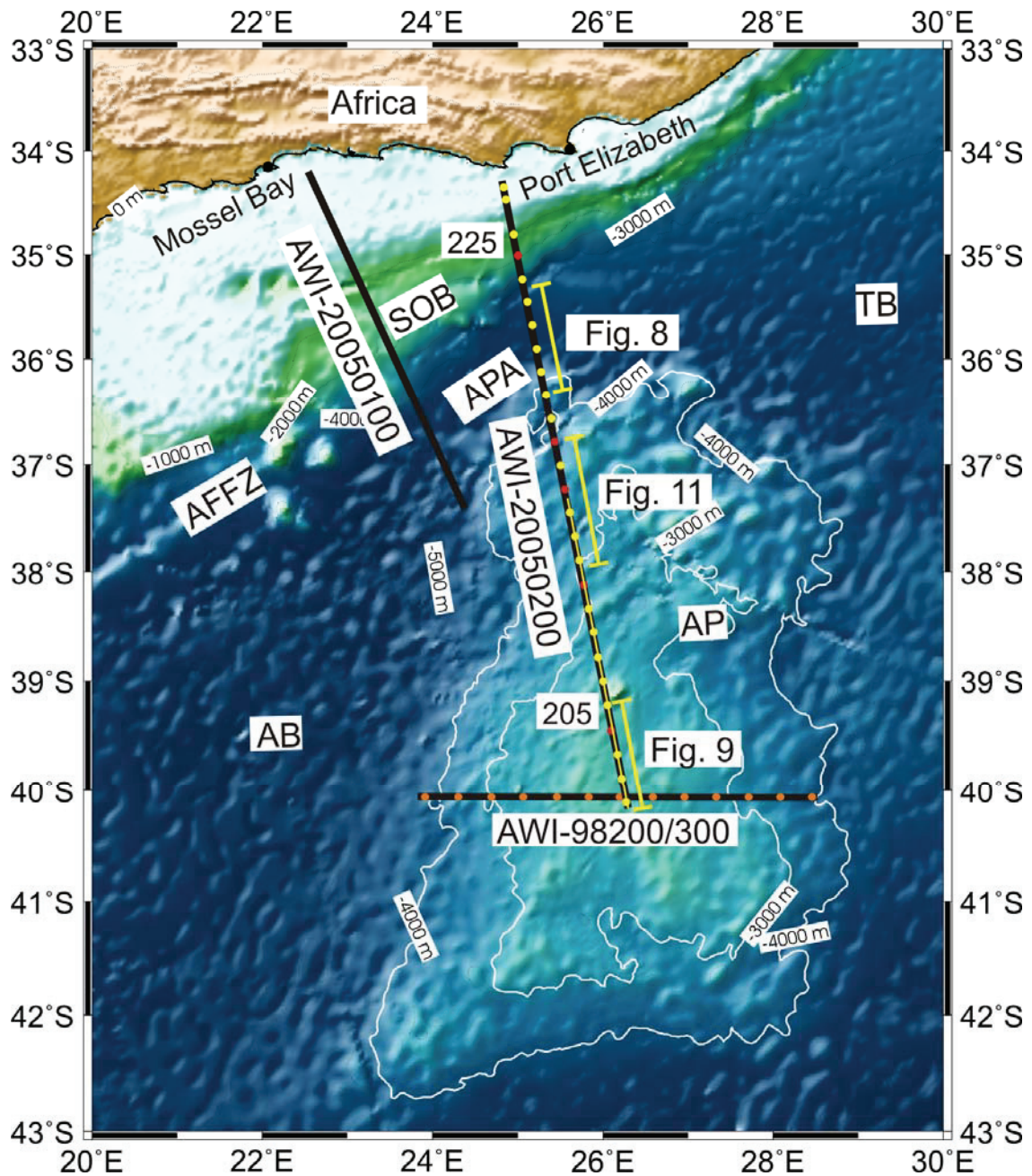


Figure 5-1: Overview map of the area of investigation with satellite derived topography (Smith and Sandwell, 1997) and location of seismic refraction lines AWI-98200/300 (orange), and AWI-20050200 (yellow) used in this paper (Figure 5-6 and Figure 5-10). Dots represent positions of ocean bottom seismometers (OBS), red dots mark OBS positions where data are shown in figures 1 3 and 1 4, thick black lines correspond to the shot profiles, yellow bars mark coincident seismic reflection sections AWI-20050201 (Figure 5-8, Figure 5-9, and Figure 5-10), the thin yellow line through the southern OBS stations of profile AWI-20050200 shows the position of the coincident shipborne magnetic profile (Figure 5-6). Positions of OBS stations 205 and 225 are labelled. Abbreviations are AB = Agulhas Basin, AFFZ = Agulhas-Falkland Fracture Zone, AP = Agulhas Plateau, APA = Agulhas Passage, SOB = Southern Outeniqua Basin, and TB = Transkei Basin.

## 5.2 Geological and tectonic background

The Agulhas Plateau is located in the present southwestern Indian Ocean where the Gondwana break-up between Africa, South America and Antarctica occurred in the Cretaceous. Today, the plateau rises up to 2500 m above the surrounding seafloor and covers an area of more than 230000 km<sup>2</sup>. It therefore presents a major bathymetric high in this region which is limited to the north by the 4700 m deep Agulhas Passage and is flanked by the Agulhas Basin in the west and the Transkei Basin in the northeast. The northern part of the plateau exhibits a rugged topography and basement morphology [Allen and Tucholke, 1981], while the central and southern part of the plateau is characterized by mostly smooth topography and basement [Allen and Tucholke, 1981].

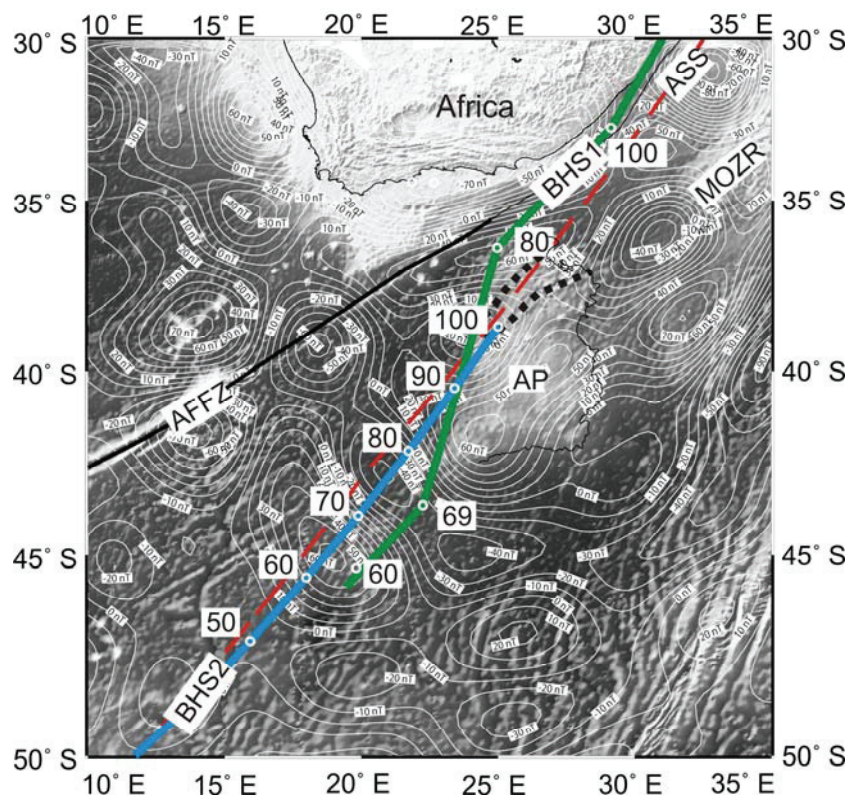


Figure 5-2: CHAMP magnetic anomalies [Maus et al., 2007] drawn as white isolines with 10 nT contour interval overlying the satellite derived topography [Smith and Sandwell, 1997]. Hotspot paths are drawn with thick lines and white circles with annotated times of the hotspot passage. Black dotted lines indicate graben-like lineations in the northern Agulhas Plateau. The southern boundary of the African Superswell [Nyblade and Robinson, 1994] is marked with a red dashed line. Abbreviations are AFFZ = Agulhas-Falkland Fracture Zone, AP = Agulhas Plateau, ASS = southern boundary of the African Superswell, BHS1 = Bouvet hotspot path after Martin [1987], BHS2 = Bouvet hotspot path after Hartnady and le Roex [1985], and MOZR = Mozambique Ridge.

## The Agulhas Plateau: Structure and evolution of a Large Igneous Province

The African, South American and Antarctic plates are joined at the Bouvet triple junction (54.5°S and 1° W). Plate-tectonic reconstructions show that this triple junction was situated near the southwestern tip of the Agulhas Plateau at about 96 Ma [Marks and Tikku, 2001]. Marks and Tikku [2001] interpret the topographic high, which extends from the southwestern Mozambique Ridge to the southern Agulhas Plateau (Figure 5-2), as the path of the Bouvet triple junction. According to Hartnady and le Roex [1985] and Martin [1987], the Bouvet hotspot track crossed the northern part of the Agulhas Plateau at approximately 100 Ma (Figure 5-2) and was therefore thought to have controlled the formation of the Agulhas Plateau together with nearby spreading centres between 80 and 100 Ma [Uenzelmann-Neben et al., 1999, Gohl and Uenzelmann-Neben, 2001]. Kristoffersen et al. [1991] and Gohl and Uenzelmann-Neben [2001] suggest a joint formation of the Agulhas Plateau together with Northeast Georgia Rise and Maud Rise. This combined area of  $0.5 \times 10^6$  km<sup>2</sup> makes the size comparable to that of the Broken Ridge LIP or a third of the Kerguelen Plateau.

### 5.3 Data acquisition and processing

The Alfred Wegener Institute for Polar and Marine Research (AWI) acquired marine seismic reflection and refraction/wide-angle reflection data [Uenzelmann-Neben, 2005] along two profiles across the southern continental margin of South Africa and the Agulhas Plateau (Figure 5-1) during the R/V Sonne cruise SO-182 as part of the Agulhas-Karoo Geoscience Transect in the German – South African cooperative project Inkaba ye Africa [de Wit and Horsfield, 2006]. Details of the western profile (Figure 5-1, AWI-20050100) are described in Parsieglä et al. [2007]. The 670 km long eastern profile AWI-20050200 (Figure 5-1) stretches from the Outeniqua Basin to the southern Agulhas Plateau, crossing the Agulhas Passage and the Agulhas-Falkland Fracture Zone. We deployed 27 ocean-bottom seismometers (OBS) with an average spacing of 20 km. Airgun shots from eight G.Guns™ and one large-volume Bolt airgun with a total volume of 96 litres were discharged every 60 seconds, corresponding to a nominal shot spacing of 150 meters. The OBS data were corrected for clock drift and relocated using the water wave arrival. A bandpass filter of 4-17 Hz and an automatic gain control with a 0.5 s window were applied before travel-time picking of refracted and wide-angle reflected phases. Most of the OBS records produced good to very good quality P-wave arrivals with maximum offsets up to 250 km in the vertical components (e.g. Figure 5-3

The Agulhas Plateau: Structure and evolution of a Large Igneous Province

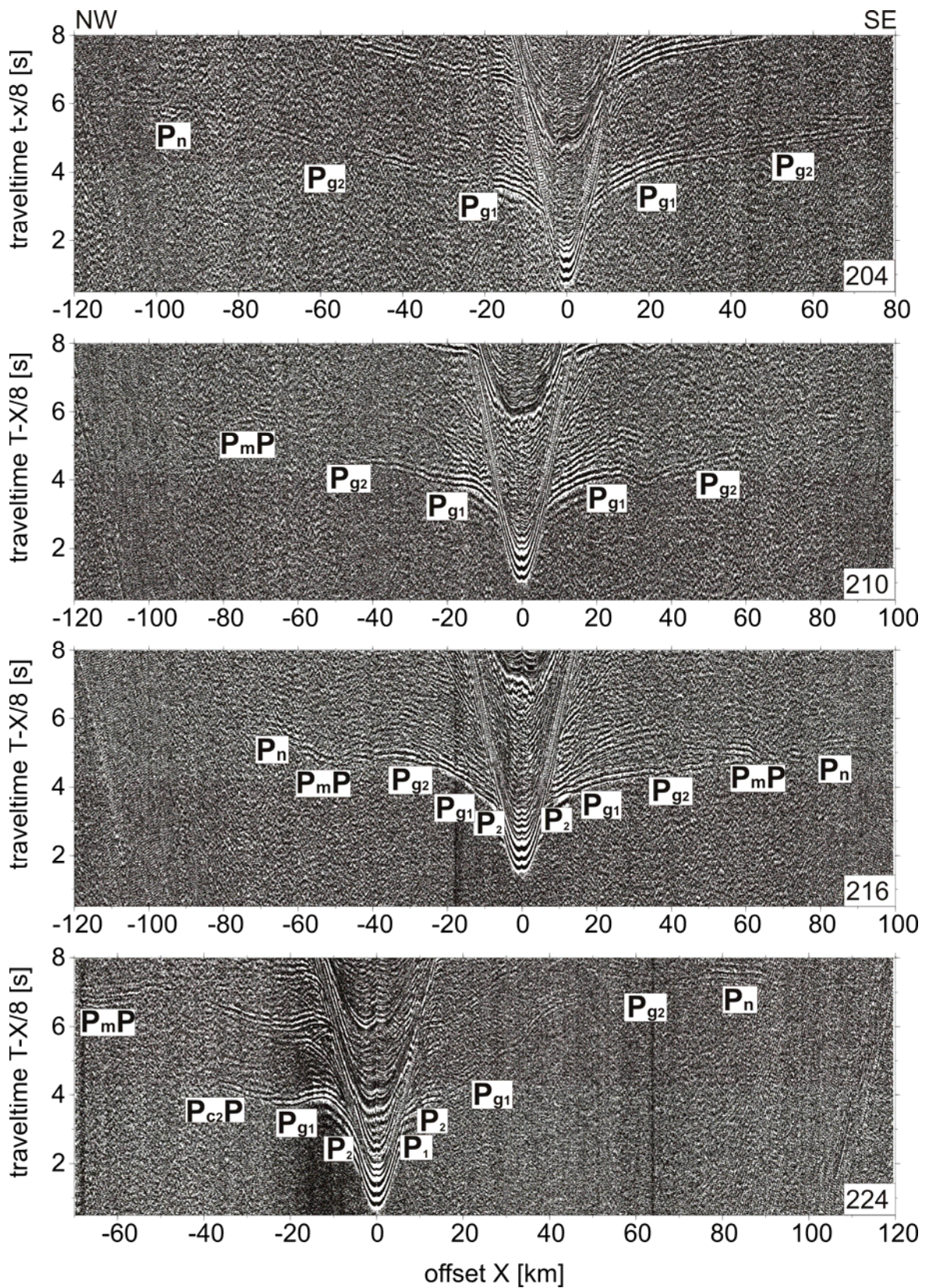


Figure 5-3: Seismic refraction data of the four OBS stations 204, 210, 216 and 224 along profile AWI-20050200 with annotated phases. For an explanation of the phases, see Table 5-1.

## The Agulhas Plateau: Structure and evolution of a Large Igneous Province

Name	Type	Origin	Stations
P <sub>1</sub>	refracted P-wave	model layer 1	3
Ps <sub>1</sub> P	reflected P-wave	top of model layer 2	3
P <sub>2</sub>	refracted P-wave	model layer 2	13
Pc <sub>1</sub> P	reflected P-wave	top of model layer 3	5
Pg <sub>1</sub>	refracted P-wave	model layer 3	24
Pc <sub>2</sub> P	reflected P-wave	top of model layer 4	7
Pg <sub>2</sub>	refracted P-wave	model layer 4	20
PmP	reflected P-wave	top of model layer 5	14
Pn	refracted P-wave	model layer 5	12

Table 5-1: Phase names of P-waves identified in the seismic refraction data and their explanation. The last column states the number of stations where a certain phase could be identified.

Normal-incidence seismic reflection data were recorded simultaneously with a sampling rate of 2 ms using a 180-channel streamer (2250 m active length, SERCEL SEAL™ system). These data were processed in a standard processing flow to depth-migrated sections. The processing flow comprised sorting (50 m CDP interval), a detailed velocity analysis to invoke the subsurface topography (every 50 CDPs), multiple suppression via a Radon transform filtering method, corrections for spherical divergence and normal moveout, application of streamer corrections, stacking, and migration. An Omega-X migration was carried out both in time and depth domain [Yilmaz, 2001]. This method allows vertical variations in velocity and is accurate for large dips ( $\leq 85^\circ$ , [Yilmaz, 2001]). The stacking velocities, which were converted into interval velocities using Dix's formula, were used to set up the velocity field used for the migration process and the embedded conversion from time to depth. The onboard SIMRAD and Parasound systems of RV *Sonne* recorded continuous multibeam bathymetry and sub-bottom profiler data. In addition, we use pre-existing crustal seismic refraction data of profiles AWI-98200 and AWI-98300 across the Agulhas Plateau (Figure 5-1) [Gohl and Uenzelmann-Neben, 2001; Uenzelmann-Neben, et al., 1999].

During the return track of RV *Polarstern* cruise ANT-XXIII/4 in 2007, shipborne magnetic data were collected along the southern 300 km of profile AWI-20050200 (between 360 and 660 km of profile distance, Figure 5-1).

The Agulhas Plateau: Structure and evolution of a Large Igneous Province

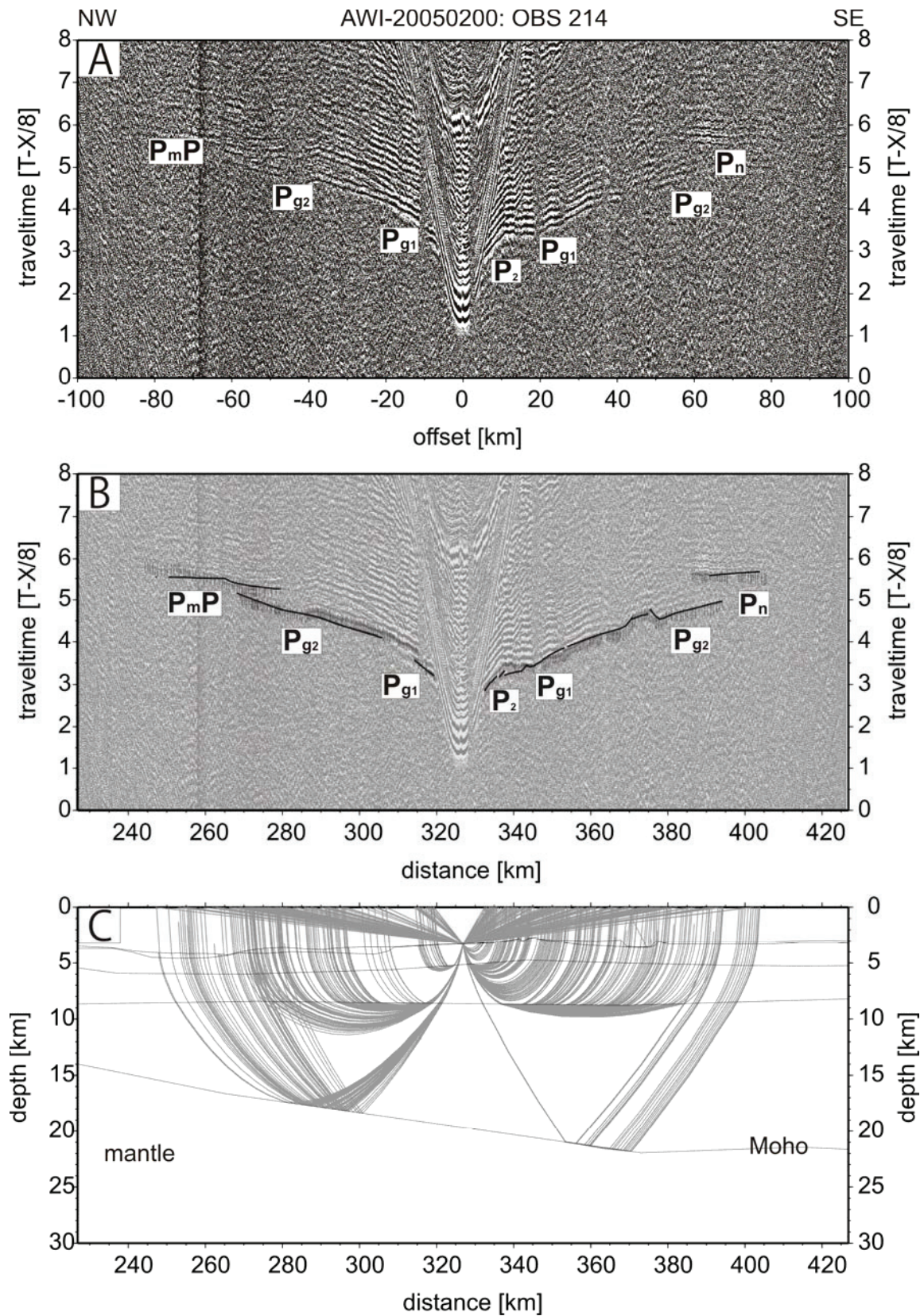


Figure 5-4: Seismic refraction data of OBS station 214 along profile AWI-20050200. The seismogram with annotated phases (A), picks and modelled travel-time curves (B) and raypaths (C) are shown. For an explanation of the phases, see Table 5-1.

## 5.4 Modelling

### 5.4.1 Seismic travel-time inversion

We identified P-wave travel times for profile AWI-20050200, where 24 stations yielded useful P-wave data. Pick uncertainties were set in the range from 40 to 150 ms, depending on the signal-to-noise ratio. We modelled the velocity-depth distribution using the 2-D travel-time inversion routine RAYINVR of *Zelt and Smith* [1992]. Station locations and shots were projected onto a line fitted through the OBS positions.

According to the main groups of identified travel-time branches from the OBS records (Table 5-1), we parameterized our initial model into five model layers beneath the water-layer with the crust (including sediments) represented by layers 1-4, and the upper mantle represented by layer 5. The horizontal spacing of the velocity nodes was chosen with respect to OBS station distance and ray coverage. It lies between 33 km and 45 km for layers 1 to 4. The refracted arrivals from the uppermost crustal layer 1 are sparse because they are masked by the arrival of the direct water-wave. Thus, the lower boundary of this layer was aligned with our interpretation of the acoustic basement from the near-vertical seismic reflection recordings. This basement was clearly identified for model distances 118-210 km, 279-309 km, 379-411 km and 550-652 km. For these model distances, the depth values were kept constant during the inversion process. In the shelf area, this layer was difficult to identify in the near-vertical seismic reflection data. In other locations, layer 1 is very thin or the acoustic basement crops out.

Phase name	Picks	RMS	Chi <sup>2</sup>
P <sub>1</sub>	56	0.076	1.073
Ps <sub>1</sub> P	29	0.048	0.260
P <sub>2</sub>	296	0.115	1.921
Pc <sub>1</sub> P	66	0.081	0.545
Pg <sub>1</sub>	2071	0.114	1.309
Pc <sub>2</sub> P	131	0.076	0.464
Pg <sub>2</sub>	2829	0.133	1.328
PmP	701	0.140	1.285
Pn	824	0.149	1.290

Table 5-2: Statistics of P-wave travel-time inversion. Number of travel-time picks, the root-mean squared (rms) error of the fitting, and the chi<sup>2</sup> value of the different phases.

## The Agulhas Plateau: Structure and evolution of a Large Igneous Province

A simple start model was improved by forward modelling. The resulting model of relatively good fit between observed and calculated travel-times went into a travel-time inversion applied in a layer-stripping manner. The model quality was continuously assessed in the inversion process (Table 5-2). Fits between measured and modelled travel-times are summarized in Figure 5-5. The calculated travel-times for the final model (Figure 5-6A) have an overall rms deviation from the observed travel-times of 0.128 s and a  $\chi^2$ -value of 1.3, which is close to the optimum value of 1. The resolution kernels are calculated for the velocity (Figure 5-7A) and depth nodes (Figure 5-7B) of the final model. Nodes with a resolution greater than 0.5 (range is 0-1) are considered as well resolved [Zelt and White, 1995]. For all layers more than 70 percent of the depth nodes are well resolved (Figure 5-7B). Less resolved depth nodes are mainly located in regions with low ray coverage at the beginning and the end of the profile (Figure 5-7C). The velocity nodes of the first layer are reasonably resolved until 100 km model distance (Figure 5-7A). The velocity resolution decreases farther south, although most of the layer thickness is constrained by our multi-channel reflection data. The second layer is well resolved with only small regions at its lower zone having a resolution of less than 0.5 (Figure 5-7A). As more rays penetrate and turn at the top of the layers (due to their incidence angle and the velocity gradient in the layer), the lower layer zones are usually less resolved. The third and fourth layers are well resolved for most parts. The fourth layer is well resolved at the Agulhas Plateau but poorly resolved in the northern part of the profile because of a low ray coverage (Figure 5-7C). As the resolution depends on the number of velocity/depth nodes as well as on the number of rays, the ray coverage provides a qualitative illustration of the model accuracy (Figure 5-7C). Layer 3 is very well covered by rays which constrain velocities from the top to the bottom of this layer. As the resolution and the ray plot (Figure 5-7) show, the velocity-depth model (Figure 5-6A) is only moderately constrained in the lower crust (layer 4) for the first 130 km profile distance. Farther south, the model is much better constrained. Rays of refracted waves mainly turn in the upper third of this layer, except for two regions (130-200 km and 460-580 km profile distance) where rays cover almost the whole thickness of the layer. The crust-mantle boundary (Moho) is constrained by large-amplitude wide-angle reflections (PmP) and upper mantle refraction (Pn) phases. They define the Moho depth and add information on the velocity-depth structure of the lower crust. The upper mantle is sampled by rays reaching up to 4 km beneath the Moho.

# The Agulhas Plateau: Structure and evolution of a Large Igneous Province

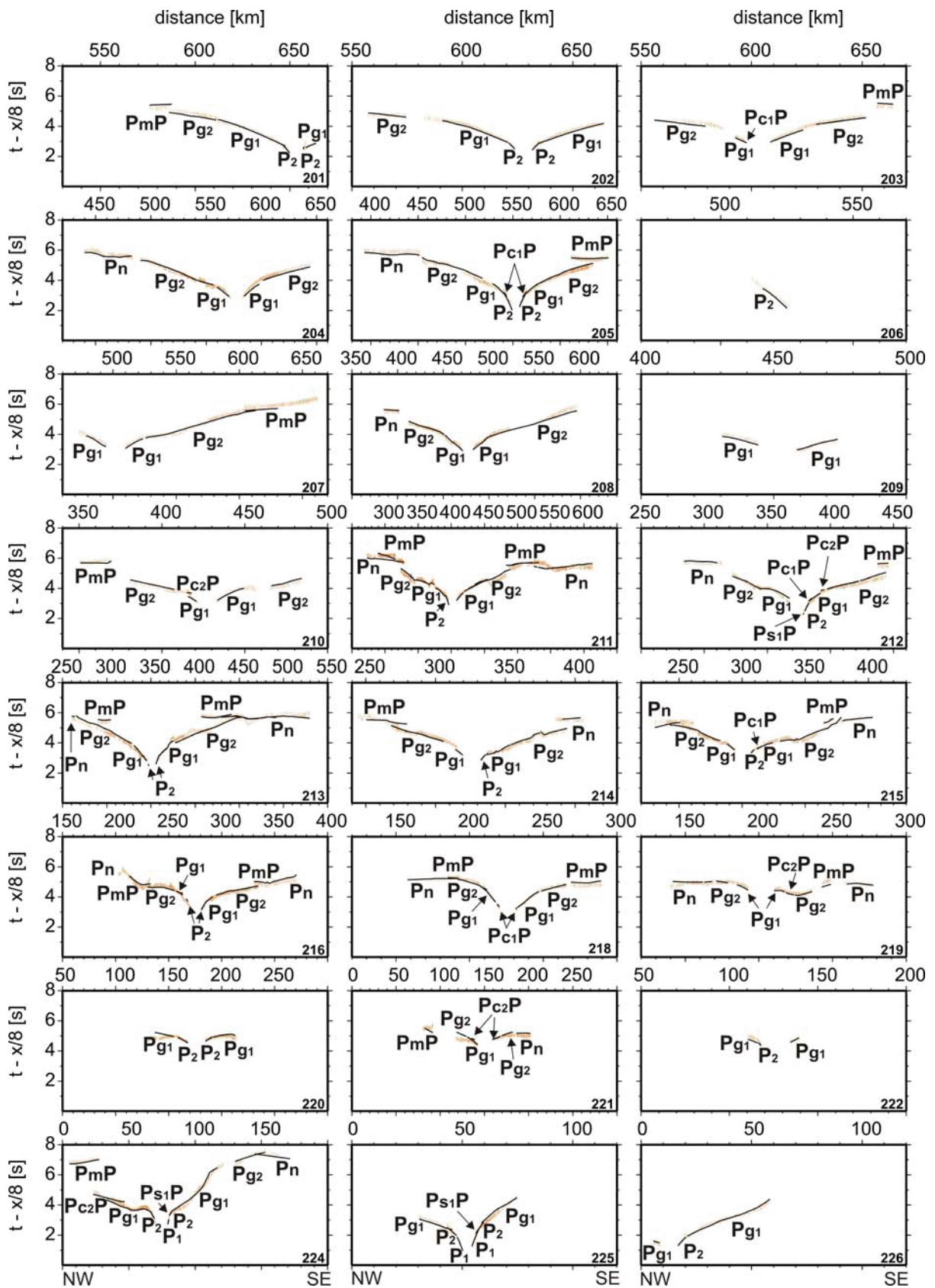


Figure 5-5: Picked (orange vertical bars) and modelled (black solid lines) seismic travel-times. The length of the vertical error bars for the picked travel times corresponds to the assigned picking uncertainties. For an explanation of the phases, see Table 5-1.

### 5.4.2 Modelling results

In the final P-wave velocity-depth model (Figure 5-6A), layer 1 consists of sediments with velocities between 1.7 and 3.4 km/s. From 0 to 90 km profile distance, this layer is up to 1.7 km thick. The sedimentary basins of the South African shelf are located in this region. In the Agulhas Passage the sediments are up to 1.3 km thick (Figure 5-8). Only small patches of sediments of some 100 m thickness exist on the northern Agulhas Plateau. From 550 to 650 km inline distance (CDP 11000-13000), sediments reach up to 0.7 km thickness (Figure 5-9). Layer 2 has velocities between 3.4 and 4.5 km/s and a thickness between 0.6 and 1.1 km beneath the shelf region. Farther south this layer thickens to an average thickness of 1.2 km. Beneath the Agulhas Passage and the northern Agulhas Plateau velocities range between 3.3 and 5.3 km/s. Layer 2 velocities in the middle/southern Agulhas Plateau are between 3.3 and 4.7 km/s. Figure 5-8 and Figure 5-9 show volcanic flows in layer 2.

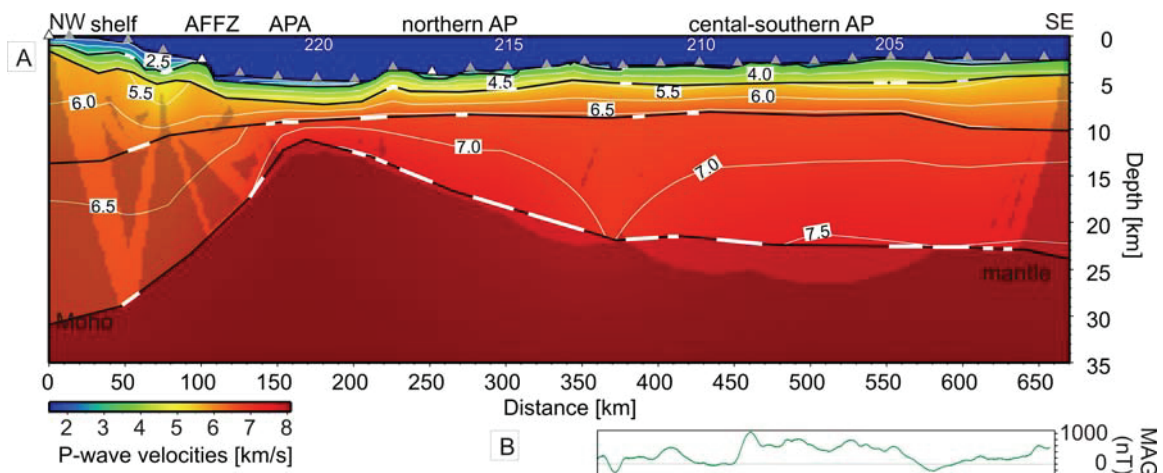


Figure 5-6: A) Seismic P-wave velocity-depth model of profile AWI-20050200. Gray triangles mark OBS positions and numbers over triangles indicate station numbers. White triangles mark OBS which did not record any data. Black lines represent model layer boundaries with thick white lines marking positions of reflected phases at these boundaries. Thin white lines are velocity isolines. Dark shaded areas are not covered by rays. Abbreviations are AFFZ = Agulhas-Falkland Fracture Zone, AP = Agulhas Plateau, APA = Agulhas Passage. B) Magnetic anomalies from shipborne measurements along this profile from 360 to 660 km profile distance.

Layer 3 (Figure 5-6A) exhibits velocities between 5.2 and 6.4 km/s in the shelf region, between 5.6 and 6.7 km/s beneath the Agulhas Passage, and 5.3 - 6.7 km/s in the Agulhas Plateau. In the northern part of the profile, this upper crustal layer has a maximum thickness of 12 km, and thins considerably down to 2 km in the Agulhas Passage. On the northern Agulhas Plateau layer 3 is 2.5-4.0 km thick and on the central to southern plateau 3.5-6.0 km.

## The Agulhas Plateau: Structure and evolution of a Large Igneous Province

In model layer 4 velocities are between 6.5-6.6 km/s beneath the shelf, 6.8-7.2 km/s at the Agulhas Passage and range between 6.7 and 7.6 km/s in the lower crustal part of the Agulhas Plateau. Noteworthy is a well-resolved sub-vertical zone (centred at 370 km profile distance) of relatively low velocities of less than 7.0 km/s compared to lower crust north and south of it with velocities between 7.0 and 7.6 km (Figure 5-6A). Above this zone, a northeast-trending trough of about 700 m depth can be observed in the ocean-floor. The Moho shows a kink here, changing its trend from southerly down dipping to almost horizontal. The Moho depth along the profile ranges from 31 km beneath the continental shelf and thins from 30 to 12 km in the Agulhas Passage. At the northern Agulhas Plateau, the Moho depth increases from 15 to 22 km followed by an almost constant depth of 23 km on average. The crustal thickness ranges from 30 km in the northern part of the profile, 8-14 km in the Agulhas Passage, 11-20 km at the northern part of the Agulhas Plateau, and 20 km in the central part on average. Upper mantle velocities range from 7.7 to 8.0 km/s. A comparison of our velocity-depth model (Figure 5-6A) in the central and southern Agulhas Plateau region with the velocity-depth model of the combined profiles AWI-98200/98300 (Figure 5-10) shows a similar velocity structure.

Most of the magnetic anomalies (Figure 5-6B) along the southern part of the seismic profile are positive with a maximum amplitude of 1055 nT. Only three regions (367-375, 431-448, and 569-591 km profile distance) exhibit negative magnetic anomaly values. The lowest magnetic anomaly of -296 nT is found at 372 km profile distance, which coincides with the position of the sub-vertical zone of relatively low velocities in the velocity-depth model (Figure 5-6A).

## The Agulhas Plateau: Structure and evolution of a Large Igneous Province

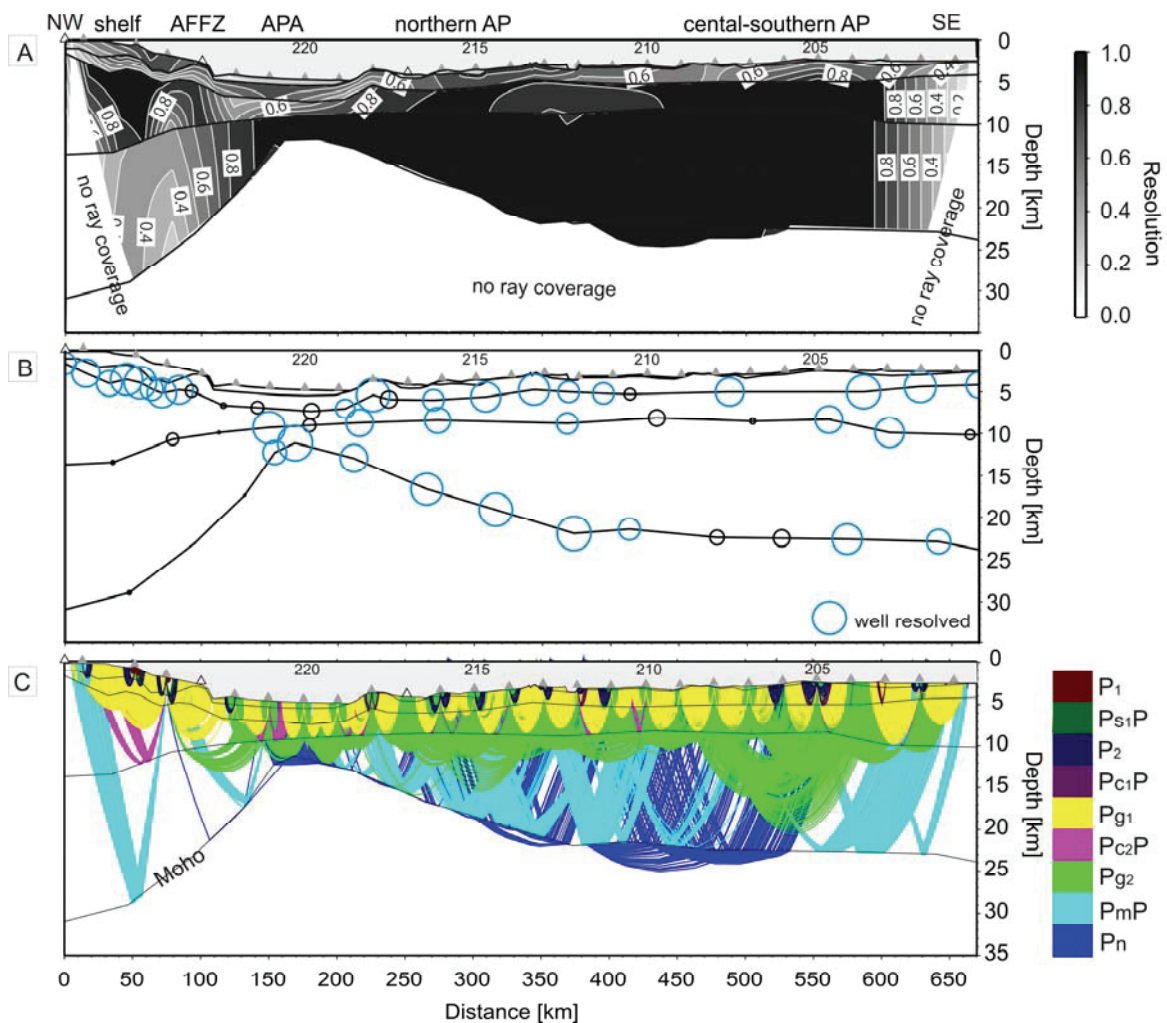


Figure 5-7: A) Resolution of the velocity nodes of the velocity-depth model of profile AWI-20050200. Abbreviations are AFFZ = Agulhas-Falkland Fracture Zone, AP = Agulhas Plateau, APA = Agulhas Passage. Contour lines are drawn with an interval of 0.1. A value higher than 0.5 represents a good resolution. Gray triangles are OBS positions, white triangles refer to stations which did not record any data and numbers over triangles indicate station numbers. B) Resolution of depth nodes of the velocity-depth model. Blue circles represent a good resolution. Black circles mark depth nodes with a resolution of less than 0.5. The circle diameter corresponds to the resolution, where circles with the largest diameter have a resolution of 0.95. For the bottom of the first layer 75 percent of all depth nodes are well resolved. The depth nodes of this layer boundary are too numerous to be clearly arranged, and are therefore not displayed in the figure. C) Plot of the ray coverage with rays modelling reflected and refracted waves. Different colours represent different phases.

## The Agulhas Plateau: Structure and evolution of a Large Igneous Province

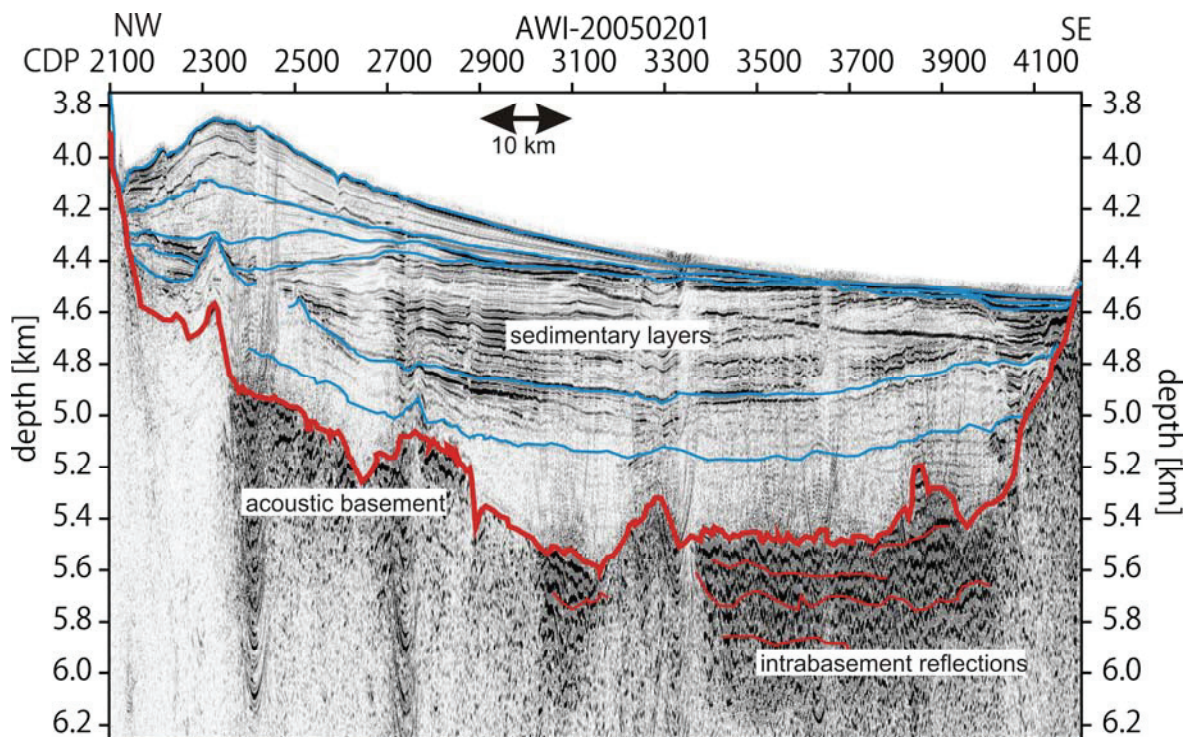


Figure 5-8: Depth-migrated seismic reflection section AWI-20050201 at the position of the Agulhas Passage showing thick sediments and intrabasement reflections interpreted as volcanic flows. Sediment layer boundaries marked with blue lines and some examples of intrabasement reflections are marked with thin red lines. The thick red line represents the top of the acoustic basement.

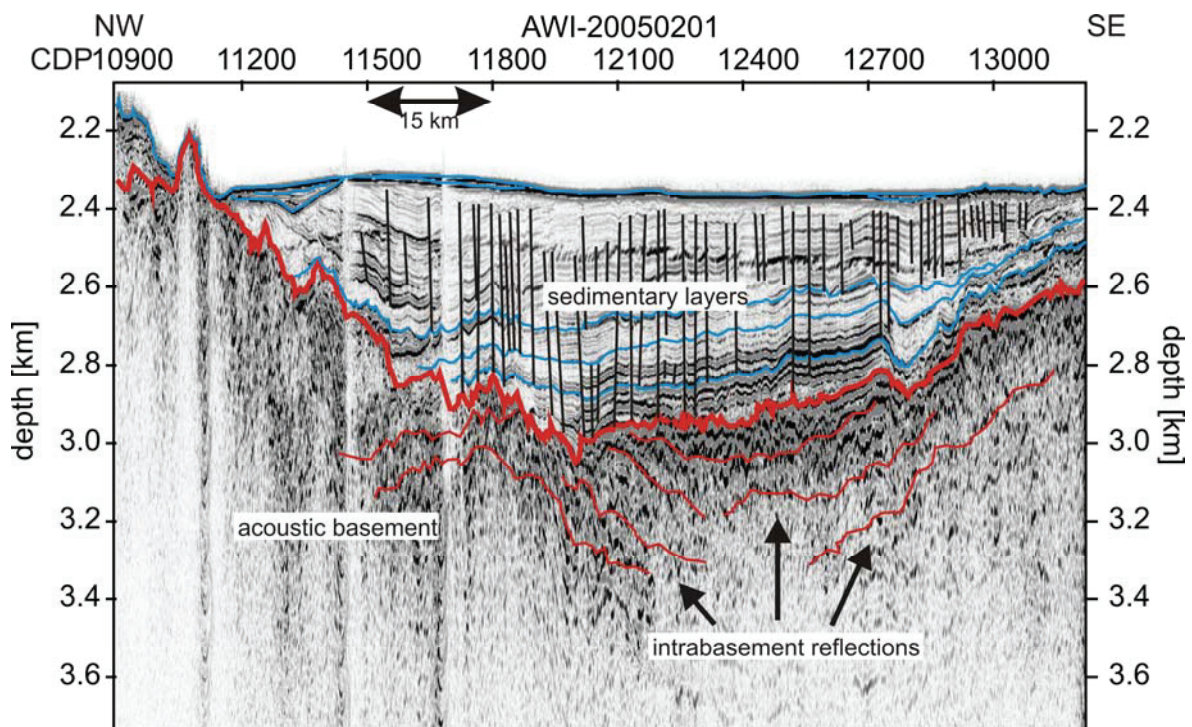


Figure 5-9: Depth-migrated seismic reflection section AWI-20050201 with intrabasement reflections (thin red lines) interpreted as volcanic flows.

## The Agulhas Plateau: Structure and evolution of a Large Igneous Province

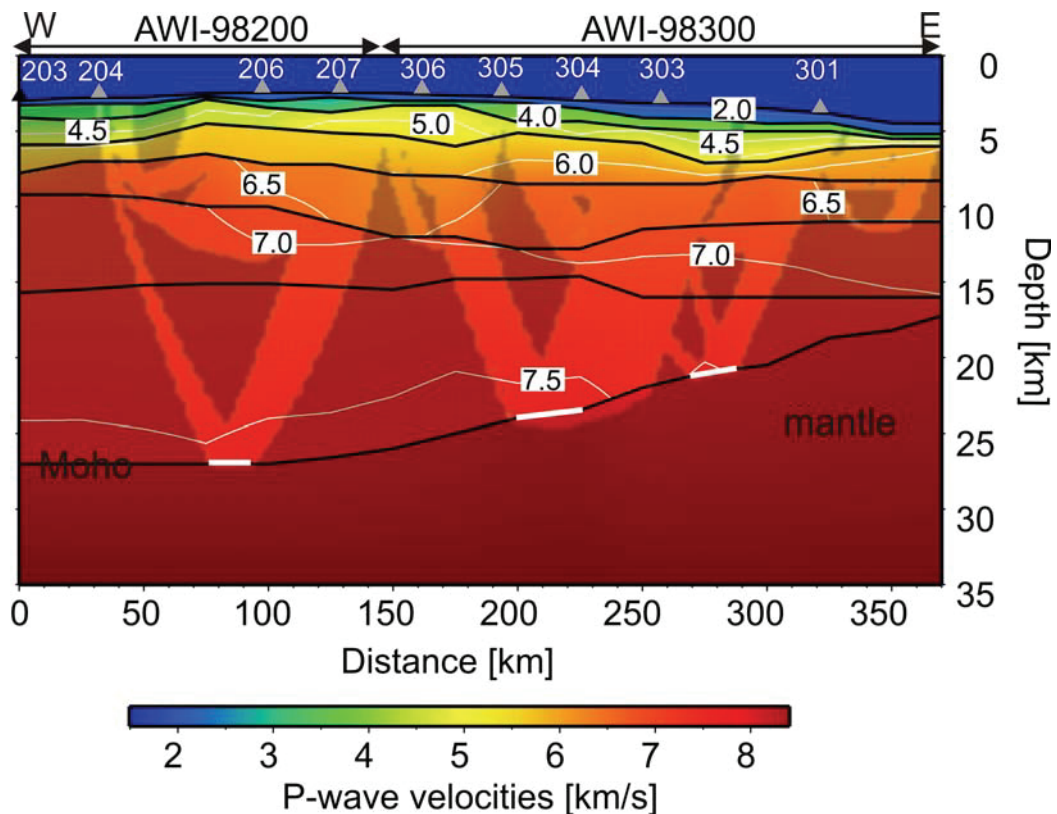


Figure 5-10: P-wave velocity-depth model of profiles AWI-98200 and AWI-98300 redrawn after Uenzelmann-Neben et al. [1999] and Gohl and Uenzelmann-Neben [2001].

### 5.5 Crustal type and structure

The Agulhas Plateau has an average crustal thickness of 20 km which can be attributed to either thickened oceanic crust or extended continental crust. In layer 2, with average velocities of 4.1 km/s, layers of volcanic flows could be identified in our seismic reflection sections (Figure 5-9). These are interpreted as a product of extrusive volcanism. Evidence for extrusive volcanism has previously been found on the southern part of the Agulhas Plateau [Gohl and Uenzelmann-Neben, 2001; Uenzelmann-Neben, et al., 1999] and could be identified as a continuous layer covering major parts of the plateau in this study (e.g. Figure 5-6, Figure 5-9, and Figure 5-11). Basalt flows, which have also been dredged on the Agulhas Plateau [Allen and Tucholke, 1981], make up major portions of this layer. Gladczenko et al. [1997a] identify a similar layer with average velocities of 4.5 km/s on the Ontong Java Plateau. Upper to mid crustal velocities on the Agulhas Plateau of 5.3 to 6.7 km/s are comparable to average velocities of the middle crust of the Ontong Java Plateau (5.3 and 6.6 km/s) [Gladczenko, et al., 1997a]. The average lower crustal velocity of the Agulhas Plateau of 7.2 km/s is slightly higher than that of the Ontong Java

## The Agulhas Plateau: Structure and evolution of a Large Igneous Province

Plateau of 7.1 km/s [Gladczenko, et al., 1997a]. On the Agulhas Plateau, the lower crustal body (LCB) with P-wave velocities between 7.0 and 7.6 km/s makes up about 50 percent of the total crustal thickness (Figure 5-6). These high seismic velocities are comparable to lower crustal velocities observed on the northern Kerguelen Plateau [Charvis, et al., 1995] and the North Atlantic Volcanic margin [Eldholm and Grue, 1994; Voss and Jokat, 2007]. The up to 10 km thick high velocity LCB of the Agulhas Plateau can be interpreted to consist of mafic to ultramafic material [Eldholm and Coffin, 2000] and is a typical feature of oceanic plateaus [Coffin, et al., 2006; Eldholm and Coffin, 2000]. The velocity-depth structure of the Agulhas Plateau is typical for overthickened oceanic crust observed at oceanic Large Igneous Provinces such as the Ontong Java Plateau [Gladczenko, et al., 1997a] and northern Kerguelen Plateau [Charvis, et al., 1995]. In comparison, average velocities as low as 6.7 km/s were observed in the lower crust of oceanic LIPs with large continental fragments such as the southern Kerguelen Plateau [Operto and Charvis, 1996]. We therefore conclude that the crust of the Agulhas Plateau must primarily be of oceanic affinity [Gohl and Uenzelmann-Neben, 2001; Uenzelmann-Neben, et al., 1999].

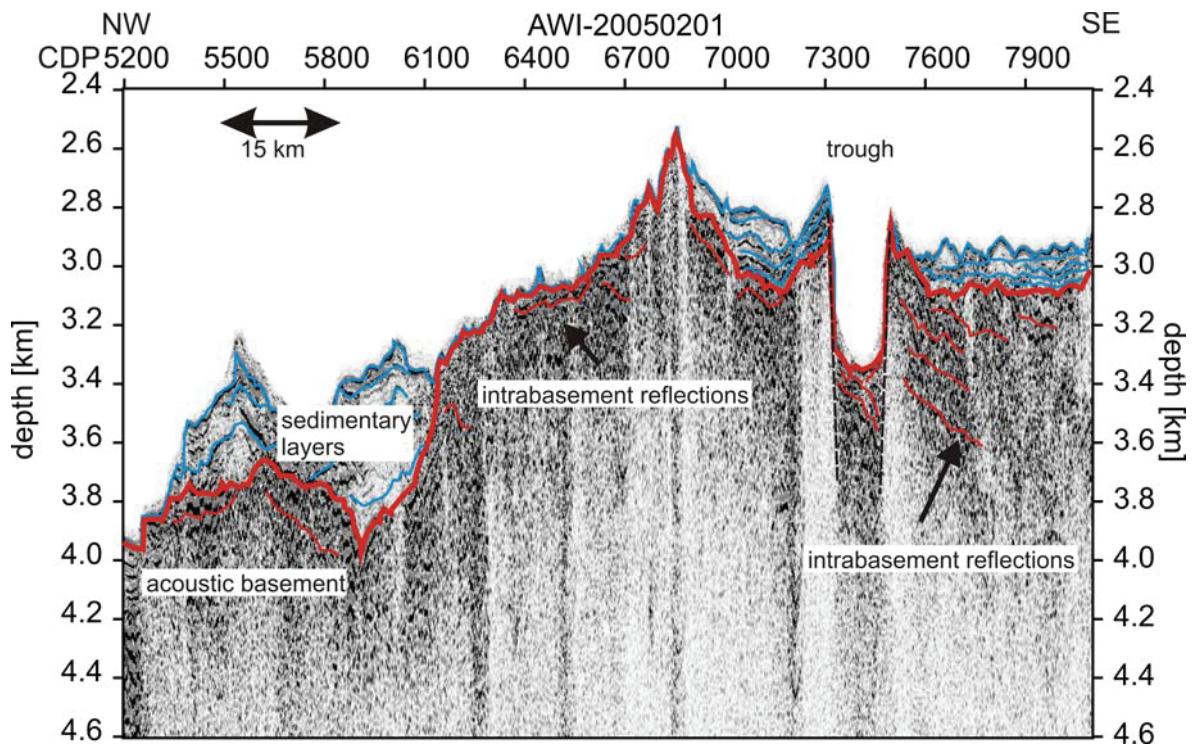


Figure 5-11: Depth-migrated seismic reflection section AWI-20050201 with graben-like structure in the northern Agulhas Plateau.

## The Agulhas Plateau: Structure and evolution of a Large Igneous Province

*Allen and Tucholke [1981]* and *Tucholke et al. [1981]* interpreted geochemical analyses of dredged rock samples as indications for continental fragments in the southern part of the Agulhas Plateau. If any continental fragments of felsic composition, and of sizes which are seismically resolvable, are included in the plateau crust, zones of velocities lower than that of the mafic surroundings can be expected. Our velocity-depth model (Figure 5-6) shows a distinct sub-vertical zone with velocities lower than those in the surrounding crust which coincides with a Moho kink at 370 km model distance. This zone coincides with a negative magnetic anomaly. A low-velocity anomaly within an oceanic plateau could be caused by embedded continental fragments. Previous geophysical studies have not confirmed any continental affinity [*Gohl and Uenzelmann-Neben, 2001; Uenzelmann-Neben, et al., 1999*]. Although large-scale continental crust, as found on the southern Kerguelen Plateau, can be excluded for the Agulhas Plateau, it may still be possible that embedded small slivers of continental fragments, which may have broken off from earlier conjugate continental crust such as the Maurice Ewing Bank (Figure 5-12A), still exist. However, plate-tectonic reconstructions show that before formation of the Agulhas Plateau, this region was occupied by the Maurice Ewing Basin (Figure 5-12A), which makes it difficult to explain how continental fragments from the Maurice Ewing Bank could have been retained there. Therefore, the presence of large-scale continental fragments is rather unlikely.

Satellite-derived topography maps show two lineations (Figure 5-2) striking in northeast-southwest direction in the region north of 38° S. Both of these lineations have coinciding lows in the ship-borne magnetic data at 370 km and 440 km profile distance. Only the northern one (370 km) is observable in the velocity-depth model. Satellite magnetic data by CHAMP [*Maus, et al., 2007*] (Figure 5-2) show centres of negative anomalies aligned with the southern linear structure (440 km). The existence of these lineations suggests an extensional regime causing trench formation, which has plate-tectonic causes discussed in the next section.

## The Agulhas Plateau: Structure and evolution of a Large Igneous Province

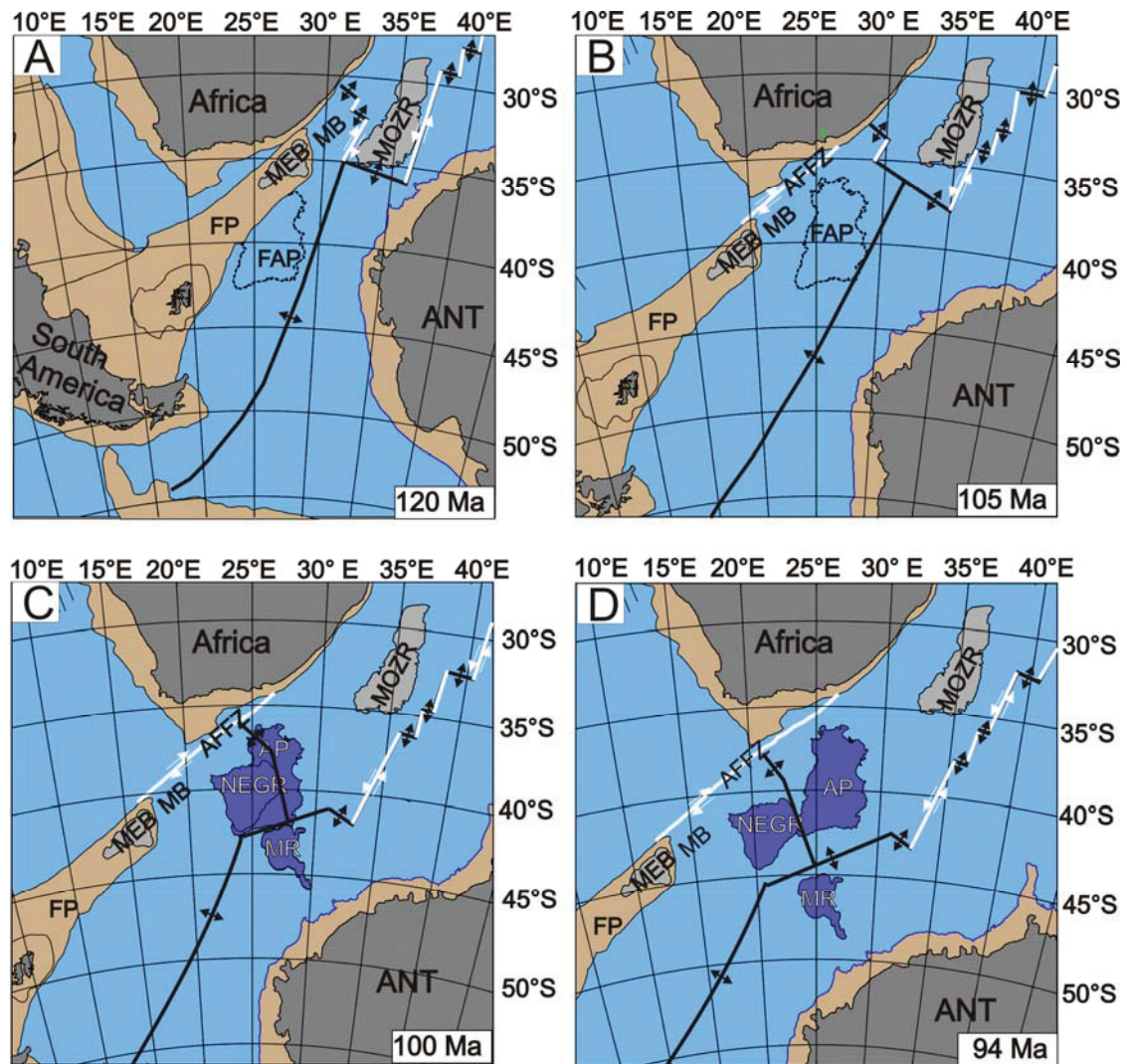


Figure 5-12: Plate-tectonic reconstructions using rotation poles published by König and Jokat [2006]. The rotation was performed with respect to Africa. In figures A-D we use the present-day coordinate system for orientation. Thick lines sketch the estimated location of the paleo-spreading system (black: spreading axis, white: transform fault). Abbreviations are AFFZ = Agulhas-Falkland Fracture Zone, ANT = Antarctica, AP = Agulhas Plateau, FAP = future position of Agulhas Plateau, FI = Falkland Islands, FP = Falkland Plateau, MB = Maurice Ewing Basin, MEB = Maurice Ewing Bank, MOZR = Mozambique Ridge, MR = Maud Rise, and NEGR = Northeast Georgia Rise. A) 120 Ma: Agulhas Plateau region was still occupied by Falkland Plateau with Maurice Ewing Bank leaving no space for the evolution of the Agulhas Plateau at this time. B) 105 Ma: The Agulhas Plateau region was cleared. This is the first possibility for the formation of the AP. C) 100 Ma: The reconstructions of Agulhas Plateau, Northeast Georgia Rise, and Maud Rise (but with the recent boundaries) show an overlap between Agulhas Plateau and Northeast Georgia Rise, which is due to different dimensions of these structures at 100 Ma. D) 94 Ma: The formation of the whole LIP (AP, NEGR, MR) is complete. The Bouvet triple junction is located at the SW tip of the Agulhas Plateau [Marks and Tikku, 2001], and subsequent spreading causes separation of the three fragments of the AP-NEGR-MR LIP.

## 5.6 The Agulhas Plateau LIP in a plate-tectonic context

*Gohl and Uenzelmann-Neben* [2001] estimate the time of plateau formation between 100 Ma and 80 Ma, while a formation age of 120 to 96 Ma is inferred by *Marks and Tikku* [2001] using a revised plate-tectonic reconstruction. We reconstructed the plate-kinematic situation in the region of the Agulhas Plateau to examine time and geometry of its formation. Rotation poles published by *König and Jokat* [2006] were used for the plate-tectonic reconstruction, where their rotation pole between South America and Africa for 130 Ma (centre: 50.00° N, 32.50° W; angle: 55.8°) was replaced by the rotation pole for 131.5 Ma (centre: 50.12° N, 32.79° W; angle: 55.2°) of *Marks and Tikku* [2001]. The reconstruction shows that the Agulhas Plateau region was still occupied by the Maurice Ewing Basin (Figure 5-12A) at 120 Ma, and therefore a formation as early as proposed by *Marks and Tikku* [2001] is unlikely. We place the time of the beginning of the Agulhas Plateau formation at about 100 ± 5 Ma (Figure 5-12B, C). At this time the plate-tectonic reconstructions show Maud Rise (MR) still attached to Agulhas Plateau (Figure 5-12C). Northeast Georgia Rise (NEGR) and Agulhas Plateau (AP) overlap at 100 Ma (Figure 5-12C). This overlap can be explained with the onset of LIP formation at that time, which did not have the same extent as today's fragments. Further rotation shows that at about 94 Ma (Figure 5-12D) AP, MR and NEGR possibly had similar dimensions as today. The identification of extrusion centres in different depths in seismic reflection data suggests a crustal growth in at least two episodes [*Gohl and Uenzelmann-Neben*, 2001]. The first episode was probably at the beginning of the 6 m.y. formation interval and caused the main crustal growth, while the second phase was initiated later possibly due to the fragmentation of the LIP. Extensional conditions during the fragmentation could be an explanation for the trench-like lineations observed on the Agulhas Plateau. On the central-southern plateau, any additional phases of excess volcanism may have masked evidence for extension in that region. Time estimates in the Cretaceous magnetic quiet time using plate-tectonic reconstruction are difficult and inexact. Lacking precise information from drilling on the Agulhas Plateau these reconstructions are a reasonable estimate to get an idea on possible formation ages and geometries.

It is not clear whether the magmatism of the Agulhas Plateau is linked to that of the Mozambique Ridge as discussed by *Gohl and Uenzelmann-Neben* [2001]. Plate-tectonic reconstructions [e.g. *König and Jokat*, 2006] suggest that their crustal growth occurred most likely at different times and places. *Marks and Tikku* [2001] suspect that the gravity and topography high from the southwestern Mozambique Ridge to southern Agulhas Plateau might be the

## The Agulhas Plateau: Structure and evolution of a Large Igneous Province

path of the Bouvet triple junction. If this is correct, a different formation time of Agulhas Plateau and Mozambique Ridge can be inferred. The Bouvet triple junction might have influenced the evolution of the Mozambique Ridge, moved southwestwards forming the topographic high east of the Agulhas Plateau and continued its motion, thus having an impact on the formation of Agulhas Plateau, Northeast Georgia Rise and Maud Rise. Therefore, the AP-NEGR-MR LIP may be an oceanic plateau that also formed at a triple junction such as the Shatsky Rise in the northwestern Pacific [Sager, *et al.*, 1999]. The Bouvet hotspot, which was located at the northern part of the Agulhas Plateau 100 Ma ago according to *Hartnady and le Roex* [1985], may have contributed to the formation of the Agulhas Plateau in two ways. The distinct difference of the topography and basement structures between the northern and southern Agulhas Plateau was already recognized by *Allen and Tucholke* [1981] and suggests a non-uniform evolution of these parts. While the northern plateau is probably directly connected to the activity of the Bouvet hotspot, the southern plateau may have experienced a different history. *Goergen et al.* [2001] recognized interactions between the Bouvet and Marion hotspots with the Southwest Indian Ridge concluding that in the vicinity of spreading centres hotspot magmatism is enforced. Therefore, we suggest that the southern AP-MR-NEGR LIP formed as a result of excessive magmatism caused by the interaction between the Bouvet hotspot and the triple junction.

Today, wide regions in southern Africa and southwest of the African continent are characterized by anomalously elevated topography and shallow bathymetry, respectively. Together, these regions are called the African Superswell (Figure 5-2) [*Nyblade and Robinson*, 1994]. *Nyblade and Robinson* [1994] suggested lithospheric heating as a possible cause. Plume events which date back to the Mesozoic are argued to be responsible for the anomalous elevation of the southern African plateau [*Nyblade and Sleep*, 2003]. Global seismic tomography studies identified a large scale low-velocity anomaly in the lower mantle beneath southern and southwestern Africa [*Su, et al.*, 1994], which is interpreted as the velocity expression of the African Superplume [*Ni and Helmberger*, 2003; *Simmons, et al.*, 2007]. *Class and le Roex* [2006] state that the African Superswell has been a long-lived feature since 130-80 Ma. *Burke and Torsvik* [2004] suggest that low-velocity regions such as beneath the African Superswell have not changed their position with respect to the spin-axis of the Earth for the last 200 Ma. The low-velocity mantle anomaly beneath the African superswell [*Burke and Torsvik*, 2004; *Lithgow-Bertelloni and Silver*, 1998; *Ni and Helmberger*, 2003] is interpreted to be caused by large-scale upwelling, which in turn can be considered as a plate driving force. It is reasonable to attribute the processes of continental break-up, triple junction

## The Agulhas Plateau: Structure and evolution of a Large Igneous Province

activity, LIP formation and Bouvet hotspot activity to the mechanism of large-scale, enduring and distributed mantle upwelling of varying intensity and at different times.

### 5.7 Consequences of crustal generation

#### 5.7.1 Crustal volume of the Agulhas Plateau

The thickness of normal oceanic crust, i.e. away from anomalous regions such as hotspot tracks, ranges between 5.0 and 8.5 km [White, *et al.*, 1992]. Regions of normal oceanic crust in the vicinity of the Agulhas Plateau have a thickness of about 6 km [Uenzelmann-Neben and Gohl, 2004]. The plateau's maximum crustal thickness of 24 km lies in the range of those of other comparable oceanic plateaus (20-40 km) [Coffin and Eldholm, 1994]. We calculated the excess crustal volume which is the additional volume compared to a 6 km thick layer of normal oceanic crust, using thickness information from our seismic velocity-depth models (Figure 5-6A and Figure 5-10) and seismic reflection records. The calculated excess crustal volume provides an important measure to quantify the amount of magmatic material involved in a LIP formation. The crustal thickness and volume calculations of the following paragraph are summarized in Table 5-3.

	Zone A	Zone B	Entire plateau
Area ( $10^5$ km <sup>2</sup> )	0.9	1.4	2.3
Av. crustal thickness (km)	16	21	18
Av. crustal volume ( $10^6$ km <sup>3</sup> )	1.9	2.2	4.1
Volume of normal oceanic crust, 6 km thickness ( $10^6$ km <sup>3</sup> )	0.5	0.8	1.3
Excess volume ( $10^6$ km <sup>3</sup> )	1.3	1.4	2.7
Extruded volume ( $10^6$ km <sup>3</sup> )	0.2	0.3	0.4
Intruded/LCB volume ( $10^6$ km <sup>3</sup> )	1.2	1.1	2.3

Table 5-3: Steps for calculating the excess volume of the Agulhas Plateau with figures for the centre of the plateau within the 3000 m depth isoline (Figure 5-13, zone A) and the area between the 3000 and 4000 m isolines (Figure 5-13, zone B). Abbreviation are Av. = average, LCB = lower crustal body.

## The Agulhas Plateau: Structure and evolution of a Large Igneous Province

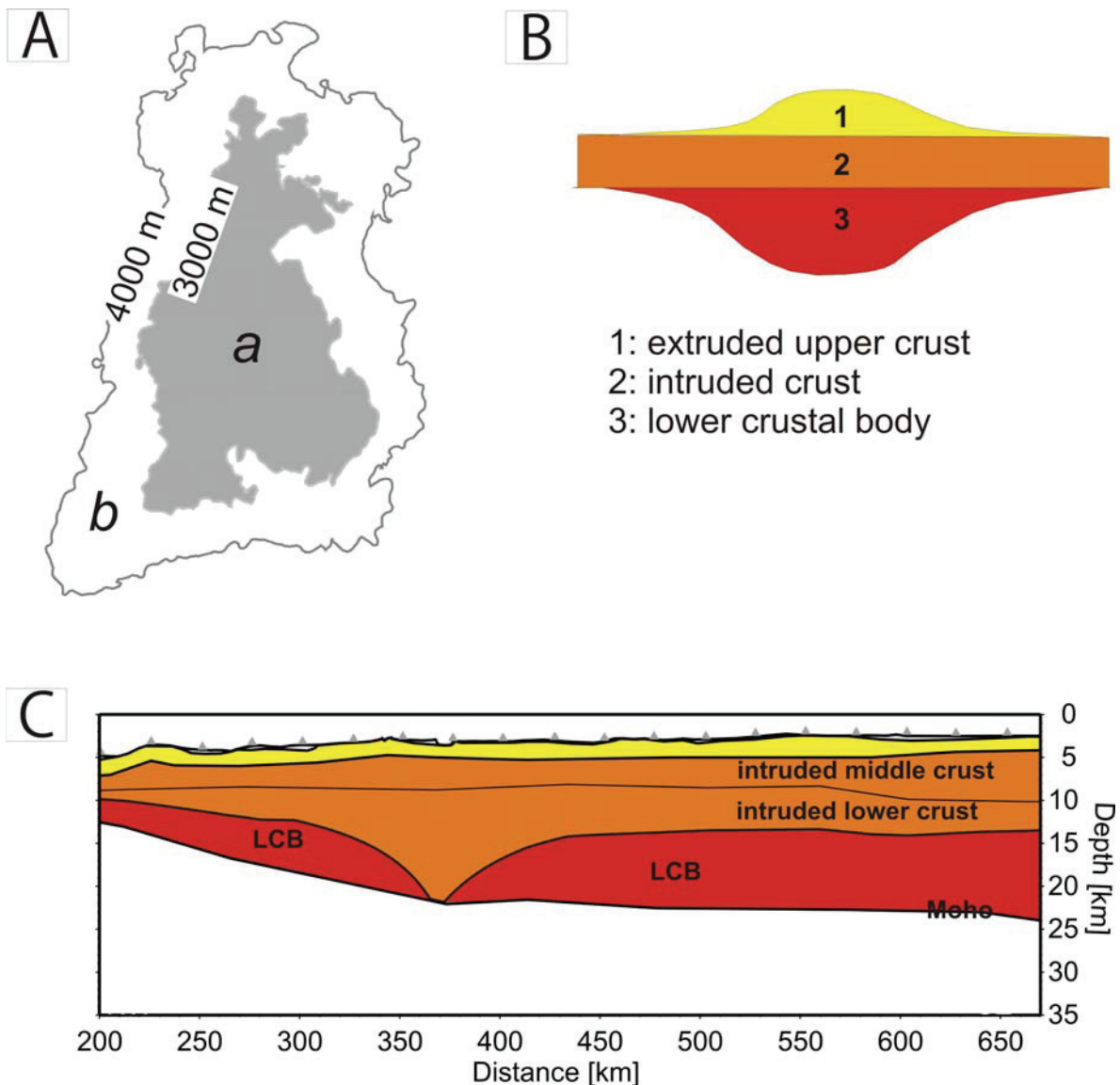


Figure 5-13: A) Subdivision of the Agulhas Plateau in zone a with average crustal thickness of 21 km and zone b with average thickness of 16 km. B) General structure of an oceanic plateau LIP [Eldholm and Coffin, 2000] consisting of an extrusive cover (yellow), an intruded middle part (orange) and lower crustal body (red). C) Crustal structure of the Agulhas Plateau along profile AWI-20050200 showing the typical structure of a LIP.

A bathymetry map (Figure 5-1) is used to distinguish two zones of the AP which differ in their crustal thickness: zone a within the closed 3000 m depth contour and zone b between the 4000 and 3000 m depth contours (Figure 5-13A). We calculated an area of  $8.9 \times 10^4 \text{ km}^2$  for zone a,  $1.4 \times 10^5 \text{ km}^2$  for zone b and  $2.3 \times 10^5 \text{ km}^2$  for the entire plateau (zone a + zone b). Crustal thicknesses in zone a are 24 km (at 125 km profile distance), 23 km (at 175 km), and 21 km (at 225 km) on profiles AWI-98200 and AWI-98300. On profile AWI-20050200, crustal thicknesses are 18 km (at 400 km), 19 km (at 500 km), and 20 km (at 600) in zone a. This leads to an average thickness for zone a of

## The Agulhas Plateau: Structure and evolution of a Large Igneous Province

21 km and a volume of  $1.9 \times 10^6 \text{ km}^3$ . The crustal thickness of zone b is determined on profiles AWI-98200 and AWI-98300 to be 17 km (at 300 km profile length) and 24 km (at 50 km) thick. The latter value is derived from a poorly constrained part of the velocity model of profile AWI-98200 [Gohl and Uenzelmann-Neben, 2001; Uenzelmann-Neben, et al., 1999] and therefore not used here. Profile AWI-20050200 shows an average thickness of 15 km (at 300 km) for zone B. These results lead to an average crustal thickness of 16 km for zone B, which corresponds to a crustal volume of  $2.2 \times 10^6 \text{ km}^3$ . The sum of both volumes is  $4.1 \times 10^6 \text{ km}^3$ , which is between a maximum volume of  $4.7 \times 10^6 \text{ km}^3$  and a minimum of  $3.6 \times 10^6 \text{ km}^3$  using 21 and 16 km as extreme values for the crustal thickness. *Eldholm and Coffin* [2000] summarize volumes of LIPs ranging from  $0.7 \times 10^6 \text{ km}^3$  for the Central Atlantic Magmatic province to  $44.4 \times 10^6 \text{ km}^3$  for the Ontong Java Plateau. Most LIP volumes are in the range of  $2 \times 10^6$  to  $1 \times 10^7 \text{ km}^3$  [Eldholm and Coffin, 2000], with the Agulhas Plateau having a comparable volume to that of the Caribbean LIP. Subtracting the volume of a 6 km thick layer of oceanic crust in the area of the plateau leads to an excess magmatic volume of the plateau of  $2.7 \times 10^6 \text{ km}^3$ .

We distinguished between an intruded/lower crustal body and an extruded component of the excess volume (Figure 5-13B, C). The extruded material is calculated using the average thickness of the layer of volcanic flows identified in the seismic reflection records (e.g. Figure 5-9). Its thickness is estimated using velocity-depth models of profiles AWI-20050200, AWI-98200 and AWI-98300 (Figure 5-6 and Figure 5-10) where the thickness of the layer with average velocities of between 3-5 km/s is sampled every 50 km. The average thickness is 1.8 km. This leads to an estimation of the extruded volume to be  $0.4 \times 10^6 \text{ km}^3$ . The remaining excess volume of  $2.3 \times 10^6 \text{ km}^3$  intruded into oceanic crust and makes up the lower crustal body. Figure 5-13 sketches the schematic structure of the Agulhas Plateau with its extrusive cover, intruded middle part (consisting of intruded middle and intruded lower crust) and its lower crustal body.

### 5.7.2 Thermal subsidence of the Agulhas Plateau

Discrimination between a marine or subaerial formation of the Agulhas Plateau is important to understand the influence of the excessive magmatism on the environment at the time of formation. Therefore, we calculated the influence of subsidence, which led to the present depth of the Agulhas Plateau between 2000 and 4000 m below sea level (Figure 5-1). In order to estimate the paleo-depth of the Agulhas Plateau between 100 Ma and 80 Ma, the thermal

## The Agulhas Plateau: Structure and evolution of a Large Igneous Province

subsidence of the Agulhas Plateau was calculated using the equation of *Parsons and McKenzie* [1978] for the 3000 and 4000 m depth isolines (Table 5-4). We calculated paleo-depths of at least 250 m above sea level for the area within the present 3000 m isobath of the Agulhas Plateau (Table 5-4). If the central part of the plateau (within the 3000 m depth isoline) already existed at 100 Ma, it was possibly subaerial, and stayed above the water surface for a maximum of 20 m.y. (Table 5-4). We did not include the additional subsidence due to loading, because our data does not provide evidence if the basalt flows on the Agulhas Plateau were erupted on already overthickened crust or occurred at the same time as crustal thickening. Therefore, the calculated subsidence is a minimum value, leading to the consequence that larger areas of the Agulhas Plateau could have been subaerial. Changes in sea level were not included in the calculations but are small enough [e.g. *Skelton*, 2003] not to change the conclusion of a partly subaerial early Agulhas Plateau.

Age [Ma]	Depth [m]	Paleo-depth [m]
100	4000	750
100	3000	-250
95	3000	-200
90	3000	-140
85	3000	-70
80	3000	-10

Table 5-4: Calculation of the thermal subsidence of the Agulhas Plateau between 100 and 80 Ma using the approximation formula after *Parsons and McKenzie* [1978] for typical water depth values of 4000 and 3000 m.

### 5.7.3 Estimation and implication of gas emissions during LIP formation

Estimations of gas emission volumes and rates of Large Igneous Provinces are sparsely published [e.g. *Caldeira and Rampino*, 1990; *Self, et al.*, 2005] although the impact of LIP formation on climate, environment and their possible correlation to mass extinctions is often discussed [e.g. *Coffin and Eldholm*, 1994; *Kerr*, 2005; *Wignall*, 2001; *Wignall*, 2005]. So far, gas emission volumes have only been estimated for continental flood basalt type LIPs but not for oceanic plateaus [e.g. *Caldeira and Rampino*, 1990; *Self, et al.*, 2005]. Such calculations are more difficult for oceanic plateaus due to their formation in a marine environment. Interactions with surrounding water such as solution or other chemical reactions are difficult to take into account. We have shown that a large part of the Agulhas Plateau possibly formed subaerially and we therefore use information from gas emissions of flood basalt provinces as a guiding example to estimate the amount of released gases during the Agulhas Plateau formation.

## The Agulhas Plateau: Structure and evolution of a Large Igneous Province

Caldeira and Rampino [1990] estimated  $6 \times 10^{10}$  moles carbon dioxide per  $\text{km}^3$  magma for the Deccan traps. Using our calculated volume of  $0.4 \times 10^6$   $\text{km}^3$  of extrusives, we can derive  $2.5 \times 10^{16}$  moles carbon dioxide, which corresponds to a mass of  $1.1 \times 10^{12}$  t. Self et al. [2005] state a value of  $13 \times 10^6$  t carbon dioxide emission per  $\text{km}^3$  of lava, which results in a total amount of  $5.4 \times 10^{12}$  t of released carbon dioxide during Agulhas Plateau formation. In comparison, the Deccan traps emitted between  $6 \times 10^{16}$  and  $2 \times 10^{17}$  mol ( $2.6$  to  $8.8 \times 10^{12}$  t) carbon dioxide [Caldeira and Rampino, 1990]. Our value for the Agulhas Plateau carbon dioxide emission is a rough estimate due to the assumptions mentioned before.

Self et al. [2005] estimated a release of  $5$  to  $10 \times 10^6$  t sulphur dioxide per  $\text{km}^3$  of magmatic material during flood basalt eruptions. Again, we use the information of a subaerial early Agulhas Plateau as a qualification to use Self et al.'s [2005] value for an estimation of sulphur dioxide amounts released during the plateau formation. Using these assumptions we calculate a release of  $2.0$  to  $4.0 \times 10^{12}$  t sulphur dioxide. Drilling and petrological analysis of the core material measuring pre- and past eruption sulphur dioxide contents [Self et al., 2005] could lead to a better estimate, but this information does not exist so far.

Carbon dioxide emission during the larger AP-NEGR-MR LIP formation was more than double that produced during the Agulhas Plateau development. However, since this amount was released in a 6 m.y. long time interval (but most likely in shorter episodes during this interval), which would correspond to  $0.4$  to  $2.0 \times 10^6$  t per year on average, it is negligible when compared to the anthropogenic carbon dioxide emission of  $\sim 10^{10}$  t per year [e.g. Saunders, 2005; Wignall, 2001; Wignall, 2005]. A comparison with the carbon dioxide release of the the Deccan traps of  $2.6$  to  $8.8 \times 10^{12}$  t [Caldeira and Rampino, 1990] demonstrates that the emission of the AP-NEGR-MR LIP ( $\sim 2.4$  to  $11.7 \times 10^{12}$  t) is of the same order of magnitude. Caldeira and Rampino [1990] calculated that carbon dioxide released by the Deccan trap basalts caused a maximum temperature increase of  $1^\circ \text{C}$  over a period of a few hundred thousand years. Consequently, the formation of the AP-NEGR-MR LIP could have caused a similar effect but possibly over a longer time scale. However, more reliable estimates for any climatic impact of this LIP complex can only be performed by deriving the timing and intensity of the volcanic eruption phases and rates from analyses of drilled rock samples.

## 5.8 Conclusions

The Agulhas Plateau consists of 20 km thick crust. Intrabasement reflections identified in the seismic reflection records were interpreted as volcanic flows which make up the upper part of the crust with seismic velocities of 4.1 km/s on average. In the middle crust average P-wave velocities of 6.0 km/s are modelled. The lower crust has an average velocity of 7.2 km/s, where the lower 10 km of the crust show high velocities between 7.0 and 7.6 km/s. This velocity-depth structure leads to the conclusion that the Agulhas Plateau consists of overthickened oceanic crust. A small part of the lower crust shows lower velocities than the surrounding areas. Due to these velocities small continental fragments are possible there, but unlikely due to plate-tectonic reasons. The Agulhas Plateau shows a similar velocity-depth structure as oceanic LIPs and consists of the same structural units: an extrusive cover, an intruded middle part and a lower crustal body. This implies that the Agulhas Plateau is a Large Igneous Province of oceanic affinity.

A plate-tectonic reconstruction was used to demonstrate a likely joint formation of Agulhas Plateau, Northeast Georgia Rise and Maud Rise with the Bouvet triple junction in the centre of the LIP. It is possible that an interaction between the Bouvet triple junction and the Bouvet hotspot caused the formation of this LIP, which was fragmented due to spreading processes. We estimated the beginning of the LIP generation at  $100 \pm 5$  Ma and the end at  $94 \pm 5$  Ma. Graben-like structures on the northern Agulhas Plateau were interpreted as remnant structures caused by extensional forces which acted during the fragmentation of the AP-NEGR-MR LIP. Any extensional features on the central-southern plateau were overprinted by later phases of magmatism.

We used two perpendicular velocity-depth models of the Agulhas Plateau to estimate its total volume to be  $4.1 \times 10^6$  km<sup>3</sup> and the excess crustal volume to be  $2.7 \times 10^6$  km<sup>3</sup>. The extruded part of the excess volume is  $0.4 \times 10^6$  km<sup>3</sup> and the volume of the intruded/LCB materials is  $2.3 \times 10^6$  km<sup>3</sup>. Thermal subsidence calculations suggest that major parts of the Agulhas Plateau have probably formed subaerially, causing a direct emission of released volcanic gases into the atmosphere. Knowing the volume of the extrusive component, we estimate carbon dioxide ( $1.1$  to  $5.4 \times 10^{12}$  t) and sulphur dioxide ( $2.0$  to  $4.0 \times 10^{12}$  t) emission during Agulhas Plateau formation. Although an interpretation is difficult because emission rates are more important than the total amount of emitted gases, these values provide an interesting input to the discussion of climate impact of LIPs as estimations of gas emissions of individual LIPs have been put forward rarely in the past.

## ***Acknowledgements***

We acknowledge the cooperation of Captain L. Mallon, the crew of RV Sonne and the AWI geophysics team who made it possible to collect the seismic data during cruise SO-182. We would like to thank the reviewers James Mechie and Frauke Klingelhöfer for their detailed, valuable and fast reviews, which helped to improve this manuscript. We would also like to thank Matthias König for his support in compiling Figure 12 and fruitful discussions on plate tectonics, Jan Grobys and Katrin Huhn for helpful suggestions as well as David Long for an English proof read. Most figures were generated with GMT [*Wessel and Smith, 1998*]. The project AISTEK-I was funded by the German Bundesministerium für Bildung und Forschung (BMBF) under contract no. 03G0182A. This is AWI contribution No. awi-n03G0182A and Inkaba yeAfrica contribution No. 28.

## **6 Deep crustal structure of the sheared South African continental margin: first results of the Agulhas-Karoo Geoscience Transect**

Parsiegla, N., Gohl, K., Uenzelmann-Neben, G.

### ***Abstract***

The southern margin of South Africa developed as a consequence of shear motion between the African and South American plates along the Agulhas-Falkland Transform Fault during the Early Cretaceous break-up of Gondwana. The Agulhas-Karoo Geoscience Transect crosses this continental margin, and includes two combined offshore-onshore seismic reflection/refraction profiles. We present results from the western offshore profile. Using ocean-bottom seismometers and a dense airgun shot pattern, a detailed image of the velocity – depth structure of the margin from the Agulhas Passage to the Agulhas Bank was derived. Modelling reveals crustal thicknesses of between 7 km and 30 km along the profile. The upper crust has P-wave velocities of between 5.6 and 6.6 km/s and the lower crust has velocities that lie between 6.4 and 7.1 km/s. Uppermost mantle velocities range from 7.8 to 8.0 km/s. The 52 km wide continent-ocean-transition zone, where the Moho rises steeply, occurs at the Agulhas-Falkland Fracture Zone.

Beneath the Southern Outeniqua Basin and the Diaz Marginal Ridge, a zone of relatively low velocities ( $\approx 5$  km/s) with a thickness of up to 3 km, can be discerned in the upper crust. We interpret this zone as an old basin filled with pre-breakup metasediments, which may be related to the Cape Fold Belt. We suggest that the origin of the Diaz Marginal Ridge is bound up with the tectonic history of this basin as it exhibits a similar velocity structure. Almost no stratified sediment cover exists in the Agulhas Passage because of strong erosion due to ocean currents. The velocity structure and seismic reflection results indicate the presence of alternating layers of volcanic flows and sediments, with a mean velocity of about 4 km/s. We suggest these volcanic flows were an accompaniment of possible re-activation events of parts of the Agulhas-Falkland Fracture Zone. Tectonic motion seems to be sub vertical instead of strike-slip along the re-activated part of the fracture zone. Therefore, a relation to the uplift of the South African crust may be possible.

## Keywords

South African continental margin; sheared margin; crustal structure; fracture zone; Gondwana break-up; seismic refraction data; seismic reflection data; Agulhas-Karoo Geoscience Transect

## 6.1 Introduction

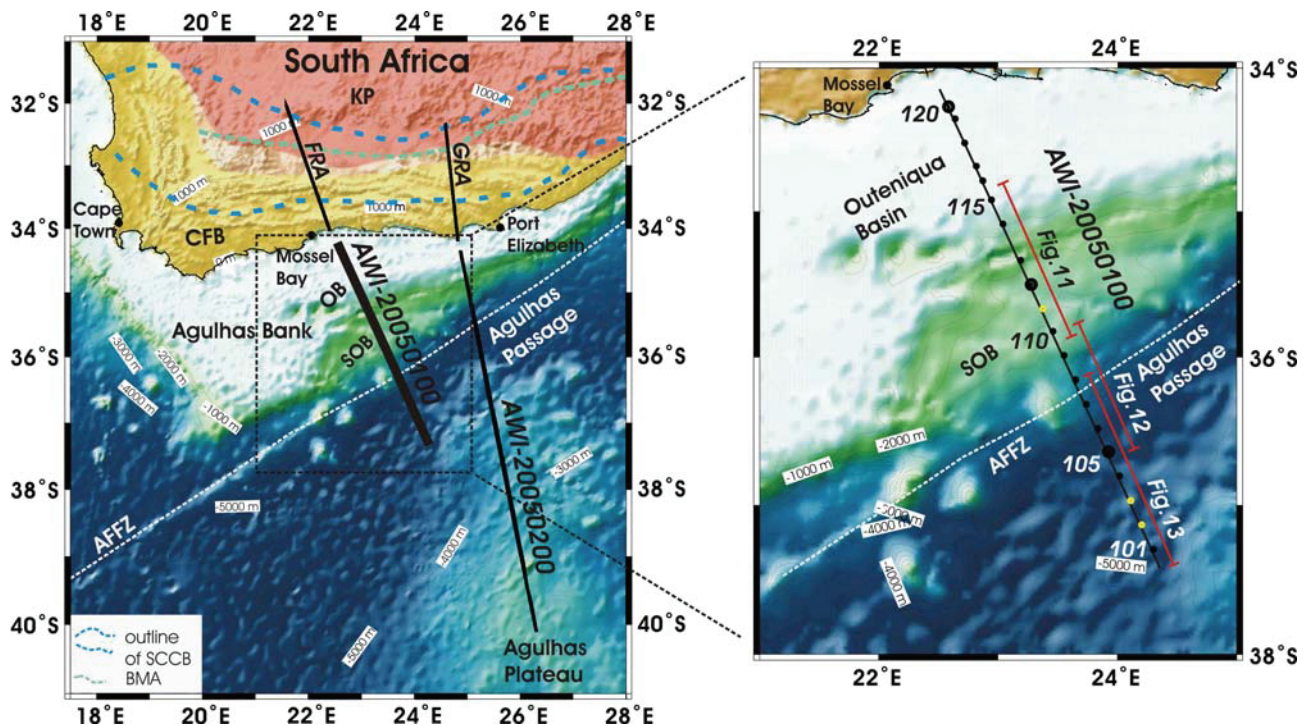


Figure 6-1: In the overview map (left) the satellite derived topography (Sandwell and Smith, 1997) of the area of investigation is shown. Offshore (AWI-20050100, AWI-20050200) and onshore (FRA, GRA) seismic lines of the Agulhas-Karoo Geoscience transect are plotted as black lines. The Agulhas-Falkland Fracture Zone (AFFZ) is marked with a white dashed line. The Cape Fold Belt (CFB) is drawn as a yellow area and the Karoo Province (KP) in light red on the map. The position of the Southern Cape Conductivity Belt (SCCB) is outlined by a blue dashed line and the location of the Beattie Magnetic Anomaly (BMA) is sketched by a green line (positions after de Beer et al., 1982). Abbreviations are OB = Outeniqua Basin, SOB = Southern Outeniqua Basin, which is part of the OB. In the enlargement (right) the shot profile AWI-20050100 is shown as black line and positions of ocean-bottom seismometers (OBS) on the profile are marked with points. Thick points mark OBS whose data are shown in Figure 6-4, Figure 6-5, and Figure 6-6. Yellow points mark OBS which did not record data. Red bars illustrate the positions of coincident seismic reflection sections on the OBS profile, which are shown in Figure 6-12, Figure 6-13, and Figure 6-11.

## Deep crustal structure of the sheared South African continental margin

Continental accretion and break-up processes can be traced back over more than 3.5 billion years in southern Africa and along its margins. The Agulhas-Karoo Geoscience Transect is part of the Inkaba yeAfrica framework project [*de Wit and Horsfield, 2006*] and is an onshore-offshore transect crossing the southern continental margin of South Africa starting in the Karoo Province, passing through the Cape Fold Belt (CFB), the Agulhas Bank, the Agulhas-Falkland Fracture Zone (AFFZ) and the Agulhas Plateau (Figure 6-1). This transect offers an unprecedented opportunity to address many different objectives concerning South Africa and its southern continental margin, applying seismic reflection and refraction, magneto-telluric, petrological, geological and geochemical methods. The main objectives of the onshore part of the survey are the identification of the sources of the Beattie Magnetic Anomaly and the Southern Cape Conductivity Belt [*Weckmann, et al., 2007*], and an explanation of the history of the CFB [*Stankiewicz, et al., 2007*]. Offshore, the structure and formation of the AFFZ and adjacent basins, and the evolution of the Agulhas Plateau and its crustal structure including its volume, age and magmatic source are addressed. The entire transect is a unique opportunity to use multidisciplinary data to create an overarching model of the architecture and dynamics of this margin. This model supplies new insights into the break-up of Gondwana in this region, the possible causes of the epeirogenic uplift of southern Africa, and the geodynamic processes that shaped the sheared continental margin.

Using seismic refraction and reflection data from the western of two offshore seismic lines (Figure 6-1), this contribution provides new detailed information on the crustal structure of the sheared South African continental margin. We discuss results with reference to the deep structure of the Outeniqua Basin, the composition of the Diaz Marginal Ridge, and the tectonomagmatic evolution of the AFFZ.

### **6.2 Tectonic framework**

The South Atlantic formed due to rifting and seafloor spreading during the break-up of Gondwana in the Early Cretaceous [e.g. *Barker, 1979; Ben-Avraham, et al., 1997*]. At the same time, shear processes along the Agulhas – Falkland Transform (AFT) caused the development of the southern margin of South Africa. Right-lateral strike-slip motion separated the African from the South American continent along this transform, which had a maximum ridge-ridge offset of 1200 km [*Ben-Avraham, et al., 1997*]. Due to a series of ridge jumps [*Barker, 1979; Tucholke, et al., 1981*] the offset has been reduced to

## Deep crustal structure of the sheared South African continental margin

about 290 km at the present day (Figure 6-2). The present Agulhas-Falkland Transform is an intraoceanic feature located between 46.3° S, 10.0° W and 46.9° S, 13.3°W (Figure 6-2) that separates the South American and African arms of the Agulhas-Falkland Fracture Zone from each other. South of the African continent, the AFFZ can be divided into four parts, from southwest to northeast: the Mallory Trough segment, Diaz Ridge segment, East London segment and Durban segment [Ben-Avraham, et al., 1997] (Figure 6-2). Ben-Avraham et al. [1995] interpreted disturbed seafloor in the eastern part of the Diaz Ridge segment as evidence for a renewal of tectonic activity in the Quaternary. The causes of the initial development of such a long offset transform boundary are still poorly understood.

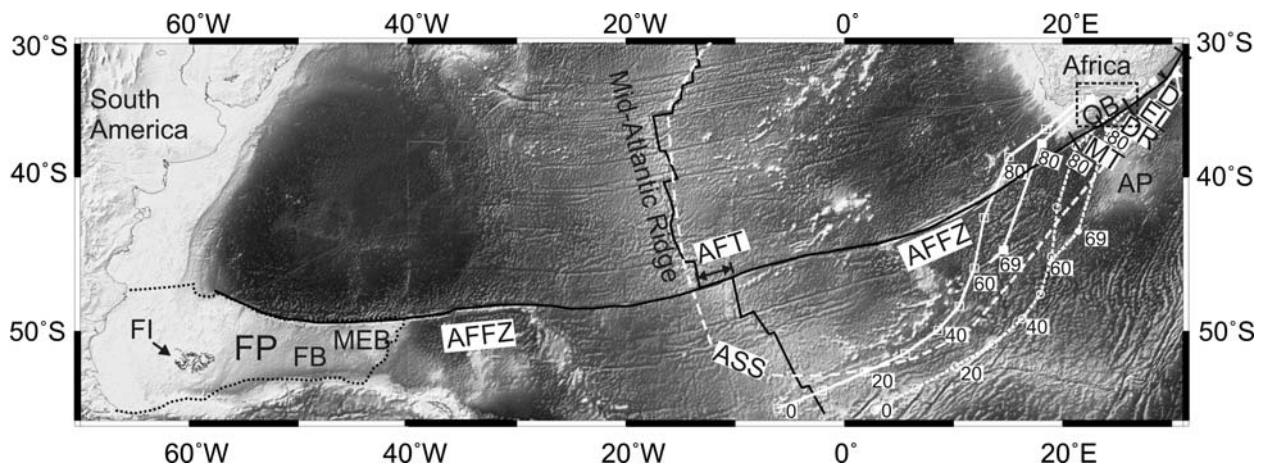


Figure 6-2: Satellite derived topography map (Sandwell and Smith, 1997) illustrating the tectonic setting. The white dashed line encircles the African Superswell (ASS). Tracks of the Shona hotspot (filled squares with solid lines according to Martin [1987]; open squares with solid lines according to Hartnady and le Roex [1985]) and the Bouvet hotspot (filled circles with dashed lines according to Martin [1987]; open circles with dashed lines according to Hartnady and le Roex [1985]) are shown and numbers refer the time in Ma when the hotspot is assumed to have reached that position. Abbreviations are FP = Falkland Plateau, FB = Falkland Basin, FI = Falkland Islands, MEB = Maurice Ewing Bank, AFT = Agulhas-Falkland Transform, MT = Mallory Trough segment, DR = Diaz Ridge segment, EL = East London segment, D = Durban segment. A detailed view of the Outeniqua Basin, as outlined in the dashed square, is shown in Figure 6-3.

## Deep crustal structure of the sheared South African continental margin

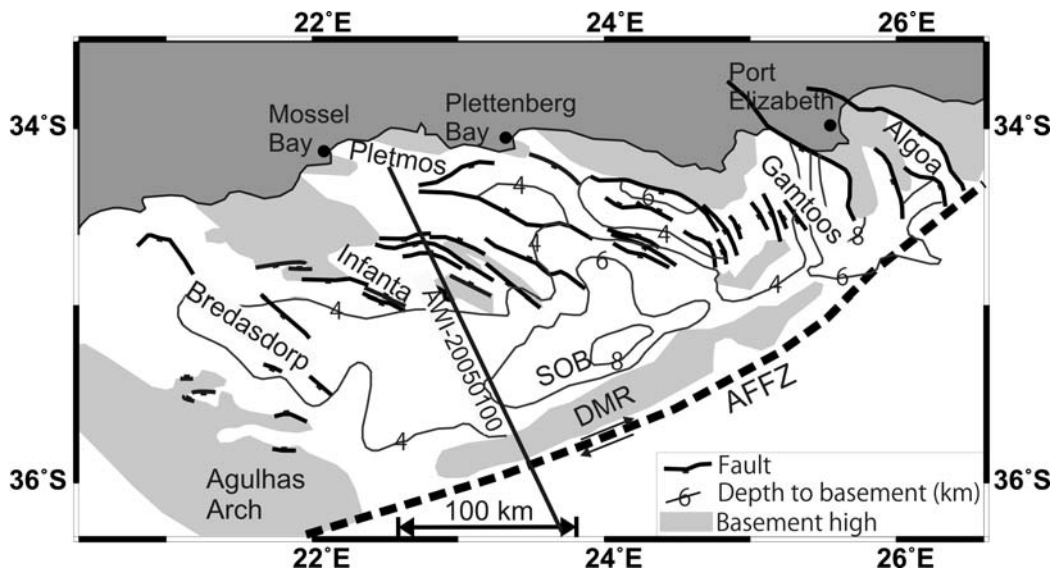


Figure 6-3: Map of the Outeniqua Basin adapted from Petroleum Agency SA (2003) showing its sub-basins (Bredasdorp, Infanta, Pletmos, Gamtoos, Algoa, and Southern Outeniqua Basin), dominant faults, and basement heights.

Complex basins and marginal ridges are typical features of sheared margins [Bird, 2001]. North of the AFFZ the Outeniqua Basin is a complex network of sub-basins (Figure 6-3). From west to east, the northern part of the Outeniqua Basin comprises the Bredasdorp, Infanta, Pletmos, Gamtoos and Algoa sub-basins (Figure 6-3). These basins are separated from each other by basement arches and faults [McMillan, et al., 1997] (Figure 6-3). The margin-parallel Southern Outeniqua Basin (SOB) lies between these sub-basins and the Diaz Marginal Ridge (DMR) (Figure 6-3). From the observation of great depths to acoustic basement (Figure 6-3), Ben-Avraham et al. [1997] concluded that the Outeniqua Basin is either underlain by oceanic or highly stretched continental crust. Reconstructions of the Falkland Plateau to its former position at the South African margin show that the Southern Outeniqua Basin and the Falkland Plateau Basin between Maurice Ewing Bank and the Falkland Island platform (Figure 6-2) were originally juxtaposed across the AFFZ [Ben-Avraham, et al., 1997; Martin, et al., 1981].

The DMR, which borders the Outeniqua Basin to the south, is usually described as a basement ridge [e.g. Scrutton, 1979] although it has no strong magnetic intensity field signature [Ben-Avraham, et al., 1993]. Ben-Avraham et al. [1993] discuss three possible compositions of the DMR; upward faulted continental basement, sedimentary rocks deformed during movement along the AFFZ, and extruded volcanic rocks. Ben-Avraham et al. [1993] prefer the second explanation, based on interpretation of seismic reflection results.

### **6.3 Seismic data acquisition**

In April-May 2005, the Alfred Wegener Institute of Polar and Marine Research (AWI) together with the Geoforschungszentrum Potsdam (GFZ) conducted a combined land-sea seismic experiment in southern Africa (Figure 6-1). During RV *Sonne* cruise SO-182, AWI acquired marine seismic reflection and refraction/wide-angle reflection data [Uenzelmann-Neben, 2005] along two sub-parallel profiles (*AWI-20050100* and *AWI-20050200*) across the southern continental margin of South Africa. Eight G.Guns™ and one Bolt airgun, with a total volume of 96 litres, were fired every 60 seconds, corresponding to a shot spacing of approximately 150 meters. The seismic reflection equipment consisted of a 180-channel streamer of 2250 m active length. The 457 km long western profile, *AWI-20050100*, starts in the Agulhas Passage, crosses the Agulhas-Falkland Fracture Zone, and carries on across the Outeniqua Basin and the Agulhas Bank (Figure 6-1). Along this profile, AWI deployed twenty ocean-bottom seismometers (OBS) with an average spacing of 20 km (Figure 6-1). The profile was extended landward by the GFZ [Stankiewicz, *et al.*, in press-b], using 48 seismic stations spaced over a distance of 240 km. Most of the OBS records produced good to very good data quality. P-wave arrivals with maximum offsets of up to 200 km can be traced on the vertical component sections.

Multibeam bathymetry and sub-bottom profile data were recorded by SIMRAD and Parasound systems onboard RV *Sonne*.

### **6.4 Data processing**

All OBS data were corrected for clock drift and converted into SEG-Y format. The data were corrected for discrepancies between the surface deployment positions and the final OBS location on the seafloor using the direct water arrivals at the OBS stations. The offset corrections were small on the continental shelf – only a few tens of meters – but significantly higher (a few hundreds of meters) in the Agulhas Passage due to strong currents. No deconvolution processing was applied as tests suggested there was no obvious improvement to the signal-to-noise ratio. During P-wave travel time picking, a bandpass filter (4-17 Hz) and automatic gain control with a 0.5 seconds window were applied. We picked the travel times of refracted and wide-angle reflected phases as parameters for a velocity-depth model.

## Deep crustal structure of the sheared South African continental margin

Seismic reflection data were processed to depth-migrated sections. The acoustic basement was picked from the depth-migrated reflection section and used to constrain the velocity-depth model of the refraction data.

### 6.5 Data and modelling

Data from 17 of the 20 stations of profile *AWI-20050100* were used for modelling (Figure 6-1). These data show refracted and reflected P-wave arrivals from the crust and upper mantle (Table 6-1).

Phase index	Type	Layer
P <sub>1</sub>	refracted wave	1 <sup>st</sup> model layer (sediments and sedimentary rocks)
P <sub>2</sub>	refracted wave	2 <sup>nd</sup> model layer (sedimentary rocks, metasediments ...)
P <sub>c1</sub> P	reflected wave	top of 3 <sup>rd</sup> model layer (upper crust)
P <sub>g1</sub>	refracted wave	3 <sup>rd</sup> model layer (upper crust)
P <sub>c2</sub> P	reflected wave	top of 4 <sup>th</sup> model layer (middle and lower crust)
P <sub>g2</sub>	refracted wave	4 <sup>th</sup> model layer (middle and lower crust)
P <sub>m</sub> P	reflected wave	top of 5 <sup>th</sup> model layer (mantle)
P <sub>n</sub>	refracted wave	5 <sup>th</sup> model layer (mantle)

Table 6-1: Phase indexes used in text and figures.

Phases refracted in the uppermost layer (P<sub>1</sub>; Figure 6-4) are not found on all records because they were often masked by direct water arrivals. Reflection phases from the acoustic basement in the seismic reflection sections provided additional constraints for this layer. The model layer below is defined by refracted arrivals (P<sub>2</sub>; Figure 6-4, Figure 6-5) at almost all stations, with the exception of stations 101 and 104 in the southern part of the profile. Wide-angle reflections from the top of the upper crustal layer (P<sub>c1</sub>P) define the downward extent of the second layer. These arrivals are often of low amplitude and hence were picked at just five stations. All stations show refracted arrivals from the upper crust (P<sub>g1</sub>; Figure 6-4, Figure 6-5, Figure 6-6). Reflections (P<sub>c2</sub>P; Figure 6-5, Figure 6-6) recorded at five stations define the boundary between the upper crust and the lower crust. Refractions from the lower crust (P<sub>g2</sub>; Figure 6-5, Figure 6-6) are sparse in the northern part of the profile, due to their long offsets. On the southern part of the profile, all data show arrivals from the lower crust. Locally it is difficult to distinguish P-wave arrivals from the upper crust

## Deep crustal structure of the sheared South African continental margin

from those of the lower crust because of changes in the gradient of the travel time branch due to topography. Upper mantle refraction phases ( $P_n$ ; Figure 6-4, Figure 6-5) are identifiable at seven stations and wide-angle reflections from the Moho ( $P_mP$ ; Figure 6-4, Figure 6-5, and Figure 6-6) with strong amplitudes are observed at 14 stations.

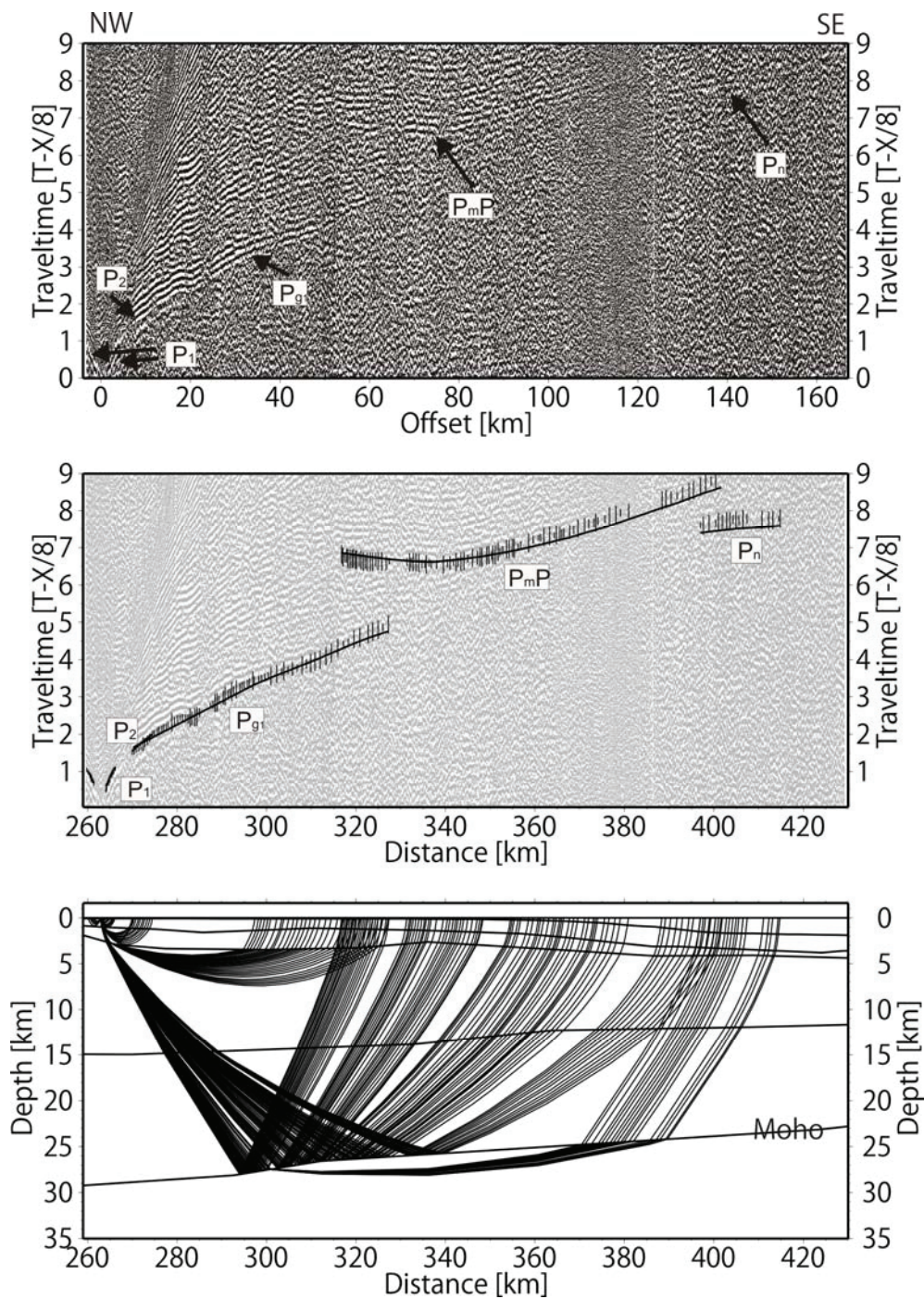


Figure 6-4: Seismic refraction data of OBS site 120. From top to bottom, the seismogram, picks and modelled travel time curves, and raypaths are shown.

Deep crustal structure of the sheared South African continental margin

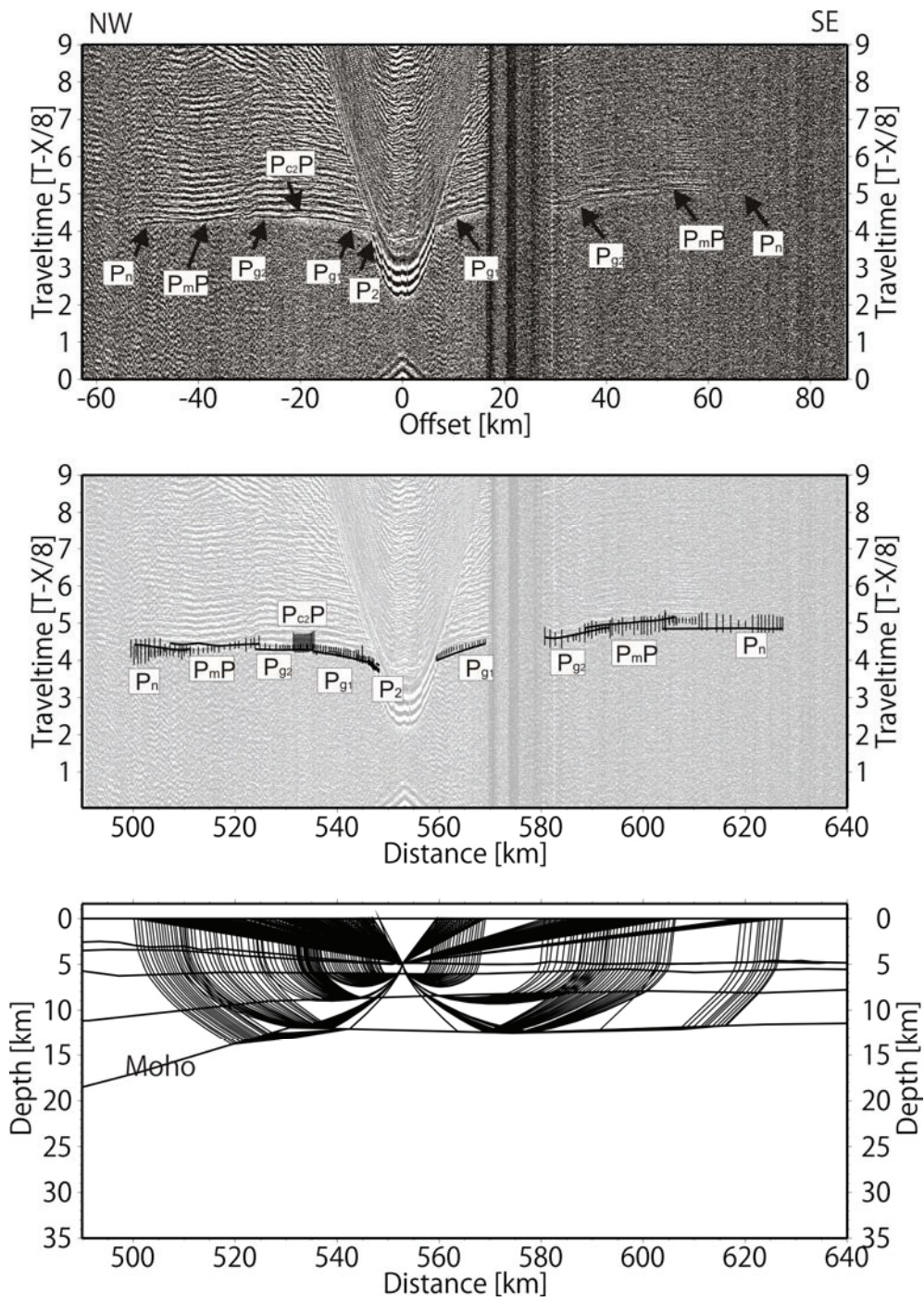


Figure 6-5: As Figure 6-4 with seismic refraction data of OBS site 105.

## Deep crustal structure of the sheared South African continental margin

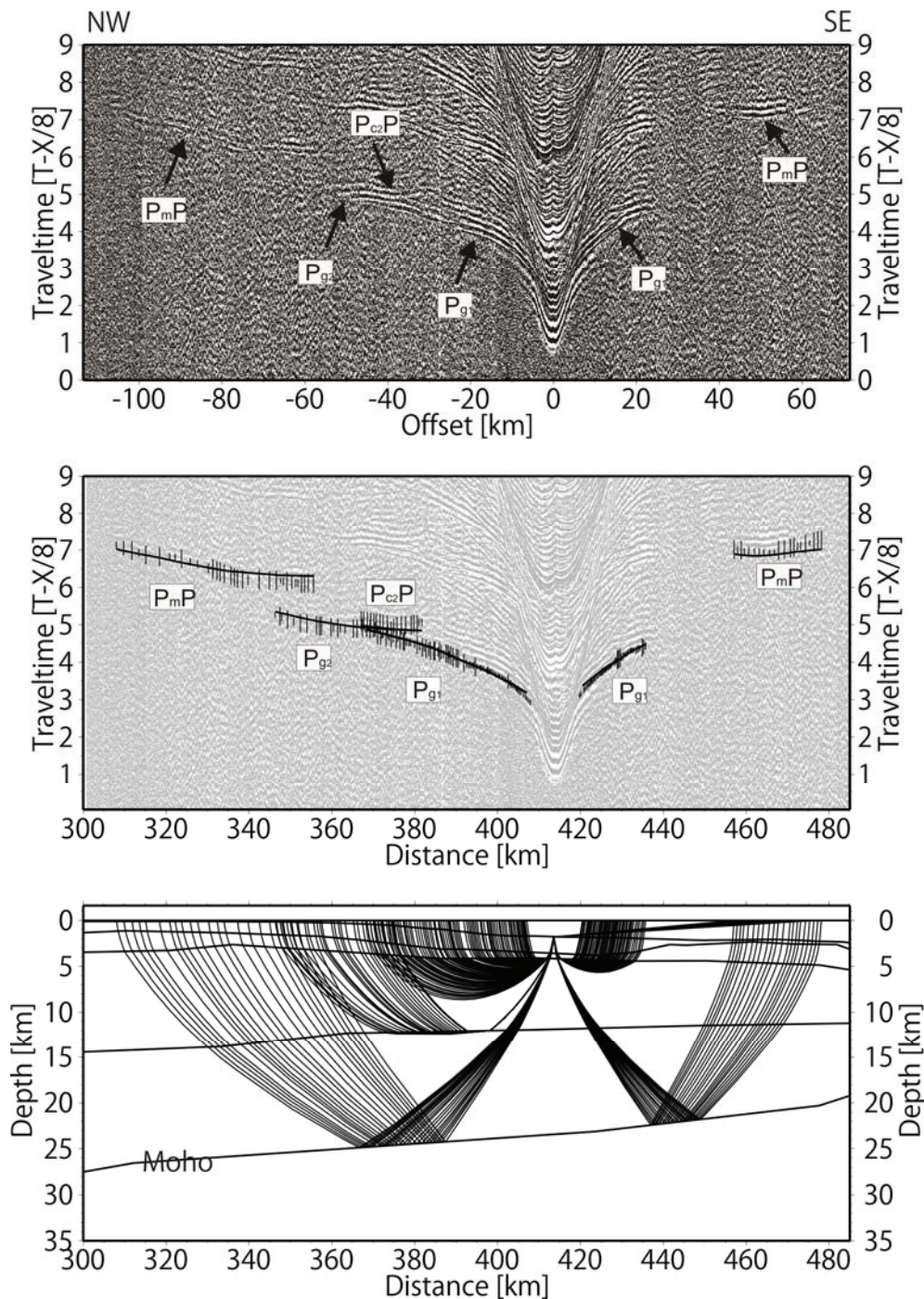


Figure 6-6: As Figure 6-4 with seismic refraction data of OBS site 112.

Modelling of the seismic refraction data was performed using the 2-D traveltimes inversion routine of [Zelt and Smith, 1992]. Their algorithm was applied assuming a sub-horizontal, laterally-continuous layering using velocity and depth nodes for parameterisation of these layers. Station and shot locations were projected onto a line fitted through the OBS positions starting at the first land station and ending at the last shot point. This leads to a total onshore-offshore profile length of 660 km, of which the offshore part is considered here.

## Deep crustal structure of the sheared South African continental margin

Pick uncertainties in the range from 40 ms to 125 ms were assigned to the picked arrival times, depending on the signal-to-noise ratio. These values were higher than the true pick uncertainty, but encompass the additional uncertainties in the discrimination of different phases with similar travel times.

A simple starting model was developed incorporating one water layer, two layers with velocities typical for sedimentary rocks, two crustal layers and the mantle. Picks from the acoustic basement in our seismic reflection sections and information from onboard bathymetry measurements were included in the layer parameterisation. Using a forward modelling technique, the initial model was improved, layer by layer, from top to bottom. The resulting model was input into travel time inversion code [Zelt and Smith, 1992], in which the differences between the observed and calculated travel times are iteratively minimised by adjustment of the velocity and depth parameters. A layer stripping approach, in which we invert for velocity and depth nodes of the first layer until a satisfactory fit is obtained, was applied. These parameters were kept fixed when inverting for the depth and velocity of the second layer. This process is repeated until all values were adjusted in order to obtain a sufficient fit.

### **6.6 Velocity-depth structure from the Agulhas Bank to the Agulhas Passage**

The final velocity-depth model of the profile *AWI-20050100* (Figure 6-7) consists of six layers. The water layer (layer 0) has a velocity of 1.5 km/s and thicknesses ranging from 0.1 to 5 km. Beneath this, layer 1 with P-wave velocities between 1.7 and 3.0 km/s, and a thickness of up to 2 km, can be observed from the continental shelf to the Southern Outeniqua Basin. These velocities suggest this layer consists of sediments. South of the Outeniqua Basin, this layer thins out and disappears in the Agulhas Passage. There, layer 2 with velocities between 3.0 – 5.0 km/s, and which can be found along the entire profile, crops out at the seafloor. Beneath this, the upper crust (layer 3) is modelled with velocities between 5.6 and 6.6 km/s. We modelled average velocities of between 6.4 and 7.1 km/s for the lower crust (layer 4), and uppermost mantle (layer 5) velocities of 7.8 to 8.0 km/s. The observed crustal thickness (including sediments) along the profile varies from 30 km on the inner continental shelf to 7 km in the Agulhas Passage.

## Deep crustal structure of the sheared South African continental margin

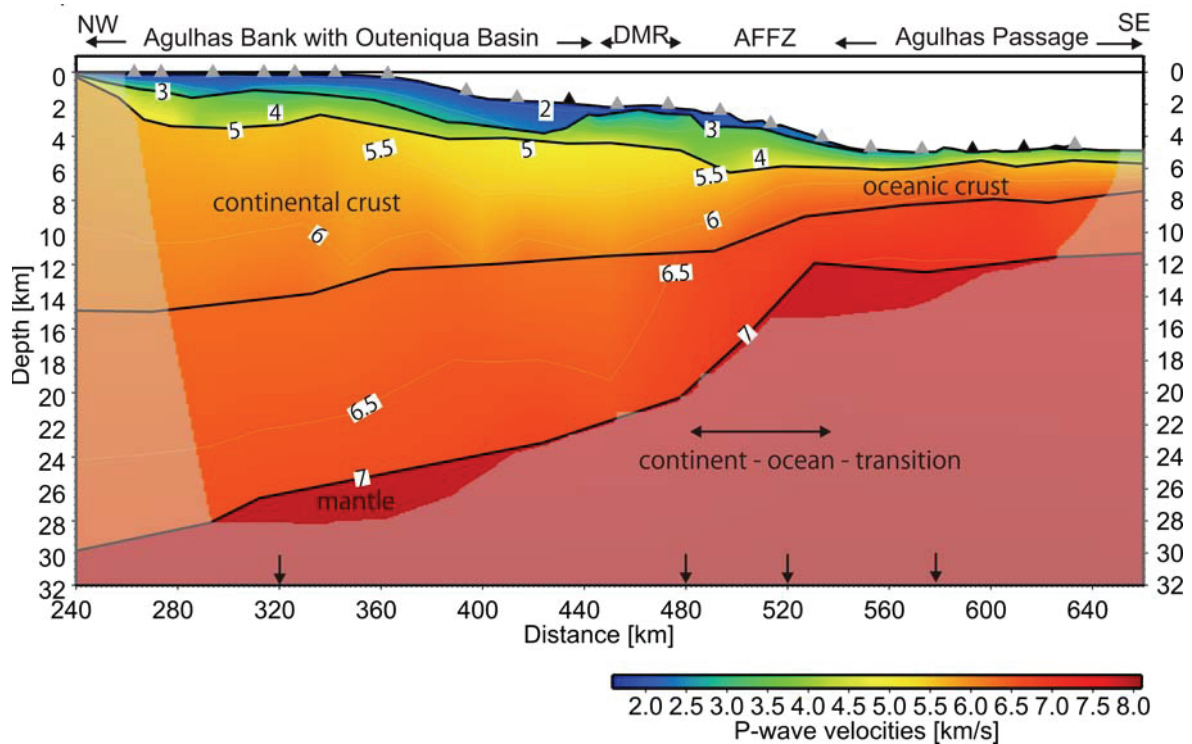


Figure 6-7: P-wave velocity model of profile AWI-20050100. Gray triangles mark positions of ocean-bottom seismometers. Arrows at base of figure show positions, where average crustal velocities (without 1<sup>st</sup> and 2<sup>nd</sup> model layer) were calculated. They are as follows  $v_{av} = 6.19$  km/s (at 320 km model distance), 6.26 km/s (at 480 km), 6.50 km/s (at 520 km), 6.64 km/s (at 580 km). DMR is abbreviation for Diaz Marginal Ridge. Numbers on white isolines refer to seismic P-wave velocities. Black lines represent model layer boundaries.

### 6.6.1 Agulhas Bank (with Pletmos Basin)

On the Agulhas Bank, the crustal thickness ranges between 26 and 30 km (Figure 6-7). A layer with P-wave velocities between 1.7 and 3.0 km/s and a thickness of 1.5 km lies on top of a 0.8 - 2.5 km thick layer with velocities between 3.0 and 5.0 km/s (Figure 6-1). The upper crust exhibits velocities of between 5.5 and 6.3 km/s. Modelled lower crustal velocities vary between 6.3 and 6.6 km/s.

### 6.6.2 Southern Outeniqua Basin and the Diaz Marginal Ridge

The uppermost crustal layer is up to 2 km thick with velocities ranging from 1.7 to 2.9 km/s (Figure 6-7). These southeastward dipping, well-stratified sediments were deposited north of the Diaz Marginal Ridge, filling the Southern Outeniqua Basin (Figure 6-12). The oldest datable sediments drilled in the Outeniqua Basin are from the Kimmeridgian, at 151-154 Ma [McMillan, et al.,

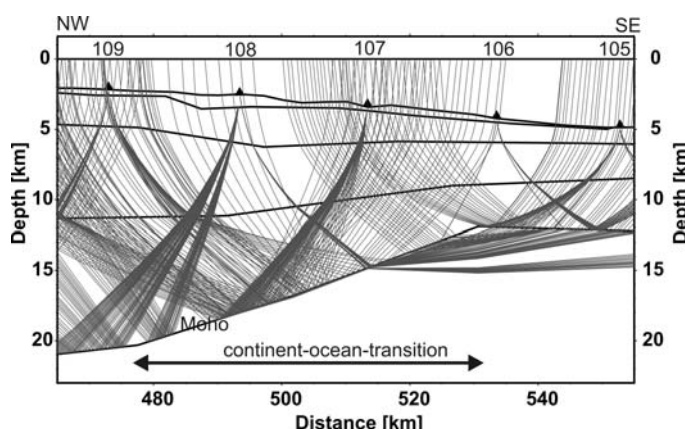
## Deep crustal structure of the sheared South African continental margin

1997]. A 0.5 - 1.5 km thick layer with seismic velocities averaging 4 km/s is located beneath the sediments of the Southern Outeniqua Basin. This layer continues beneath the Diaz Marginal Ridge, albeit with a broader range of velocities, from less than 3 km/s to more than 4 km/s. A sediment cover of 0.5 km thickness buries the ridge.

A broad, thick region (130 km in north-south direction and up to 3 km thick) with velocities in the range of 5.0 – 5.5 km/s occurs beneath the Southern Outeniqua Basin and the Diaz Marginal Ridge in the upper crust. The lower crust is modelled with velocities between 6.2 and 6.7 km/s. The thickness of the crust underlying the Southern Outeniqua Basin declines from 25 km in the north to 22 km in the south. Beneath the Diaz Marginal Ridge, the crust thins from 22 km to 19 km thick.

### 6.6.3 Agulhas-Falkland Fracture Zone

At the Agulhas-Falkland Fracture Zone, we observe a 0.5 to 1 km thick layer with sedimentary P-wave velocities (Figure 6-7) lying on top of a 2 km thick layer with average velocities of 4 km/s. In the upper crust, the P-wave velocities range from 5.5 to 6.4 km/s. Velocities between 6.6 and 6.8 km/s dominate the lower crust. A north-to-south increase in seismic velocities is observed at the AFFZ. The model shows lines of equal velocity curving upwards, which means that P-waves travel faster in shallower regions than they do farther north. A distinct Moho incline of about 10° to the southeast, which is well constrained by good ray coverage (Figure 6-8), is observed at 476 km



model distance. The Moho becomes almost horizontal again at 530 km.

Figure 6-8:  $P_mP$  and  $P_n$  raypaths at continent-ocean-transition. OBS numbers are annotated on top of figure.

### 6.6.4 Agulhas Passage

Stratified sediments are only thin or absent in the Agulhas Passage (Figure 6-7). The second model layer, with velocities between 3.0 and almost

## Deep crustal structure of the sheared South African continental margin

5.0 km/s, crops out at the seafloor. Upper crustal velocities range from 5.7 to 6.6 km/s, and lower crustal velocities range from 6.6 to 7.1 km/s. The crust in the region of the Agulhas Passage is significantly thinner at 7 km than in all other parts of the profile. The Moho is almost flat-lying, forming just a small depression between 550 and 600 km model distance, where overlying velocities of up to 7.1 km/s are modelled.

### 6.7 Model quality

The quality of the model (Table 6-2) is assessed using statistical parameters such as the normalised misfit parameter  $\chi^2$ , the root-mean-squared (rms) travel time residual of the fits, and the numerical resolution of the model [Zelt and Smith, 1992].

When  $\chi^2 = 1$ , the data have been fitted within their assigned uncertainties, whereas  $\chi^2 < 1$  indicates that the data are overfitted, i.e. more tightly than warranted by the picks' uncertainties [Zelt and Forsyth, 1994].  $\chi^2 > 1$  indicates that small-scale features sampled by the data have probably not been resolved [Zelt and Smith, 1992]. For our model, the overall average  $\chi^2$  value is 0.971, meaning that the chosen uncertainties for the picks are slightly overestimated. In the second layer (Table 6-2, phase P<sub>2</sub>),  $\chi^2$  is greater than 1, which we interpret as indicating there are unresolved small-scale features and three-dimensional effects such as out-of-plane refractions. An rms-misfit value of 0.120 was obtained during modelling, which is within the assigned uncertainty bounds of the travel time picks.

Phase	number of picks	RMS misfit [s]	$\chi^2$
All	3244	0.120	0.971
P <sub>1</sub>	116	0.072	0.803
P <sub>2</sub>	265	0.128	1.835
P <sub>c1</sub> P	57	0.188	0.962
P <sub>g1</sub>	1413	0.107	0.962
P <sub>c2</sub> P	102	0.152	0.655
P <sub>g2</sub>	438	0.119	0.790
P <sub>m</sub> P	636	0.129	0.844
P <sub>n</sub>	217	0.143	0.989

Table 6-2: Statistics of the velocity-depth model.

## Deep crustal structure of the sheared South African continental margin

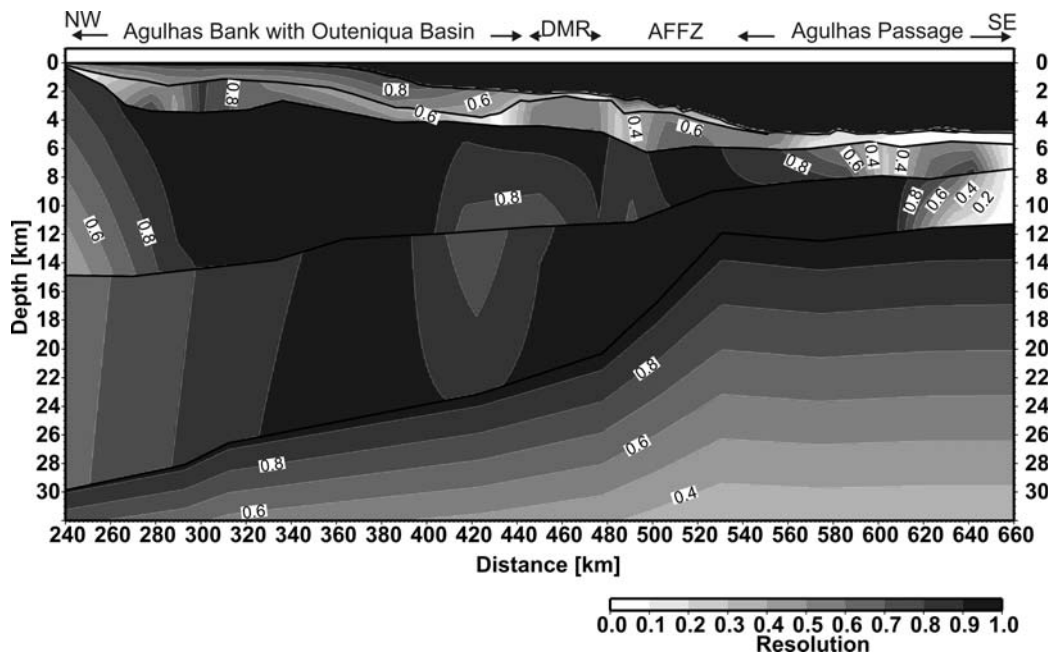


Figure 6-9: Numerical resolution of the P-wave velocity model of profile AWI-20050100.

We applied *Zelt and Smith's* [1992] travel time inversion method in order to assess the resolution of the velocity-depth model (Figure 6-9). This qualitative approach is based on the relative number of rays that determine the parameterisation of the model. Values greater than 0.5 are considered to be well-resolved [*Zelt and Smith, 1992*], which is the case for the upper sedimentary layer. Some parts of layer 2 have a resolution of less than 0.5, including two small zones north and south of the Diaz Marginal Ridge. A larger numerically unresolved zone in this second layer extends from 600 km model distance to the end of the profile. In this area only, two of four stations recorded data and these returned no refracted arrivals from layer 2. This low numerical resolution, however, is dominantly caused by the model parameterisation in this region rather than the number of rays. The numerical resolution decreases because many more nodes are needed here to parameterise the pinchout of the upper sedimentary layer. On the other hand, seismic rays that travel through layer 2 into deeper layers provide indirect information on this layer. This information is confirmed by seismic reflection data. Both layers of the crystalline crust are resolved very well, having large areas with a resolution between 0.7 and 1. Only at the borders of the model do the resolution values decrease to  $< 0.5$ . Velocities in the upper mantle are numerically well resolved, although this is mainly due to the small number of nodes rather than the large number of rays.

## 6.8 Discussion

### 6.8.1 Continental and oceanic crust

Continental crust, with velocities between 5.6 and 6.3 km/s in the upper crystalline crust and 6.4 and 6.7 km/s in the lower crust (Figure 6-7), is located from the Agulhas Bank to the Agulhas-Falkland Fracture Zone (model distance 260 - 510 km, Figure 6-10). Beneath the Agulhas Bank, this continental crust has a thickness of between 24 and 30 km. The crust thins towards the south. This thinning can be attributed to extensional forces that acted during the Valanginian rifting phase in the Falkland Plateau [Richards, *et al.*, 1996] and Outeniqua Basin [Dingle, *et al.*, 1983].

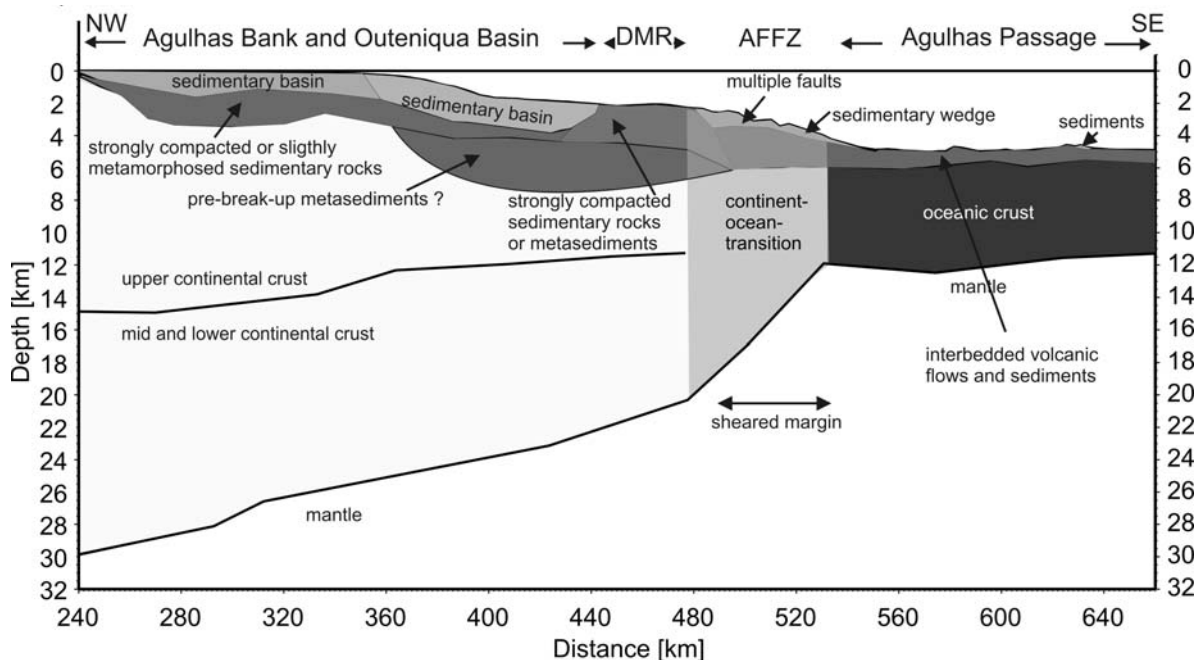


Figure 6-10: Interpreted structure of the sheared South African continental margin along profile AWI-20050100 using information from the P-wave velocity model and seismic reflection sections.

The Agulhas-Falkland Fracture Zone separates the continental side of the South African continental margin with its Agulhas Bank and Outeniqua Basin from the oceanic side with its Agulhas Passage (Figure 6-10). The transition zone from continental to oceanic crust is 52 km wide (profile distance 478 - 530 km), which is a typical value for sheared margins [Bird, 2001]. It is characterised by a sharp decrease in crustal thickness from 30 km on the continental side to 7 km on the oceanic side (upper crust: 5.7 – 6.6 km/s, lower crust: 6.7-7.1 km/s) and by a southeastward increase in average crustal P-wave velocity (Figure

6-7). The slight increase in seismic velocity (Figure 6-7) in the lower crust, especially in the southern part of the continent-ocean-transition, is interpreted as indicating the presence of magmatic intrusions. Additional thinning may have occurred as a result of the shear process itself, where such deformation would require a ductile rather than a rigid crust. In this case it would be possible that parts of the African plate were dragged along the AFFZ and bent before frictional tension was released. Evidence of such a process seems to be preserved today in the curved strikes of the bounding faults in the northern reaches of the Outeniqua Basin (Figure 6-3). The Bouvet-Shona hotspot cluster (Figure 6-2) [Ben-Avraham, *et al.*, 1997] would have produced a heat source that may have led to a more ductile rather than rigid behaviour of the plate.

### **6.8.2 A possible precursor of the Outeniqua Basin and the origin of the Diaz Marginal Ridge**

The Outeniqua Basin is a complex basin, which consists of shallow basins in the north with horst, graben and half graben structures, separated from each other by basement ridges and faults, and the deep Southern Outeniqua Basin [McMillan, *et al.*, 1997] (Figure 6-3). The Diaz Marginal Ridge blocks southward sediment transport so that sediments are trapped north of it and fill the Outeniqua Basin. The OBS profile crosses the Pletmos and Southern Outeniqua basins (Figure 6-3). The geometry of fault strikes (Figure 6-3), especially in the northern parts of the Outeniqua Basin, has been ascribed to the influence of pre-existing structures of the Cape Fold Belt [e.g. McMillan, *et al.*, 1997], whereas other authors have attributed the fault pattern to the strike-slip motion along the AFT [Ben-Avraham, *et al.*, 1993; Thomson, 1999]. We suggest a combined explanation. Some structures are possibly inherited zones of weakness, i.e. old faults of the Cape Fold Belt. These faults are likely to have been re-activated due to extensional forces causing the development of horst and graben structures. Additional faults were generated during the active episodes of the AFT in the Cretaceous. During shear motion between the African and South American plates, a ductile African crust was dragged along the AFT resulting in a bending of existing and newly developed fault structures.

## Deep crustal structure of the sheared South African continental margin

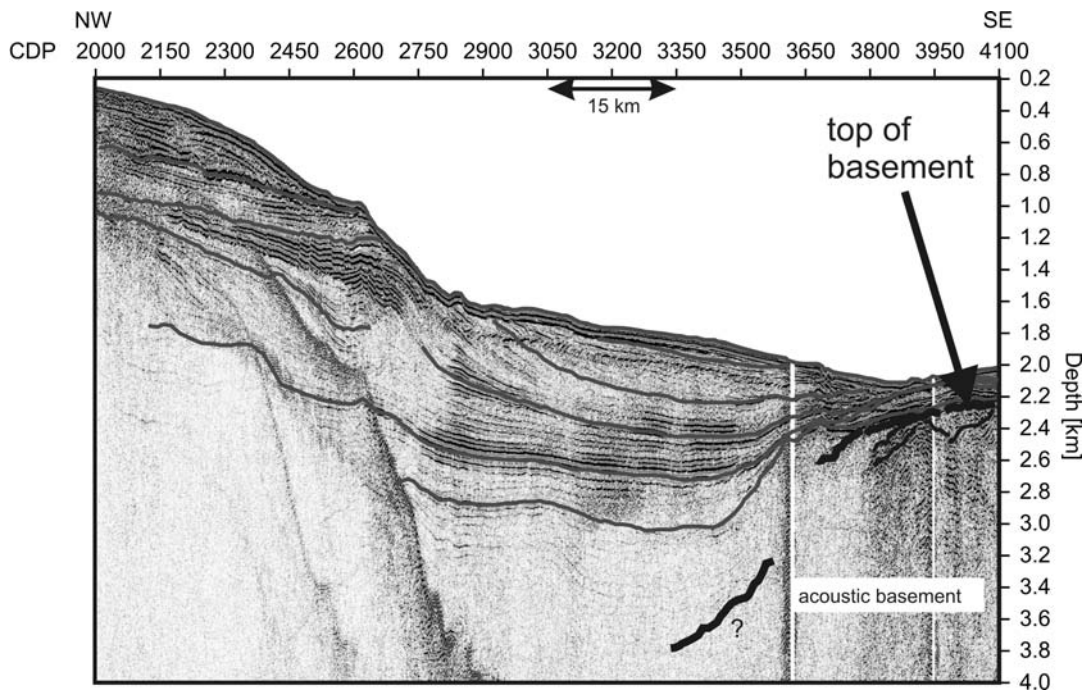


Figure 6-11: Part of the depth-migrated seismic reflection profile crossing the southern part of the Outeniqua Basin.

Beneath the Southern Outeniqua Basin and the Diaz Marginal Ridge, a 3 km thick and 130 km long zone of relatively low P-wave velocities (5.0 km/s – 5.5 km/s) is evident within the upper crust (Figure 6-7, model distance  $\approx$  360 – 490 km, model depth  $\approx$  4.5 km). This suggests the presence of either sedimentary rocks (e.g. sandstone, limestone, and dolomite) or metamorphic rocks (e.g. gneiss, marble, and schist) as these rock types have velocities in this range [Schön, 1983]. Further S-wave modelling and the derivation of Poissons ratios will help to narrow down the variety of possible rocks. Dingle *et al.* [1983] reviewed the sedimentary structure of the Agulhas Bank from results of wide angle reflection and refraction studies and reported three layers with mean P-wave velocities of 2.0, 3.4 and 4.6 km/s. We suggest that the observed velocities of around 5 km/s originate from sedimentary rocks of upper Palaeozoic age, which are part of the third layer of Dingle *et al.* [1983], but which underwent further diagenesis and light metamorphism. We interpret this structure, therefore, as a precursor to the Outeniqua Basin, filled with pre-break-up metasediments (Figure 6-10). If this is correct, then before extensional forces formed the present Outeniqua Basin, an older basin (Pre-Outeniqua Basin) existed within the southern regions of the Permo-Triassic CFB. This basin was likely to have developed during the collision process that formed the CFB. Erosion of the CFB provided the sedimentary fill of the older basin. Our seismic reflection records show no obvious stratification of this infill (Figure 6-11). This suggests that the sediments of this basin were heavily deformed

## Deep crustal structure of the sheared South African continental margin

during tectonic events that shaped the South African continental margin. These processes may have also been responsible for the generation of zones of crustal weakness which were (re)activated during the extensional process and caused the development of the present Outeniqua Basin. The sedimentary rocks of the older basin may have experienced metamorphism as a result of the proximity to the Bouvet-Shona hotspot cluster.

Earlier studies [Ben-Avraham, et al., 1993] suggest that the DMR is composed of sedimentary rocks of Jurassic to Early Cretaceous age, which were deformed due to motion along the AFFZ. Our modelling (Figure 6-7) leads us to a different conclusion. The DMR can be interpreted as a former part of the Pre-Outeniqua Basin (Figure 6-10). In addition to the strike-slip motion along the AFFZ, episodes of compression and extension are likely to have occurred. Compressional forces may have pushed parts of the metasedimentary infill of the older basin upwards to form the DMR. Thus, the metasediments underwent decompression that resulted in fracturing of the sediments which in turn caused the seismic velocities to decrease to an average of 4 km/s (Figure 6-7). The lack of any significant signature in the magnetic intensity field of the DMR [Ben-Avraham, et al., 1993] supports the theory of a metasedimentary origin.

### 6.8.3 New implications for re-activation of the AFFZ and a possible explanation

Plate-tectonic reconstructions suggest an end of the tectonic activity in this region, when the active parts of the AFFZ passed to the west at  $\approx 100$  Ma [Martin and Hartnady, 1986]. Ben-Avraham [1995] suggests a possible re-activation of the AFFZ occurred in the Quaternary from observations of deformed seafloor. Ben-Avraham et al. [1995] and Ben-Avraham [1995] noted that volcanic glasses with no significant alteration and interpretations of volcanic intrusions in seismic reflection records were consistent with the idea of neotectonic activity in this region.

A depth-migrated section of the seismic reflection line (AWI-20050100) illustrates the presence of several faults at the position of the AFFZ (Figure 6-12). These faults can be followed from the basement into the overlying sedimentary layers, suggesting re-activation of parts of the AFFZ past deposition of the sediments. This younger tectonic motion along parts of the AFFZ does not necessary have to have a strike-slip nature but may be related to vertical motions of the African Superswell (Figure 6-2), a zone of anomalously elevated topography and bathymetry in southern and western

## Deep crustal structure of the sheared South African continental margin

Africa. Nyblade and Robinson [1994] suggest the elevated topography/bathymetry is a result of heating of the lithosphere. We suggest that the AFFZ may have acted as a zone of crustal weakness to accommodate the uplift process.

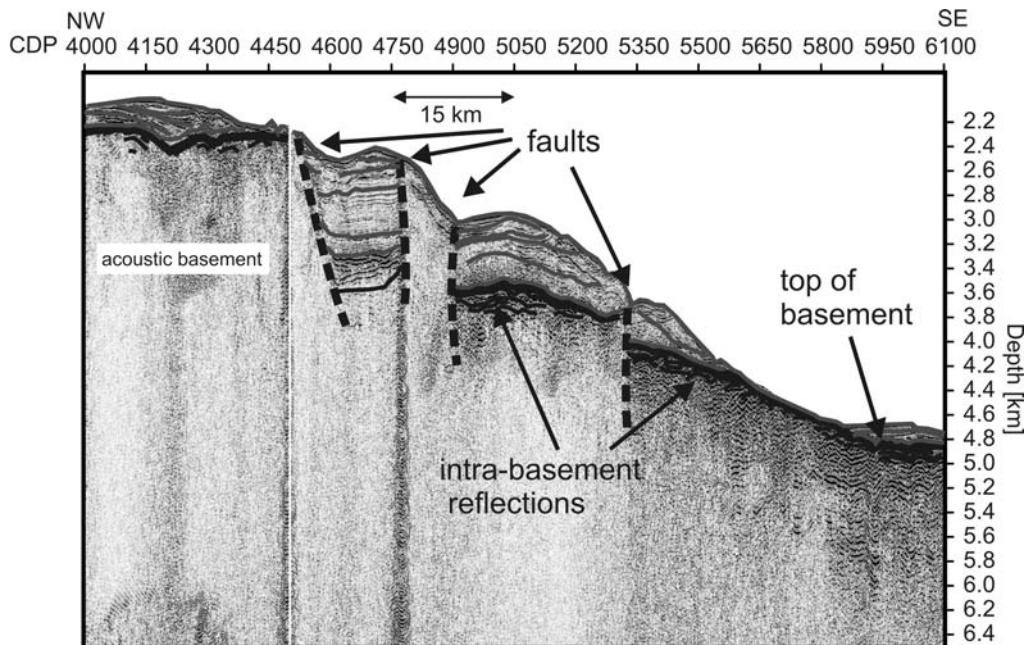


Figure 6-12: Part of the depth-migrated seismic reflection profile crossing the Agulhas-Falkland Fracture Zone.

The combination of tectonic activity in the western part of the Diaz Ridge segment of the AFFZ and reported neotectonic activity on its eastern part [Ben-Avraham, et al., 1995] leads to the conclusion that the entire Diaz Ridge segment of the AFFZ may have experienced phases of re-activation. If the neotectonic activity, for which we observe evidence on our profile, was caused by uplift processes related to the superswell, it is possible that other sectors of the AFFZ south of the African continent were also involved.

### 6.8.4 Volcanic activity in the Agulhas Passage

Stratified sediments are absent or very thin on top of the acoustic basement of the Agulhas Passage due to erosion driven by strong ocean currents [Uenzelmann-Neben, in press]. The uppermost kilometre exhibits P-wave velocities of between 3.5 and 4.5 km/s. Strong reflections within the acoustic basement can be clearly seen on the seismic reflection records (Figure 6-13). These reflections may be caused by interbedded strata of sediments and volcanic flows, because such alternating layers of sediments and volcanic flows

## Deep crustal structure of the sheared South African continental margin

could combine to explain the observed bulk velocities. Volcanic activity in the Agulhas Passage may be related to seamounts like those observed on our seismic reflection records (Figure 6-13). It is difficult to assess the timing of the volcanism as no dredge samples or other clues for the age of these seamounts are available, which in turn makes it difficult to identify the source of the volcanism. We speculate that this volcanism, like the re-activation of the AFFZ, might be attributable to uplift during heating of the lithosphere.

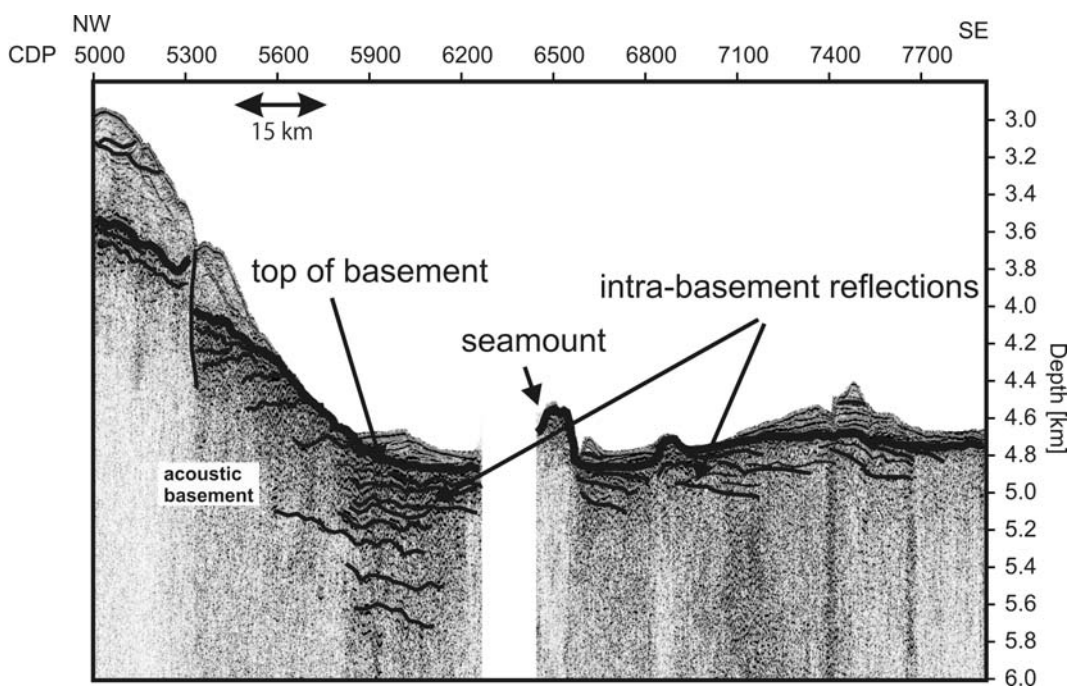


Figure 6-13: Part of the depth-migrated seismic reflection profile crossing the Agulhas Passage.

### 6.9 Conclusion

We obtained new insights into the structure and evolution of South African continental margin by modelling the western offshore seismic refraction profile of the Agulhas-Karoo-Geoscience transect. The profile provides detailed information on the seismic velocity structure of this sheared margin from the Agulhas Bank to the Agulhas Passage. Coincident seismic reflection data gives a detailed view of the uppermost kilometres along the profile.

The main results and conclusions are:

- 1) The crust along the profile thins from 30 km beneath the continental shelf to 7 km in the deep sea.

## Deep crustal structure of the sheared South African continental margin

- 2) The continent-ocean-transition is located at the AFFZ and extends over a  $\approx 52$  km wide zone that is characterised by a Moho gradient.
- 3) The seismic reflection sections show faults that continue into sediments above the AFFZ. These faults are probably caused by re-activation of the Diaz Ridge segment of the AFFZ and may be part of an even larger regime of re-activation related to thermal uplift of southern Africa.
- 4) Further indications for neotectonic and triggered volcanic activity have been identified in the Agulhas Passage. Here are indications of volcanic flows interbedded with sediments overlying basement. This volcanic activity may have accompanied the re-activation of the AFFZ.
- 5) In the upper crust beneath the Southern Outeniqua Basin and Diaz Marginal Ridge, a zone of about 130 km length and with a maximum thickness of 3 km has relatively low velocities ( $\approx 5$  km/s) compared to the adjacent basement. This region is interpreted as the metasedimentary fill of a pre-break up basin. The basin probably formed coevally with the Cape Fold Belt and was filled with sediments shed from it, which were subsequently reworked due to magmatic and tectonic processes.
- 6) The Diaz Marginal Ridge is probably neither a volcanic feature nor a crystalline basement ridge, but instead may consist of metasediments. These metasediments may have been pushed upward out of the Pre-Outeniqua Basin as a result of compressional forces.

## **Acknowledgements**

We acknowledge the cooperation of the captain and crew of RV Sonne who made it possible to collect the seismic data and thank the participants of SO-182 cruise for their support. We thank Graeme Eagles for improving the English of this manuscript. We would like to thank Gesa Netzeband and an anonymous reviewer for their helpful comments. Most of the figures were generated with the Generic Mapping Tools [*Wessel and Smith, 1998*]. The project AISTEK-I was funded by the German Bundesministerium für Bildung, Forschung und Technologie (BMBF) under contract no. 03G0182A. This is Inkaba yeAfrica contribution 9 and AWI publication no. AWI-n16537.

## **7 Crustal structure of the southern margin of the African continent: Results from geophysical experiments**

J. Stankiewicz, **N. Parsiegl**a, T. Ryberg, K. Gohl, U. Weckmann, R. Trumbull and M. Weber.

### ***Abstract***

A number of geophysical onshore and offshore experiments were carried out along a profile across the southern margin of the African Plate in the framework of the Inkaba yeAfrica project. Refraction seismic experiments show that Moho depth decreases rapidly from over 40 km inland to around 30 km at the present coast, before gently thinning out towards the Agulhas-Falkland Fracture Zone, which marks the transition zone between continental and oceanic crust. In the region of the abruptly decreasing Moho depth, in the vicinity of the boundary between the Namaqua-Natal Mobile Belt and the Cape Fold Belt, lower crustal P-wave velocities up to 7.4 km/s are observed. This is interpreted as metabasic lithologies of Precambrian age in the Namaqua-Natal Mobile Belt, or mafic intrusions added to the base of the crust by younger magmatism. The velocity model for the upper crust has excellent resolution, and is consistent with the known geological record. A joint interpretation of the velocity model with an electrical conductivity model, obtained from magnetotelluric studies, makes it possible to correlate a high velocity anomaly north of the centre of the Beattie Magnetic Anomaly with a highly resistive body.

### ***7.1 Introduction***

A number of features make southern Africa a key site for integrated geophysical and geological research on continental accretion and break-up. Bounded to the south by the Agulhas-Falkland Fracture Zone (AFFZ, Figure 7-1), this region represents one of the world's best examples of a sheared continental margin which formed during break-up of Western Gondwana from about 130 Ma [*Ben-Avraham et al.*, 1997]. At the same time, a classic volcanic rifted margin was developing at the western margin of South Africa. The deep crustal structures and physical properties on these two contrasting margin types, and the nature of the continent-ocean transition across them, are key to

## Crustal structure of the southern margin of the African continent

understanding the processes of continental break-up and passive margin development. The southern margin of Africa is also of great interest because progressively older crustal provinces are crossed as one moves inboard from the coast (Cape Fold Belt, Namaqua-Natal Mobile Belt, Kaapvaal Craton). The boundaries between these crustal provinces are first-order features relating to continental assembly and information on their 3-D geometry is largely lacking. Particularly important in this respect are the Beattie Magnetic Anomaly and the Southern Cape Conductivity Belt (Figure 7-1), which run roughly parallel to the boundary of the Cape Fold Belt and Namaqua-Natal Belt, and are among the largest and strongest geophysical anomalies on the African continent. Despite the nearly 100 years since their discovery, the geologic nature of these anomalies is still a mystery. Finally, and superimposed on the crustal mosaic, is the huge and economically important Karoo sedimentary basin of Triassic to Jurassic age and the associated lavas and sills of the Karoo Large Igneous Province (LIP) of about 175-185 Ma age.

All of these aspects are addressed in a coordinated program of marine and terrestrial geophysical experiments that has been carried out along the so-called Agulhas-Karoo Geoscience Transect extending from the Agulhas Plateau across the sheared margin and inland as far as the Kaapvaal Craton border (Figure 7-1). Beginning in 2004, this work has been one of the main research targets of the Inkaba ye Africa project [*de Wit and Horsfield, 2006*]. Seismic experiments included wide angle refraction [*Stankiewicz et al., 2007*], and near-vertical reflection [*Lindeque et al., 2007*] surveys across the Cape Fold Belt and into the Karoo Basin, magnetotelluric profiles (partially coincident with the seismic survey) across the Beattie Anomaly and Cape Conductivity Belt [*Branch et al., 2007; Weckmann et al., 2007a,b*], and offshore refraction and reflection seismics [*Parsieglä et al., 2007, 2008*]. This paper combines and jointly interprets these different data sets along the Western Karoo-Agulhas Profile.

## Crustal structure of the southern margin of the African continent

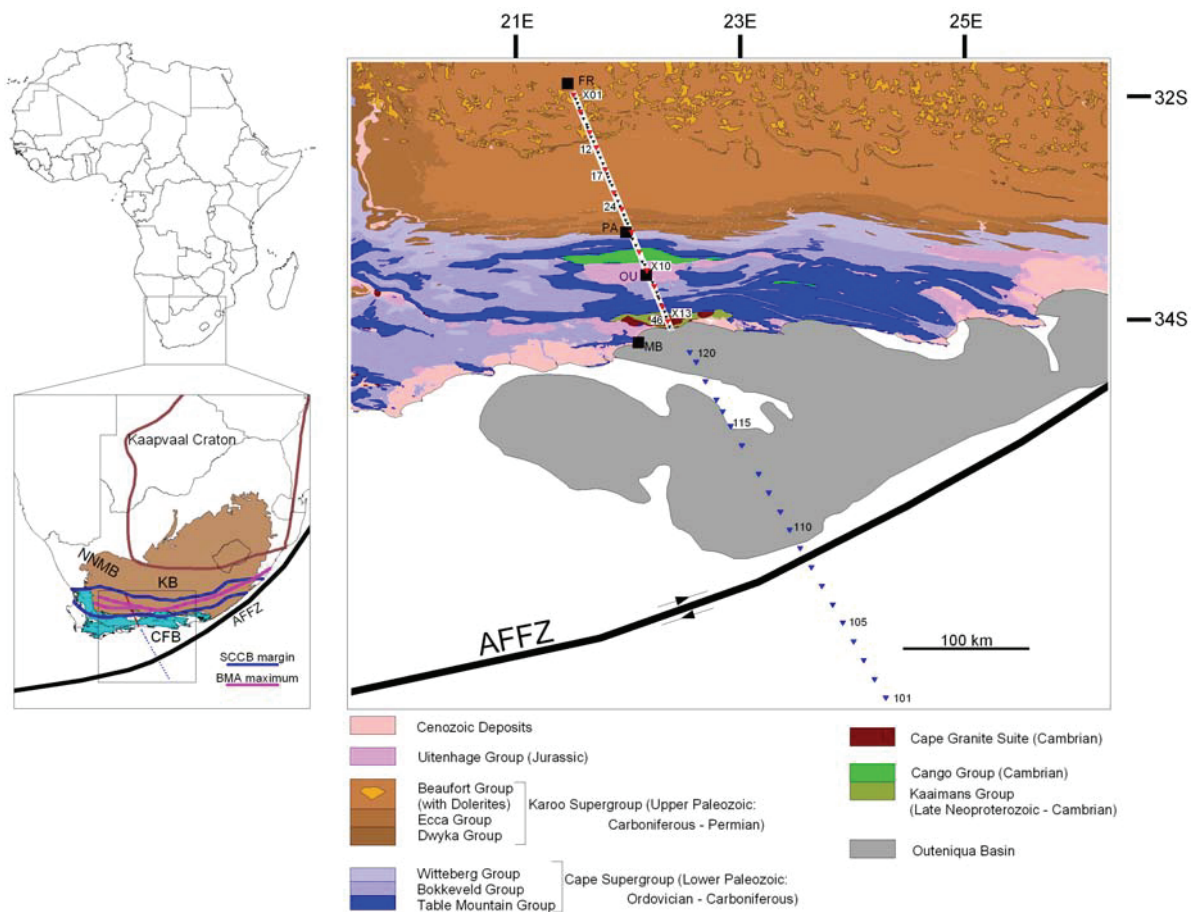


Figure 7-1: Study area: Map of southern Africa shown the relevant large-scale features, like the Kaapvaal Craton, Karoo Basin (KB), Cape Fold Belt (CFB), the location of the Namaqua Natal Mobile Belt (NNMB), the Agulhas-Falkland Fracture Zone (AFFZ), as well the Southern Cape Conductivity Belt and the Beattie Magnetic Anomaly. The detailed map shows the geological setting of the study area. The onshore section of the profile is indicated by the red triangles (13 shots, numbered X01-X13) and smaller black triangles (48 receivers, numbered 01-48). Four cities are shown on the map to aid location: Fraserburg (FR), Prince Albert (PA), Oudtshoorn (OU) and Mossel Bay (MB). The 20 Ocean Bottom Seismometers used in the offshore part are marked as blue triangles, and are numbered 101-120 following the notation of Parsieglia et al. [2007].

## 7.2 Profile setting

The northern part of the profile runs through the Karoo Basin (KB, Figure 7-1). This retroarc foreland basin is believed to have formed during the accretion of the palaeo-Pacific plate to the Gondwana plate during the Late Carboniferous [Cole, 1992]. The basin contains up to 12 km of Late Carboniferous to Mid Jurassic sedimentary strata (Karoo Supergroup) dominated by shale, siltstone and sandstone [Broquet, 1992; Cole, 1992; Cloetingh et al., 1992; Catuneanu et al., 1998]. Cole [1992] and Cloetingh et al.

## Crustal structure of the southern margin of the African continent

[1992] report a thickness of about 4600 m near the northern end of our profile. The Karoo Supergroup is subdivided from the top downwards into the Beaufort, Ecca and Dwyka Groups. An important marker horizon in the Karoo Basin is a series of deep water carbonaceous shales within the Ecca Group (~40 m thick Whitehill and ~180 m thick Prince Albert Formations). In the southern part of the basin along the geophysical profile, the Karoo strata are tightly folded with north-vergence whereas deformation intensity decreases northward and strata have gentler dips.

To the south the Karoo Basin is terminated by the Cape Fold Belt (CFB, Figure 7-1). This belt comprises a thick sequence of Neoproterozoic to early Palaeozoic metasedimentary rocks (Cape Supergroup), which were deposited in a marginal basin created by inversion of a Pan-African mobile belt [*de Wit*, 1992]. The stratigraphy of the Cape Supergroup consists of a lower series up to ~3 km of Neoproterozoic to Cambrian metasediments in local basal rift sequences [e.g., Kango Inlier, *Barnett et al.*, 1997], which are overlain by ~8 km Ordovician to Carboniferous clastic sediments and orthoquartzites [*Hälbich*, 1983, 1993; *Tankard et al.*, 1982; *Broquet*, 1992; *Catuneanu et al.*, 1998]. Together with the lower units of the Karoo Basin (see above), the Cape Supergroup rocks were deformed at ~250 Ma, with the formation of north-vergent asymmetric or overturned folds and thrust faults [*Hälbich*, 1993; *Hälbich and Swart*, 1983]. The dominant CFB thrusts are south dipping and may coalesce into a common décollement [*Hälbich*, 1983, 1993; *Newton*, 1992; *Paton et al.* 2006]. Drill cores discussed by *Eglinton and Armstrong* [2003] show that some of the Cape Supergroup underlies the Karoo Basin, but it is not known how far north the Cape Supergroup extends.

The Cape Supergroup, and farther north the KB, unconformably overlie the Namaqua-Natal Mobile Belt (NNMB, Figure 7-1). This Mesoproterozoic complex has accreted to the lithospheric core of the Kaapvaal Craton, and experienced successive periods of extension and compression between 2.0 and 1.0 Ga [*de Wit*, 1992]. During the Late Proterozoic / Early Cambrian, eroded material from uplifts in the NNMB filled basins to the south, forming the Kango and Kaaimans Inliers [*Hälbich*, 1993]. The NNMB is a highly complex polymetamorphic province that constitutes three sub-provinces or terranes, which were amalgamated and attached to the Archaean Kaapvaal Craton during the late Mesoproterozoic [*Robb et al.*, 1999; *Eglinton and Armstrong*, 2003; *Raith et al.*, 2003; *Dewey et al.*, 2006; *Eglinton*, 2006 and references therein]. The age of peak metamorphism across all terranes was 1.02-1.04 Ga [*Eglinton*, 2006], and assemblages indicate upper amphibolite to granulite-facies conditions with locally extensive generation of crustal melts now

## Crustal structure of the southern margin of the African continent

represented by megacrystic orthogneisses. The structural history of the NNMB includes regional ductile deformation with refolded recumbent folds, thrusting and listric shear zones that produced strong shallow to steeply-dipping fabrics and regionally extensional shear zones. Interpretation of a seismic refraction profile across the NNMB in the western Cape Province indicated crustal thickness of about 42 km and intermediate P-wave velocity of 6.2-6.9 km/s in the lower crust [Green and Durrheim, 1990]. Similar results were reported by Hirsch *et al.* [2008] from a combined interpretation and modelling of gravity and seismic data along an offshore-onshore profile which crosses the Orange Basin off the western coast of Southern Africa, and extends 100 km inland. The crustal thickness and lower-crustal P-wave velocity values at the inland end of this profile are 36-38 km and 6.7 to 7.0 km/s, respectively. The eastern exposures of the NNMB in KwaZulu-Natal comprise a number of litho-tectonic terranes dominated by upper amphibolite to granulite-facies gneisses with occasional charnockites, separated by subvertical ductile shear zones [Jacobs *et al.*, 1993; Jacobs and Thomas, 1994; Eglington, 2006; McCourt *et al.*, 2006].

The profile crosses two major continental geophysical anomalies: the Beattie Magnetic Anomaly (BMA), and the Southern Cape Conductive Belt (SCCB). Both features stretch for more than 1000 km in a roughly east-west orientation (Figure 7-1). The BMA, a positive anomaly, was first observed by Beattie [1909]. Following a magnetometer array study, Gough *et al.* [1973] concluded that a large body with high electrical conductivity underlies the NNMB and parts of the KB. Gough [1973] interpreted this Southern Cape Conductive Belt as the signature of a linear plume in the upper mantle. However, de Beer *et al.* [1974] suggested that, due to their spatial coincidence, the two geophysical anomalies are likely to have a common source, and that such a plume could not account for the BMA. de Beer and Gough [1980] then used Curie isotherms to show that if a common source exists, it must be a crustal feature. Pitts *et al.* [1992] suggested a sliver of serpentinised oceanic crust, 30 km broad and dipping south from a depth of 7 to 30 km as the source. However, a recent magnetotelluric study by Weckmann *et al.* [2007a] found no evidence for the existence of such an extensive high conductivity body, which could be the source of the magnetic anomaly at the same time.

The offshore section of this western profile starts about 20 km off the coast and stretches over 400 km south, past the Agulhas-Falkland Fracture Zone (AFFZ, Figure 7-1). Between the AFFZ and the present coast a network of basins, collectively referred to as the Outeniqua Basin (Figure 7-1), is located [e.g. Fouche *et al.*, 1992, McMillan *et al.*, 1997, Broad *et al.*, 2006]. This complex basin developed due to extensional episodes in Oxfordian /

## Crustal structure of the southern margin of the African continent

Kimmeridgian and Valangian times exploiting the structural gain of the underlying Cape Fold Belt [e.g. *McMillan et al.*, 1997]. The Outeniqua Basin is bounded to the south by a marginal ridge, which was first described by *Scrutton and du Plessis* [1973] and renamed into Diaz Marginal Ridge (DMR) by *Ben-Avraham et al.* [1997]. While earlier studies [e.g. *Scrutton and du Plessis*, 1973] describe it as a basement ridge, more recent studies by *Parsiegla et al.* [2007] suggest a metasedimentary composition of this ridge. South of the DMR, the AFFZ, a large scale fracture zone, is located. The magnetic signature of this fracture zone was first identified by *Oguti* [1964] south of Africa. The AFFZ marks the southern boundary of the African continent [*Talwani and Eldholm*, 1973]. This sheared continental margin developed as a consequence of dextral strike-slip motion between today's African and South American continents during the Cretaceous break-up of Gondwana [e.g., *Barker*, 1979; *Rabinowitz and LaBrecque*, 1979]. During this shear process the originally juxtaposed Southern Outeniqua and Falkland Plateau Basins were separated [e.g. *Martin et al.*, 1981; *Ben-Avraham et al.*, 1997] and the major faults of the Outeniqua Basin were bent [e.g. *Ben-Avraham et al.*, 1993; *Thomson*, 1999; *Parsiegla et al.*, 2007].

### **7.3 Seismic data acquisition**

The wide angle seismic experiment was carried out in April-May 2005. The 240 km onshore part [*Stankiewicz et al.*, 2007] consisted of 13 shots (each 75-125 kg of explosives) fired from boreholes 20-30 metres deep (Figure 7-1). Forty-eight stations (average spacing of ~5 km) each consisting of a GPS synchronised electronic data logger (EDL) and a three-component seismic sensor were used to record the data. The offshore part [AWI-20050100, *Parsiegla et al.*, 2007] consisted of 20 four-component (three component seismometer and a hydrophone component) ocean bottom seismometers (OBS) deployed over 400 km profile length. Eight G-guns and one Bolt-airgun (volume of 96 l) were fired every 60 seconds during cruise SO-182 of the RV Sonne. This gave a shot spacing of approximately 150 metres. As the onshore and offshore parts were carried out simultaneously, the airgun shots were recorded by the land receivers, improving the profile's ray coverage, especially beneath the coast. Land shots were not detected by OBSs.

## 7.4 Wide-angle seismic data processing

Figure 7-2 shows the high quality of the traces resulting from land shots, recorded by the land receivers. The direct (refracted) P-wave arrival ( $P_g$  – red), as well the Moho reflection ( $P_mP$  – blue) are clearly seen. Examples of airgun shots picked up by land receivers are illustrated in Figure 7-3, where, due to the longer offsets, the P-waves refracted in the upper mantle ( $P_n$ ) are also seen. The airguns produce much less energy than the land shots, but because of their small spacing prominent arrivals can be easily identified. Examples of airgun signals registered by the OBS can be seen in Figure 7-4. All together, 24045 arrivals were manually picked (Table 7-1). Pick uncertainty was in the range of 0.05 – 0.25 seconds, depending on the signal to noise ratio.

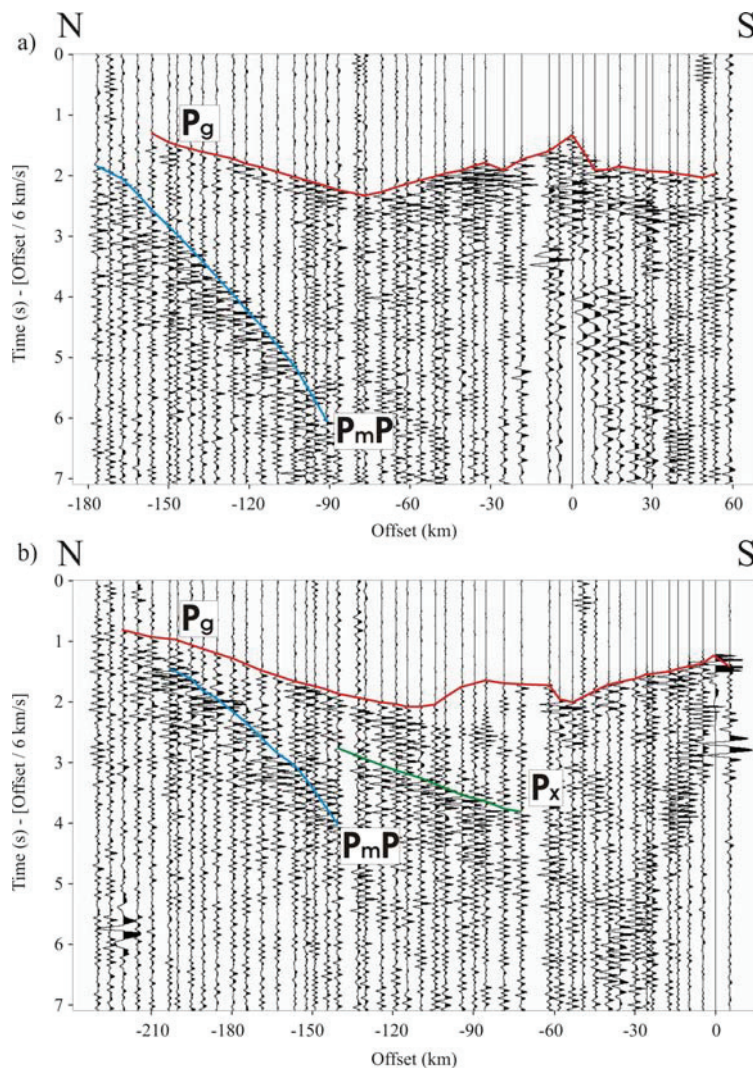


Figure 7-2: Examples of data recorded by land receivers from land shots. Top: shot X10. The refracted P-waves ( $P_g$ ) marked in red, and Moho reflections ( $P_mP$ ) in blue. Bottom: shot X13. Phases reflected off the “floating” crustal reflector ( $P_x$ ) are marked in green. Reduced travel times are shown with a reduction velocity of 6 km/s.

Crustal structure of the southern margin of the African continent

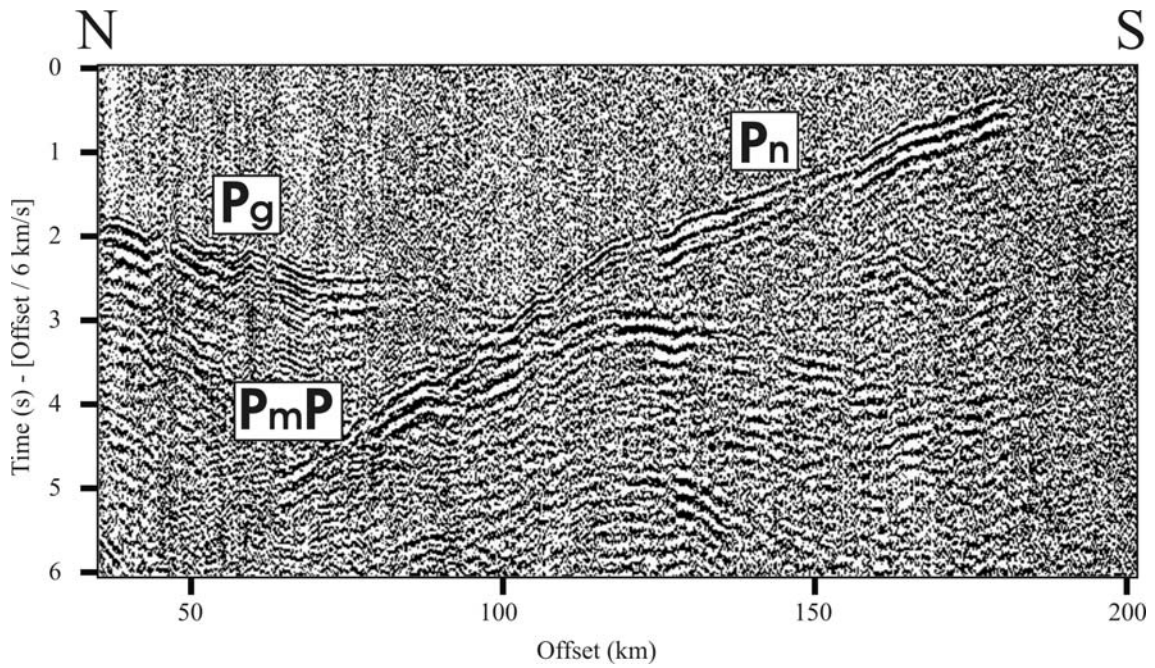


Figure 7-3: Example of the data from air gun shots picked up by land receiver 46. Direct P-waves from the crust ( $P_g$ ), from the mantle ( $P_n$ ) and Moho reflections ( $P_mP$ ) are clearly visible. Reduced travel times are shown with a reduction velocity of 6 km/s.

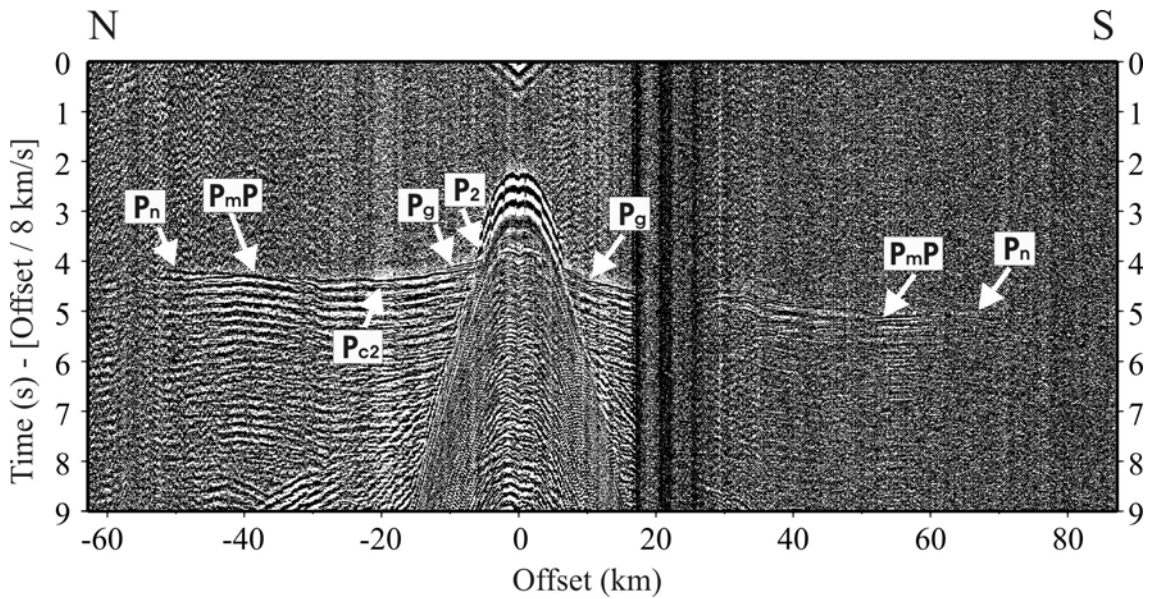


Figure 7-4: Air gun shots recorded by OBS 105. Phases  $P_g$ ,  $P_n$  and  $P_mP$  as in Figure 7-3.  $P_2$  corresponds to P-waves refracted in the upper-crust low-velocity sediments, and  $P_{c2}$  P-waves reflected inside the crust (notation from Parsieglia et al., 2007). Reduced travel times are shown with a reduction velocity of 8 km/s.

## Crustal structure of the southern margin of the African continent

phase	Air Gun – OBS	Air Gun – EDL	Land Shot – EDL	$\Sigma$
<b>Crustal Refraction</b>	2329	5030	445	7804
<b>Mantle Refraction</b>	225	13861	0	14086
<b>Moho Reflection</b>	642	1028	132	1802
<b>Intracrustal Reflection</b>	332	0	21	353
$\Sigma$	3528	19919	598	24045

*Table 7-1: Number of picked arrival times.*

Two travel-time inversion techniques have been used in this study. Standard 2-dimensional tomography involves dividing the cross section beneath the profile into rectangular cells. An initial velocity model needs to be provided, and its values temporarily assigned to the cells. A simple one-dimensional model was used here. Synthetic travel times are then computed, and compared to real (picked) ones. An iterative algorithm adjusts the individual values until an optimal model is reached. This study uses the software package FAST (First Arrival Seismic Tomography), which was released by *Zelt and Barton* [1998]. This package is a modification of the algorithm developed by *Vidale* [1988] to ensure a better detectability of high velocity contrasts. To minimize the influence of the starting model, we have used an iterative approach developed by *Ryberg et al.* [2007], which repeats the inversion 5 times, using increasingly smaller cell sizes. We have performed the inversion using vastly different starting models, and found no significant differences in the resulting models. A ratio of 1:8 was used for the vertical-to-horizontal smoothing constraints.

The above technique was used to compute the velocity model for the upper crust beneath the land section of the profile, as well as the northernmost 100 km of the offshore section. The final cell size used was 2 km horizontal by 1 km vertical. For first-arrival tomography calculations it is important to have individual rays crossing each other in every individual cell, so having airgun shots spaced in only one direction from the receivers is not an optimal situation. For this reason only a small part of the offshore section was used, with the purpose of improving the onshore ray coverage rather than trying to compute a detailed offshore model. The resolving capabilities of the algorithm can be tested with checkerboard tests, where checkerboard of alternate positive and negative velocity anomalies is added to the originally computed velocity model. Synthetic travel times are then generated, and an inversion is performed using these times. The inversion result is then subtracted from the initial model. If the blocks can be observed in the final model, we can assume that a real feature corresponding to the block's size, position and velocity perturbation would be

## Crustal structure of the southern margin of the African continent

resolved by our inversion algorithm, and therefore an observed feature like that is likely to be real, and not an inversion artefact.

A disadvantage of FAST is that reflected phases cannot be incorporated in the model. For this reason, the travel-time routine RAYINVR [Zelt and Smith, 1992] was used. In this program the 2-D velocity model is defined in terms of layers. Velocity is specified at a number of nodes along the layer boundaries, and a linear velocity gradient is assumed between nodes (both along boundaries, and with depth). Rays may refract in a particular layer, reflect off any boundary, or travel as head waves along it. As with FAST, model quality is determined by comparing synthetic travel times to the manually picked real ones. Modelling is done as an iterative combination of forward modelling and inversion [Zelt and Forsyth, 1994]. The resolution of the velocity model depends (among other things) on the number of layers defined, and the node density along them. The marine model of *Parsiegla et al.* [2007] was computed using this package. Their model consists of 6 layers: a water layer, two sedimentary layers, two crustal layers and the mantle.

To produce a starting velocity model for the joint onshore-offshore analysis of the entire profile, the two separate models had to be merged. As a number of reflected phases are available, RAYINVR was considered the more appropriate package to use. For this reason, the onshore FAST model needed to be converted into a layered model, with layers matching the ones in the offshore model. The uppermost sedimentary layer (marine sediments), and obviously the water layer, exist only in the offshore section, so the onshore part consisted of 4 layers. The uppermost of these was a shallow (not exceeding 3 km) zone with velocities typical for sedimentary rocks. The next 2 layers represented the crystalline crust. In the starting model they were separated at a depth of 15 km, using velocities obtained from the FAST at nodes spaced 20 km apart. The boundary between the 3<sup>rd</sup> and 4<sup>th</sup> layer was the Moho, set in the starting model at 42 km [after *Lindeque et al.*, 2007]. The combined starting velocity model is then iteratively updated, using forward and inverse modelling, until the calculated synthetic travel times match the data as well as possible. While converting from FAST to RAYINVR decreased the resolution of small-scale features in the onshore part, the two modelling techniques complement each other, and our final results are better than what could be achieved using either of the techniques alone.

## 7.5 Results

### 7.5.1 Crustal features beneath the continent

The upper crust model computed with FAST using first arrivals of land shots (445 P-wave arrivals), as well as airgun shots less than 100 km from coast (3351 P-wave arrivals), is shown in Figure 7-5. The RMS travel time residual was 0.045 seconds, and the chi-squared misfit parameter 2.60. Figure 7-5 needs to be viewed in conjunction with Figure 7-6, which shows the checkerboard tests conducted on the model. These tests confirm that the model is better resolved beneath the land, where features barely twice as wide as the receiver spacing can be resolved in the upper 10 or 15 km. Large scale features, 40 km wide, can be confidently resolved almost to the maximum ray penetration, even beneath the ocean.

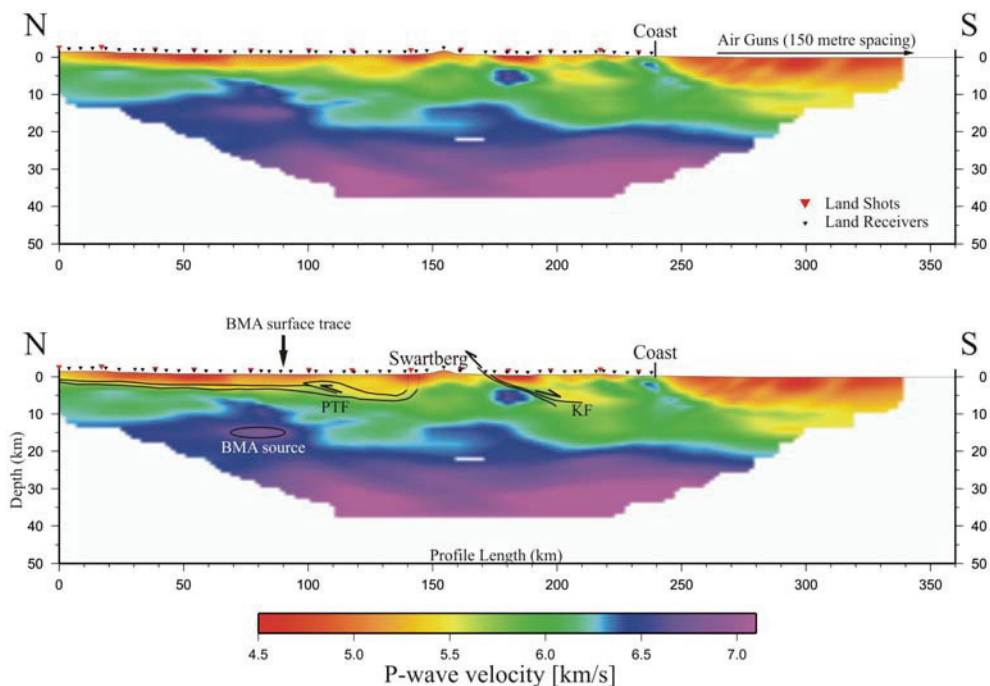


Figure 7-5: P-wave velocity model computed for the onshore part of the profile, as well as the first 100 km of the offshore part. Upper panel shows just the model, the lower panel includes interpretations. Starting in the north, 140 km of the inferred distribution of the Karoo Supergroup, and the Cape Supergroup underlying it, has been drawn. The location of the blind thrust fault which we believe marks the northernmost deformation of the Cape Supergroup has been marked by an arrow (PTF). We see the thickening of the basement at profile km 130, which is consistent with the syncline at which it tapers out. The actual edge of it, however, is not resolved, and has been drawn in dotted lines. Farther south, the geometry of the normal listric Kango Fault (KF, surfacing at 170 km) has been drawn. A high velocity anomaly most likely related to the BMA has been indicated with an ellipse at a depth of ~15 km, at profile km 80. The centre of the surface trace of the BMA has also been indicated.

## Crustal structure of the southern margin of the African continent

The model in Figure 7-5 is consistent with the model computed using only onshore shots [Stankiewicz *et al.*, 2007]. However, the improved ray coverage increased the maximum depth of the model from less than 30 km to almost 40 km, and many of the upper crustal features are better resolved. In the northern half of the profile, the slow velocities (4.6 – 5.3 km/s, red and orange in Figure 7-5) characterising the Karoo Basin are clearly visible to depths not exceeding 5 km. Slightly faster (5.4 – 5.8 km/s, yellow and pale green) velocities beneath indicate the relatively thin Cape Supergroup. The resolution of the model does not clearly indicate the contact of the two Supergroups. The checkerboard tests indicate that the thinning of the basin at profile length of 100 km is a real feature – this is consistent with our earlier results [Stankiewicz *et al.*, 2007], which suggested a blind Paleozoic Thrust Fault, which could mark the northernmost deformation of the Cape Supergroup. The thickening of the basin at profile length of approximately 130 km (also well within the resolving capability of the model) is consistent with the large asymmetric syncline inferred from field observations [Cole, 1992].

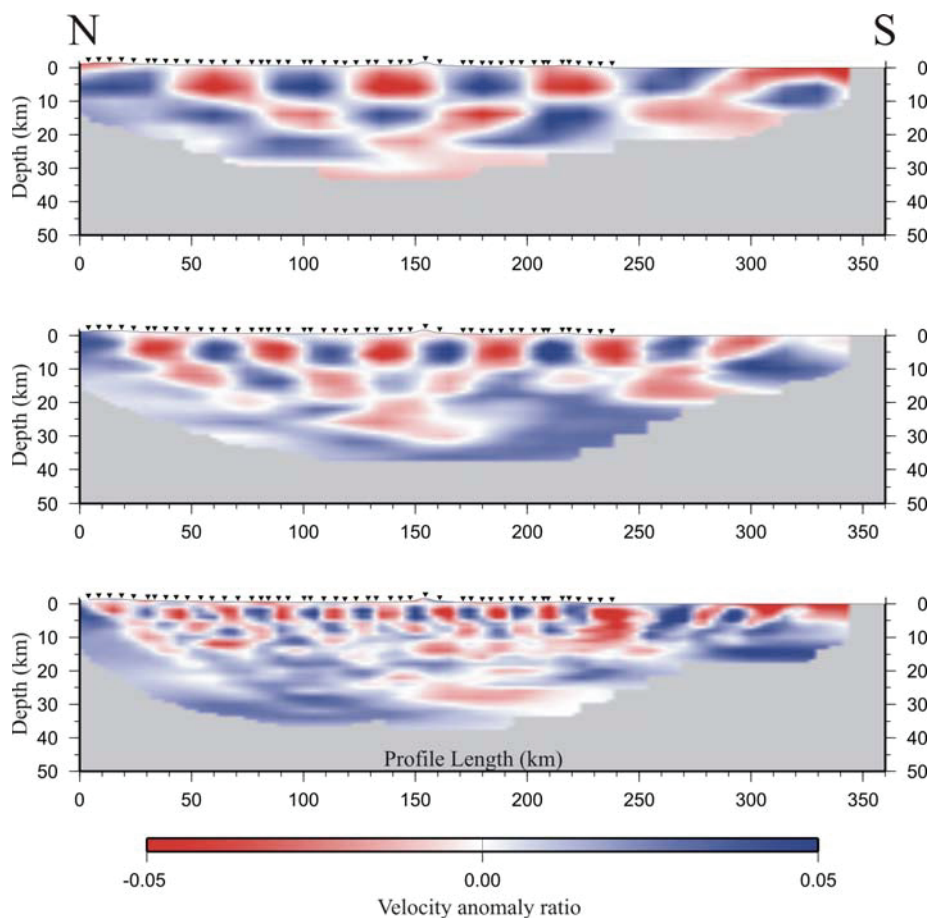


Figure 7-6: Resolution tests for the model in Figure 7-5. Original checkerboard sizes are 40 km by 10 km (top), 25 km by 10 km (middle) and 12 km by 5 km (bottom); velocity perturbation of 5% used in each case.

## Crustal structure of the southern margin of the African continent

Farther south, the geometry of the listric Kango Fault (KF) is resolved much more clearly than in the earlier results [Stankiewicz *et al.*, 2007]. Near the surface (at ~170 km profile length) this fault marks the northern edge of the Jurassic Uitenhage basin, characterised by very low velocities (~4.5 km/s). The offshore section of the model is not well resolved, which was expected from the shot-receiver geometry explained in the previous section. However, the very low velocities representing the sediment cover (< 5 km/s) are clearly seen to be significantly deeper than onshore.

### 7.5.2 Combined onshore-offshore model

The final RAYINVNR model is shown in Figure 7-7. The programme used 21,868 travel times (over 90 % of the picks). The RMS travel time residual was 0.134 seconds, which is within the uncertainty bounds of individual picks. The chi-squared misfit parameter was 1.74. Table 7-2 shows how these uncertainties vary for different phases. A value greater than 1 for the chi-squared parameter means the small-scale features of the model have not been resolved [Zelt and Forsyth, 1994], so we will concentrate our discussion on the large-scale features. A likely explanation for a large value of chi-squared is the presence of 3-D effects, in particular the fact that the onshore and offshore parts of the profile are not perfectly aligned (Figure 7-1). Examples of ray paths in the model are shown in Figure 7-8. The relative ray coverage available is shown in Figure 7-9, with red areas indicating poor ray coverage.

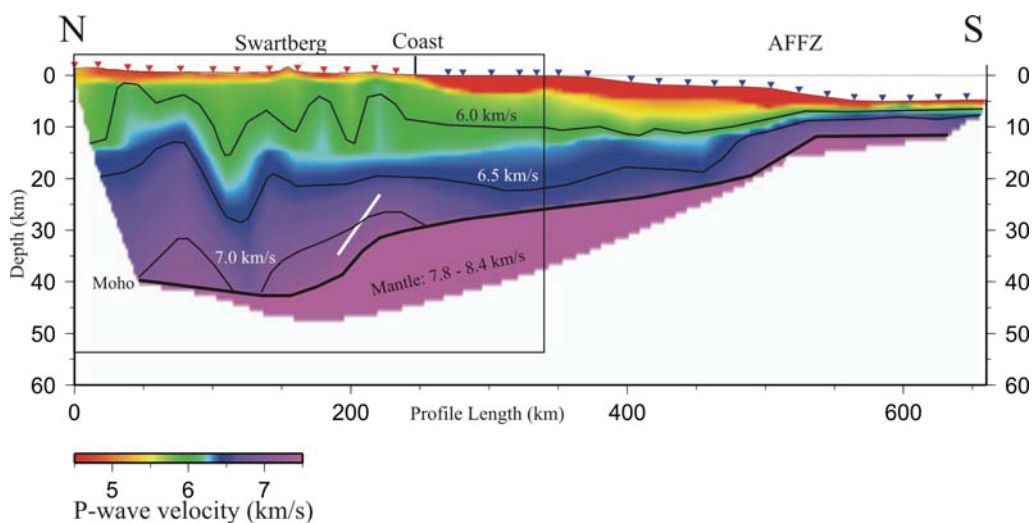


Figure 7-7: P-wave velocity model for the entire profile. To help location with Figure 7-1, land shots (red triangles) and OBSs (blue triangles) have been indicated. Velocity contours corresponding to 6.0, 6.5 and 7.0 km/s have been drawn. The thick white line marks the “floating” reflector. Black rectangle indicates the northern 340 km that are shown in Figure 7-5 and Figure 7-6.

## Crustal structure of the southern margin of the African continent

phase	rms	$\chi^2$
<b>Crustal Refraction</b>	0.132	1.70
<b>Mantle Refraction</b>	0.132	1.70
<b>Moho Reflection</b>	0.161	2.40
<b>Intracrustal Reflection</b>	0.173	0.88
$\Sigma$	0.134	1.74

Table 7-2: Model quality for different phases.

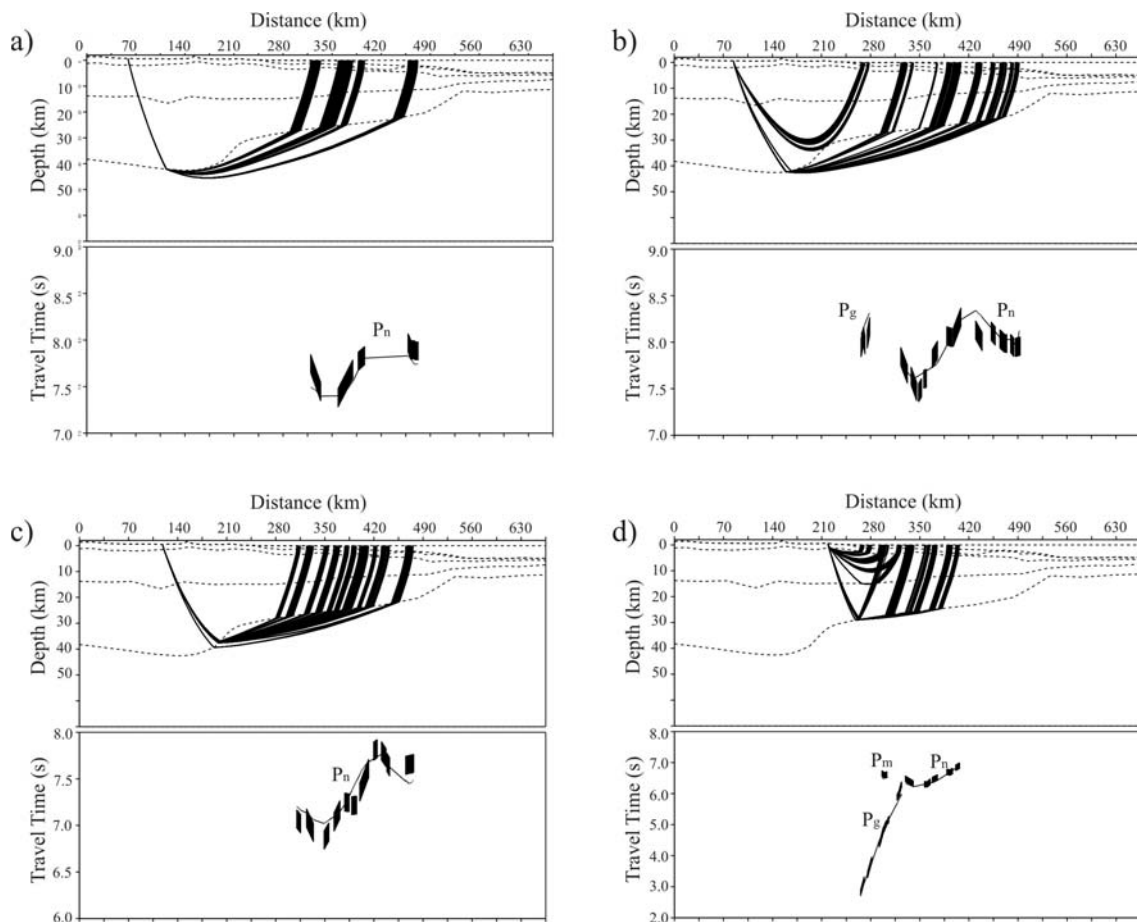


Figure 7-8: Airgun shots recorded by 4 land receivers (a: receiver 12; b: 17; c: 24; d: 44). In each figure the top panel shows the raypaths; the bottom panel the observed travel time (steeples corresponding to uncertainty bars), and the travel time expected from the model for the given source-receiver distance (solid line).

In addition to the standard phases  $P_g$  and  $P_mP$ , an unusual phase has been observed on the traces recorded from the two southernmost shots ( $P_x$  – Figure 7-2). The amplitude of this phase is of similar order of magnitude to the  $P_mP$ . Furthermore, the phase is most prominent in the vertical component, so we interpret it as P-waves reflected inside the crust. As a reflected phase, these travel times could not be included in the FAST model, and the corresponding

## Crustal structure of the southern margin of the African continent

reflector location was derived with RAYINVR using the floating reflector technique. The position of the reflector that best fits the observed travel times was found to be between profile km 190 and 220, rising steeply southwards from a depth of 35 km to 23 km (Figure 7-7). The steep landward dip of this reflector makes it impossible to detect reflections of airgun shots off it, the same way the steeply rising Moho was invisible.

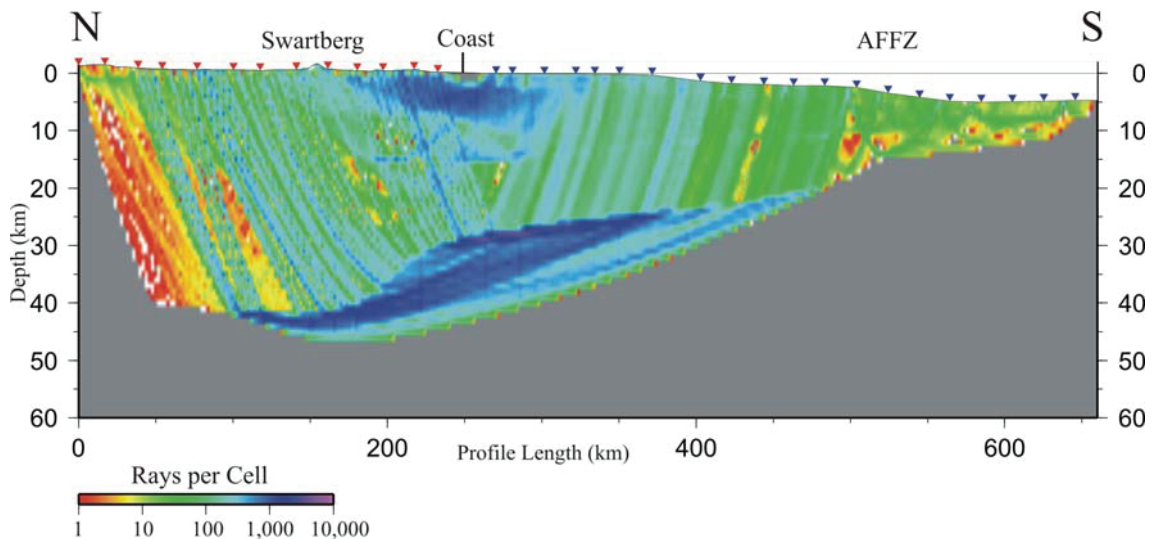


Figure 7-9: Ray coverage for the model presented in Figure 7-7. A logarithmic scale of number of rays crossing each 2 km by 1 km cell highlights regions of relatively high or low coverage.

The most interesting feature of the joint model shown in Figure 7-7 is the Moho discontinuity, clearly visible as a high-velocity contrast. The Moho depth beneath the Karoo Basin is ~40 km, and slightly deeper (~42 km) beneath the CFB. The crustal thickening beneath the CFB is consistent with receiver function analyses [Harvey *et al.*, 2001; Nguuri *et al.*, 2001]. However, the study by Nguuri *et al.* [2001], while detecting the thickening, consistently locates the Moho approximately 5 km deeper than reported here. This could be due to the fact that these authors use an average crustal velocity of 6.5 km/s. This value is typical for the Kaapvaal Craton at which their study was aimed, but is too high for off craton analysis. Our results are much closer to those of Harvey *et al.* [2001], who subdivided the crust into regions of different velocity at different depths.

South of the CFB the Moho depth becomes more shallow very abruptly, reaching 30 km at the present coast. The depth is consistent with values obtained from an east-west reflection profile of Durrheim [1987], which runs approximately 10 km south of the coast. Farther south the crust continues to thin, albeit much more gradually, for another 250 km, underneath the Agulhas Bank, Outeniqua Basin and the Diaz Marginal Ridge, until it reached the

## Crustal structure of the southern margin of the African continent

Agulhas-Falkland Fracture Zone (AFFZ). This fracture zone marks the continent-ocean transition (COT). This transition to oceanic crust begins around profile distance of 480 km, where the Moho depth of 20 km is reduced to 12 km over a little over 50 km horizontal difference [Parsiegla *et al.*, 2007]. This is a typical length, as well as depth change, for the transition at sheared margins [e.g., White *et al.*, 1992; Bird, 2001]. The depth of 11-12 km (i.e. 6-7 km of crust under 5 km of ocean) is observed in the Agulhas Passage, where the southernmost 130 km of the profile stretches.

### **7.6 Discussion**

#### **7.6.1 Crustal features beneath the continent**

Most of our shallow results are consistent with the results of the magnetotelluric profile [Weckmann *et al.*, 2007a] coinciding with the northern 140 km of the seismic line. These authors traced the highly conductive Whitehill Formation (pyrite-rich black shales at the bottom of the Eccca Group) for virtually the entire length of their profile, which correlates well with the geometry of the basin obtained with our tomography. The accuracy of the Whitehill's location in the MT depth section is confirmed by excellent correlation with drill cores [Eglington and Armstrong, 2003; Branch *et al.*, 2007]. Weckmann *et al.* [2007a] also observe an offset in the depth to the shales at the same location as our basement thinning, and also suggest a south dipping thrust as a likely explanation.

There is also some correlation between the velocity model and the electrical conductivity image of Weckmann *et al.* [2007a] for deeper features (Figure 7-10). Our model shows a zone of anomalously high velocity (~7 km/s) at a depth of ~15 km between profile km 60 and 90. The size of the body certainly falls within the model's resolving capability. The southern edge of this anomaly is in the vicinity of the centre of the BMA. In the 2D image of the electrical conductivity distribution, a zone of high electrical resistivity is found at the same location. To the north this zone is flanked by a large mid-crustal region of stacked layers of high electrical conductivity, possibly imaging mineralisations in synforms, and, to the south, by a narrow, southward dipping conductor at 7-15 km depth under the maximum of the BMA. The top of this anomaly is exactly coincident with what a seismic reflection study [Lindeque *et al.*, 2007] called a "complex seismic reflectivity patch". However, a comparison of magnetic models explaining the magnetic response of the BMA with the

## Crustal structure of the southern margin of the African continent

electrical conductivity model clearly shows that the electrical conductivity anomaly located beneath the centre of the BMA is too narrow to be a possible source of the BMA [Weckmann *et al.*, 2007b]. Figure 7-10 shows the two magnetic bodies outlined by black lines, each with a magnetic susceptibility of 0.05 SI. Weckmann *et al.* [2007b] show that these simple magnetic bodies would produce a response similar to the signature of the BMA. The bodies are separated by a fault, which cuts through at the same inclination as the conductivity anomaly. The gap (some 100 metres wide) representing the fault has an induced magnetic susceptibility of 0.0 SI, the same value as the background susceptibility. The location of the fault correlates well (at least in the upper 20 km) with the velocity contrast marking the northern edge of the synclinal low velocity zone between 100 and 140 km along the profile, while the top of the northern body correlates very well with both the high velocity anomaly and the zone of high resistivity north of the surface maximum of the BMA [Weckmann *et al.*, 2007a, Quesnel *et al.*, 2008].

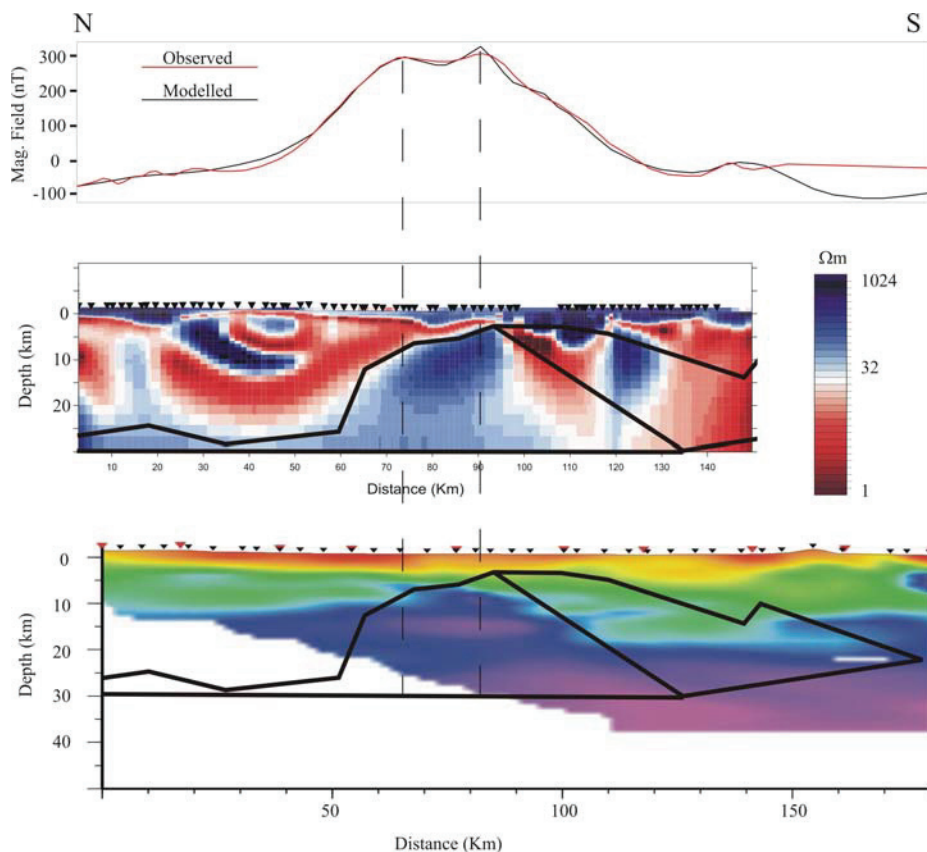


Figure 7-10: Top panel: Surface magnetic field (red line) along the profile, compared to the modeled magnetic signature of two magnetic bodies intersected by a few 100 m wide non-magnetic region [Weckmann *et al.*, 2007b]. Middle panel: the two magnetic bodies drawn over the MT depth section of Weckmann *et al.* [2007a]. Lower panel: the magnetic bodies drawn over the northern 180 km of the P-wave velocity model shown in Figure 7-5. Vertical dashed lines across all three panels project the locations of the maxima of the BMA onto the depth sections.

### 7.6.2 Combined onshore-offshore model

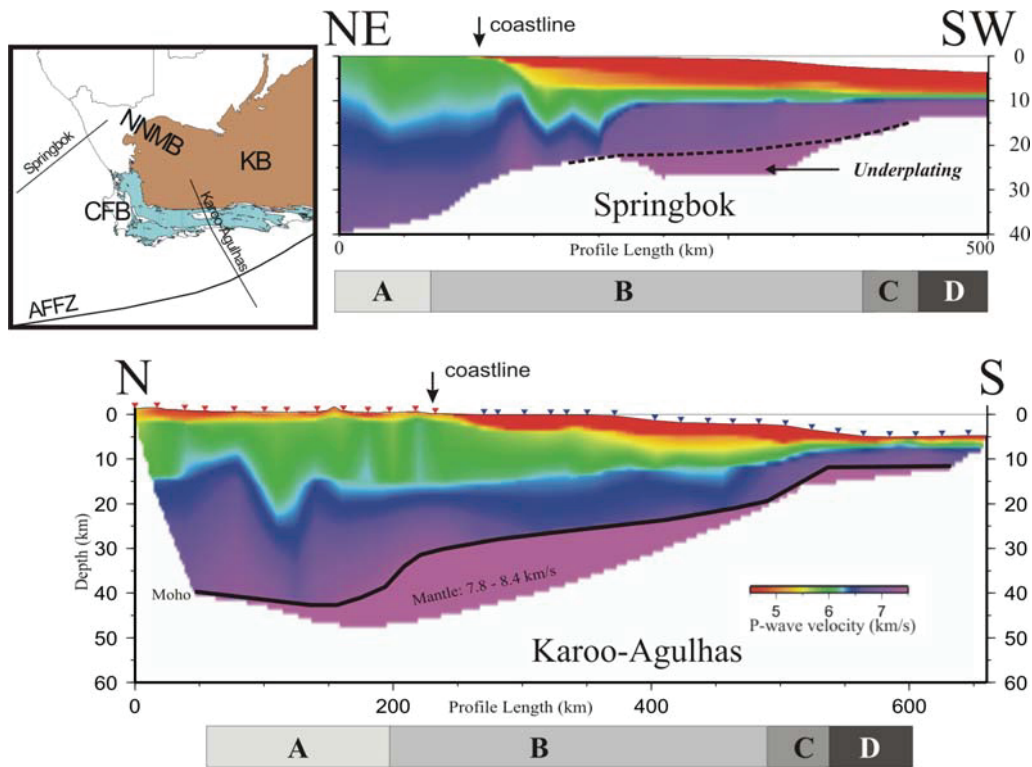


Figure 7-11: P-wave velocity model comparison between the Springbok profile on the western coast of South Africa (top panel, after Hirsch et al., 2008], and this study (bottom panel). Based on Moho geometry, four segments of the crust can be distinguished in both profiles: thick continental (A), stretched gradually thinning (B), steeply thinning (C), and thin oceanic crust (D).

The geometry and seismic velocity structure derived from a joint interpretation of onshore and offshore Vp tomography (Figure 7-7) provides one of the best available geophysical images of a sheared continental margin in cross-section. It also allows a detailed comparison with features from profiles across the classic volcanic rifted margins on the western coast of South Africa. The most direct comparison is with the seismic profile across the Orange Basin [Hirsch et al., 2008], because this profile also extends oceanward from the Namaqua-Natal Mobile Belt. The sheared and volcanic margin profiles are compared at the same scale on Figure 7-11. Both profiles show similar wedge-shaped geometry and furthermore, the crustal thickness (Moho depth) does not reduce uniformly but stepwise, with inflection points separating segments of rapid and gradual change. Comparing these segments in turn, from the continental crust (A in Figure 7-11) outward, we consider the following observations most important:

- Both profiles begin at the landward end in the Namaqua-Natal Mobile

## Crustal structure of the southern margin of the African continent

Belt, in the case of the Karoo-Agulhas profile this is covered by the Karoo sequence. The crustal thickness at this end of both profiles is about 40 km, but there is a major difference in the seismic velocity structures of the lower crust. The Karoo-Agulhas profile shows a zone up to 7 km thick with seismic velocity above 7.0 km/s (maximum  $V_p = 7.4$  km/s), whereas the basal velocity at the Springbok profile does not exceed 6.8 km/s. The significance of the high velocity lower crust is discussed in more detail below. The high-velocity zone on the Karoo-Agulhas profile is interrupted at profile distance 120 km by a “keel” of material with intermediate velocity (green on Figure 7-7, Figure 7-11). The higher resolution of the upper crustal seismic image (Figure 7-5) shows that this feature has a complex shape that appears consistent with the north-vergent folds and thrust faults known in the upper crust.

- Over much of the segment of stretched continental crust (B in Figure 7-11) between continental crust (segment A) and the steep decrease in Moho depth (segment C), the crustal thickness at the Karoo-Agulhas profile is significantly greater at the Springbok profile. This is likely due to the presence of the Cape Fold Belt, which is not intersected by the Springbok profile on the west coast.
- The stretched crust shows a gradual and uniform thinning on the sheared Agulhas margin. The lower crustal seismic velocity in this segment is also uniform, with  $V_p$  values of 6.5 to 7.0 km/s that are in the same range as the lower crust observed in other parts of the NNMB [Green and Durrheim, 1990; Durrheim and Mooney, 1994; Hirsch et al., 2008]. This is in marked contrast to the corresponding segment on the Springbok VRM, which shows a down-warping of the lower crust in the middle part of the segment. This “keel” has a higher seismic velocity ( $V_p > 7.0$  km/s) than the lower crust elsewhere along the profile, and even the crust above the keel has a higher velocity than at the same depth outside the keel region. High-velocity lower crust are very common features at volcanic rifted margins and interpreted as underplated basaltic magma that intruded and ponded at the crust-mantle boundary [Menzies et al., 2002]. Hirsch et al. [2008] showed that this interpretation is consistent with gravity modelling of the Springbok profile and also noted that the high-velocity keel underlies a zone of seaward-dipping reflector wedges in the upper crust, also characteristic features of volcanic rifted margins and interpreted as submerged basalt flows on the foundering margin [Menzies et al., 2002]. Note that if the high-velocity keel on the Springbok profile is considered to be accretion of new crust by magmatism, the

## Crustal structure of the southern margin of the African continent

geometry of the Springbok margin in this segment is very similar to that of the Agulhas margin, with a uniform, moderate thinning (dashed line, Figure 7-11).

- Both margins exhibit an abrupt rise of the Moho over about 50 km (segment C). In the case of the Agulhas margin, the lower crust at this rise shows a higher seismic velocity than in the "stretched" segment, with values of about 7 km/s. This represents the continent-ocean transition across the sheared margin. For the Springbok profile this increase in seismic velocity at the steep rise is not observed, because it is part of a much longer (~200 km) continent-ocean transition zone.
- The oceanic crust (segment D) on both sections has the global average thickness of about 7 km and a velocity structure that is also typical of oceanic crust worldwide. The post-rift sedimentary cover on the oceanic crust at the Springbok profile is considerably thicker than at the Agulhas profile because it crosses the Orange River Basin.

A number of theoretical and empirical models exist that link observed geometry and seismic properties with the processes of rifting and magmatism at volcanic rifted margins [e.g., *Menzies et al.*, 2002]. It is clear from their work that seaward-dipping reflector sequences in the upper crustal section land-ward of the ocean-continent transition zone, and thick, high seismic-velocity lower crust (>7.0 km/s) underneath the reflector sequences result from massive intrusion of breakup-related magma. Classic examples of these features were documented from the Walvis Basin in Namibia by *Bauer et al.* [2000], and *Trumbull et al.* [2002] showed that the thickness (20 km) and high V<sub>p</sub>-values (7.2-7.4 km/s) of underplated lower crust in NW Namibia require high mantle temperatures and active mantle upwelling, consistent with the proximity to the Walvis Ridge and Paraná-Etendeka Large Igneous Province. The volcanic rifted margin at the Orange River Basin (Springbok profile) is located some 1500 km south of the Walvis Ridge and the underplated crustal body is considerably thinner and has a lower average V<sub>p</sub> velocity [*Hirsch et al.*, 2008]. *Trumbull et al.* [2007] found that dolerite dykes exposed along the coast from NW Namibia to the Cape Province showed a systematic decrease in their maximum MgO contents, both in whole-rock and in olivine, which is consistent with a waning plume influence from north to south expressed in lower mantle potential temperature and less active upwelling.

On the sheared Agulhas margin, neither seaward-dipping reflectors nor high-velocity lower crust are revealed by the geophysical surveys, nor is there

## Crustal structure of the southern margin of the African continent

geologic evidence for syn-rift magmatism onshore. This margin can thus be considered as non-magmatic with respect to the time of breakup. There is, however, seismic evidence of post-breakup magmatism on the profile. Seismic reflection sections in the Agulhas Passage found signs of volcanic seamounts and intra-basement reflectors interpreted as basaltic flows [Parsieglia et al., 2007]. A late Cretaceous age of extensive volcanism (ca. 100 Ma) is also suggested from seismic data from the Agulhas Plateau [Uenzelmann-Neben et al., 1999; Parsieglia et al., 2008].

One feature of the Karoo-Agulhas profile that deserves further comment is the zone of high seismic velocity ( $V_p > 7.0$  km/s) in the lower crust inland of the coast (from profile km 150 to the coast). Whereas the velocity of this zone is like that encountered in underplated lower crust at volcanic rifted margins, the position of this zone in relation to the continental margin makes it unlikely to represent breakup-related magmatism. Also, as mentioned above, there are no matching expressions of magmatism in the upper crustal seismic data, or on land. Crustal rocks with P-wave velocities greater than 7 km/s are most likely to represent mafic igneous rocks rich in olivine, or their metamorphosed equivalents (amphibolites, mafic granulites). Seismic velocities of metabasic rocks are particularly high if they are rich in garnet [e.g., Durrheim and Mooney, 1994; Christensen and Mooney, 1995]. Gerignon et al. [2004] discussed the likelihood of older high-pressure rocks (garnet granulite, eclogite) as an explanation for high  $V_p$  lower crust on parts of the rifted Vøring Basin in the Norwegian Sea. Considering the geologic setting of the Karoo-Agulhas profile, there are principally two possible explanations for the high-velocity crust. Either it represents metabasic lithologies of Precambrian age in the NNMB, or mafic intrusions added to the base of the crust by younger magmatism. The dominant exposed lithologies of the high-grade unit in the NNMB (Namaqualand terrane) are intermediate to felsic gneisses and meta-granitoids [Dewey et al., 2006]. These authors suggested that the heat source for granulite-grade metamorphism and crustal melting was “massive underplating” of mafic magmas at around 1050 Ma. The evidence cited for this underplating was a seismic refraction study by Green and Durrheim [1990], who reported lower crustal velocities of 6.6 – 6.9 km/s for the western Namaqualand crust. Similar values of 6.8 km/s were derived for the base of the crust in the NNMB at the landward end of the Springbok profile [Hirsch et al., 2008]. Even under the thick Kaapvaal Craton, seismic data indicate a generally sharp transition from the Moho to crustal rocks with intermediate to felsic properties [Durrheim and Mooney, 1994; Nair et al., 2006] and no evidence for widespread high- $V_p$  lower crust. Crustal xenoliths of garnet granulite are not uncommon in kimberlites from the NNMB [Schmitz and Bowring, 2004], and thus some high- $V_p$  material

## Crustal structure of the southern margin of the African continent

must be present in the crust, however the seismic surveys so far undertaken indicate that such material cannot be a major component of the lower crust. Therefore, although we do not rule out the possibility that the high- $V_p$  zones at the base of the crust in the Karoo-Agulhas profile are part of the Proterozoic basement, all other studies of the NNMB and cratonic crust failed to detect velocities above 6.9 km/s.

The alternative explanation for the high  $V_p$  values observed at the landward end of the Karoo-Agulhas profile is that Phanerozoic magmatism added thick intrusions of gabbroic material in the lower crust. This is of course the same scenario offered to explain the very common thick underplated crust at volcanic rifted margins, and it is clear from many studies that appropriate volumes of material and bulk seismic properties would fit the observations (7 km thickness,  $V_p = 7.0\text{-}7.4$  km/s – see Fig. 7). From the regional geology and location of the profile, the most likely candidate for producing extensive mafic underplating is the mid-Jurassic Karoo-Ferrar-Chon Aike Large Igneous Province. This was one of the major episodes of mafic magmatism on a global scale, and it is unlikely that the huge volumes of magma represented by Karoo lavas, dykes and sill complexes could be emplaced at upper crustal levels without an intrusive equivalent at depth. Unfortunately, the seismic experiments used in this study did not produce enough S-wave information to allow calculation of  $V_p/V_s$  ratios which would provide better lithologic discrimination, but from the available shape, location and  $V_p$  values of the lower crustal zone we believe an origin from underplated magmas related to the Karoo LIP provides the best explanation.

*de Wit* [2007] already noted the surprising lack of seismic evidence for mafic underplating of the Karoo magmas, whereas such evidence is clear and abundant for the Paraná-Etendeka LIP on the western margin. We argue from the results of this study that significant Karoo underplating did occur. Its paucity in seismic studies under the craton probably relates to the deflecting action of the thick Kaapvaal lithosphere. Why there is no seismic expression for underplating in the other surveys of the NNMB surveys is less clear but it may be related to the fact those surveys were located farther west than the Karoo-Agulhas profile whereas the locus of strongest Karoo magmatism is to the east, in the Lebombo-Natal and Lesotho regions.

## 7.7 Summary

In this study we have used tomographic inversion of reflected and refracted travel times to construct a P-wave velocity model along an off-onshore profile across the southern margin of Africa. The findings are summarized in Figure 7-12. A number of the model's features agree with known geological record, and are consistent with the results of the separate onshore [Stankiewicz *et al.*, 2007] and offshore [Parsieglia *et al.*, 2007] analyses. These include the rough geometry of the Karoo and Cape Supergroups, the presence of a blind Paleozoic Thrust Fault ~ 40 km north of the farthest Witteberg Group outcrop which possibly marks the northern edge of deformation in the Cape Supergroup, and the geometry of the Agulhas-Falkland Fracture Zone which marks the continent – ocean transition.

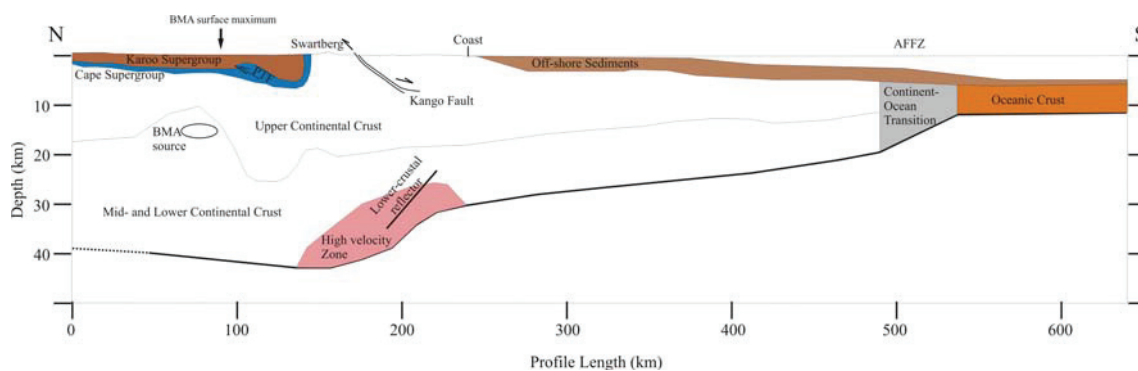


Figure 7-12: The combined onshore/offshore profile, showing the summary of the findings of this study. To the north the Karoo and Cape Supergroups taper out in an asymmetric syncline. The division between Upper and Middle/Lower Crust roughly follows the P-wave velocity of 6.5 km/s contour. Near its most shallow point, the high velocity anomaly most likely is related to the BMA is found in the Middle Crust. Immediately south a large synclinal feature was identified in the Upper Crust. In the Lower Crust high velocity material has been observed on top of the steeply rising Moho, as was a reflector roughly parallel to the Moho. Offshore the layer of sediments can be seen, as is the structure of the AFFZ, which separates continental from oceanic crust.

New findings of this study are:

- A high velocity anomaly north of the centre of the BMA is much better resolved than previously. This feature is coincident with an extensive zone of high resistivity and a magnetic body required to reproduce the magnetic signature of the BMA.
- A synclinal low velocity feature was identified in the Mesoproterozoic

## Crustal structure of the southern margin of the African continent

basement beneath the front of the Cape Fold Belt, south of the above mentioned feature. The northern edge of this feature correlates with the second magnetic body necessary to account for the BMA's signature.

- A steep decrease in crustal thickness (from 40 to 30 km over lateral distance of 40 km) occurs under the present coast.
- A zone of high velocity material is observed in the lower-most crust beneath the present coast. This either represents metabasic lithologies of the Mesoproterozoic Namaqua-Natal Metamorphic Complex, or intrusions of gabbroic material added to the base of the crust by younger magmatism.

### ***Acknowledgements***

J.S. thanks the GeoForschungsZentrum Potsdam for providing a scholarship to conduct research in Potsdam as part of the capacity building program of the Inkaba yeAfrica project. Equipment for the onshore experiments was provided by the Geophysical Instrument Pool, Potsdam. We thank the seismic and MT field teams, as well as the farmers who granted us access to their land. Many thanks go to the captain, the crew and the scientific participants of the RV Sonne cruise SO-182. We are grateful to Ernst Flüh of IfM-GEOMAR for lending us OBS systems. The SO-182 cruise (project AISTEK-I) and N.P.'s position was funded by the German Bundesministerium für Bildung und Forschung (BMBF) under contract no. 03G0182A. The German Academic Exchange Service (DAAD) funded a one month research visit of N.P. to the University of Cape Town (South Africa). We thank Maarten de Wit for his continuous involvement in the project, as well as Klaus Bauer and Oliver Ritter for many discussions. The manuscript benefited from constructive reviews by Ray Durrheim and an anonymous reviewer. This is Inkaba ye Africa publication 29.

## 8 The southern African continental margin – dynamic processes of a transform margin

Parsiegla, N., Stankiewicz, J., Gohl, K., Ryberg, T., Uenzelmann-Neben, G.

### ***Abstract***

Dynamic processes at sheared margins associated with the formation of sedimentary basins and marginal ridges are poorly understood. The southern African margin provides an excellent opportunity to investigate the deep crustal structure of a transform margin and to characterize processes acting at these margins by studying the Agulhas-Falkland Fracture Zone, the Outeniqua Basin and the Diaz Marginal Ridge. To do this, we present the results of the combined seismic land-sea experiments of the Agulhas-Karoo Geoscience Transect. Detailed velocity-depth models show crustal thicknesses varying from ~42 km beneath the Cape Fold Belt to ~28 km beneath the shelf. The Agulhas-Falkland Fracture Zone is embedded in a 50 km wide transitional zone between continental and oceanic crust. The oceanic crust farther south exhibits relatively low average crustal velocities (~ 6.0 km/s), which can possibly be attributed to transform-ridge intersection processes and the thermal effects of the adjacent continental crust during its formation. Crustal stretching factors derived from the velocity-depth models imply that extension in the Outeniqua Basin acted on regional as well as more local scales. We highlight evidence for two episodes of crustal stretching. The first, with a stretching factor  $\beta$  of 1.6, is interpreted to have influenced the entire Outeniqua Basin. The stresses possibly originated from the break-up between Africa and Antarctica. The second episode can be associated with a transtensional component of the shear motion along the Agulhas-Falkland Transform from ~ 136 Ma. This episode caused additional crustal stretching with  $\beta = 1.3$  and is established to only have affected the southern parts of the basin. Crustal velocities directly beneath the Outeniqua Basin are consistent with the interpretation of Cape Supergroup rocks underlying most parts of the basin and the Diaz Marginal Ridge. We propose that the formation of this ridge can be either attributed to a transpressional episode along the Agulhas-Falkland Transform or to thermal uplift accompanying the passage of a spreading ridge to the south.

## **Keywords**

sheared margin, transform margin, fracture zone, seismic refraction, seismic reflection, plate-tectonics, crustal stretching, basin formation, Agulhas-Karoo Geoscience Transect

## **8.1 Introduction**

The southern African margin is a transform margin which developed as a result of the relative motion between Africa and South America along the Agulhas-Falkland Transform Fault which is conserved in the present Agulhas-Falkland Fracture Zone (AFFZ) (Figure 8-1). In general, such a sheared margin develops in three phases [Bird, 2001; Lorenzo, 1997; Scrutton, 1979] starting with the continent-continent stage (rift stage) in which a continental shear zone develops, such as the San Andreas [e.g. Furlong and Hugo, 1989] or Dead Sea faults [e.g. Pe'eri, et al., 2002]. Following the onset of sea-floor spreading at a neighbouring stretched margin segment, oceanic crust slides past the continental crust on the sheared margin, which is now in its continent-ocean shear stage (drift stage). The transform margin becomes inactive in its post shear stage, a term usually used for the southern African margin [Scrutton, 1976]. Although in this sense the AFFZ is no longer an active plate boundary, there are several indications for neotectonic processes whose causes are still under discussion (Figure 8-1) [Ben-Avraham, 1995; Ben-Avraham, et al., 1995; Parsieglä, et al., 2007].

The AFFZ stretches from the northern boundary of the Falkland Plateau through the south Atlantic to the southern boundary of the African continent (Figure 8-2) and had an original transform offset of 1200 km [Ben-Avraham, et al., 1997]. North of the fracture zone, the Outeniqua Basin (Figure 8-3) consists of a set of small fault-bounded sub-basins in the north and a distinctively deeper sub-basin (the Southern Outeniqua Basin) in the vicinity of the AFFZ. The cause of this variability, the amount of stretching, and the structure of the crust underlying the basins and the AFFZ, are not understood. There is also an ongoing discussion about whether these basins are underlain by rocks of the Cape Fold Belt (Figure 8-1) [e.g. Broad, et al., 2006; McMillan, et al., 1997; Thomson, 1999] and, if so, whether the belt's structures had an impact on basin formation. As the basins are close to the AFFZ it is also possible that the shear process itself had an influence on basin geometry and sedimentation processes. Plate-tectonic reconstructions [Eagles, 2007; König and Jokat, 2006; Martin, et al., 1982] show that the sedimentary basins of the Falkland Plateau

## Dynamic processes of a transform margin

(Figure 8-2) were conjugate to the Outeniqua Basin before Gondwana break-up, which leads to the question to what extent these basins have shared histories.

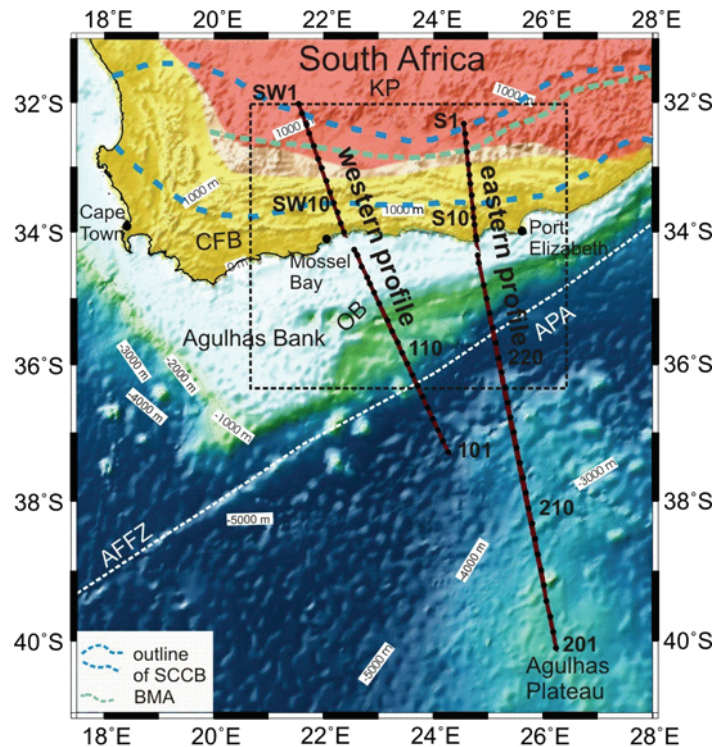


Figure 8-1: Overview map of the investigation area with the satellite derived topography [Smith and Sandwell, 1997] showing the location of both combined onshore-offshore seismic profiles (western profile, eastern profile) of the Agulhas-Karoo Geoscience Transect. Brown lines represent the profile location, dots in the onshore part are positions of land-shots, dots in the offshore part are positions of ocean-bottom seismometers (OBS). Some shot positions (SW for the western profile and S for the eastern profile) and OBS positions are labelled for orientation. The locations of seismic land stations are not plotted in this figure but can be found in Figure 8-4. The Agulhas-Falkland Fracture Zone (AFFZ) is marked with a dashed white line. The Cape Fold Belt (CFB) is drawn as a yellow area and the Karoo Province (KP) in light red on the map. The position of the Southern Cape Conductivity Belt (SCCB) is outlined by a blue dashed line and the Beattie Magnetic Anomaly (BMA) is sketched by a green line (positions after de Beer [1982]). The dashed box shows the position of the detail map of the onshore geology and structure of the offshore basins (Figure 8-3). APA = Agulhas Passage, OB = Outeniqua Basin.

In order to find answers to these questions and to understand the processes that shaped this margin and its structures, the Alfred Wegener Institute for Polar and Marine Research (AWI) and the Geoforschungszentrum Potsdam (GFZ) acquired seismic refraction/wide-angle reflection data along two combined onshore-offshore profiles across the southern continental margin of South Africa [Uenzelmann-Neben, 2005] (Figure 8-1). Parts of these profiles are published by Parsieglä *et al.* [2007; 2008] and Stankiewicz *et al.* [in press-a;

## Dynamic processes of a transform margin

2007]. In this study, we present both profiles at their full lengths (Table 8-1) and incorporate as-yet unpublished data. In the following, we will refer to these combined land-sea profiles, which are part of the Agulhas-Karoo Geoscience Transect in the German – South African cooperation program Inkaba yeAfrica [de Wit and Horsfield, 2006], as the *eastern profile* (AWI-20050200-GRA) and *western profile* (AWI-20050100-FRA) (Figure 8-1, Figure 8-3).

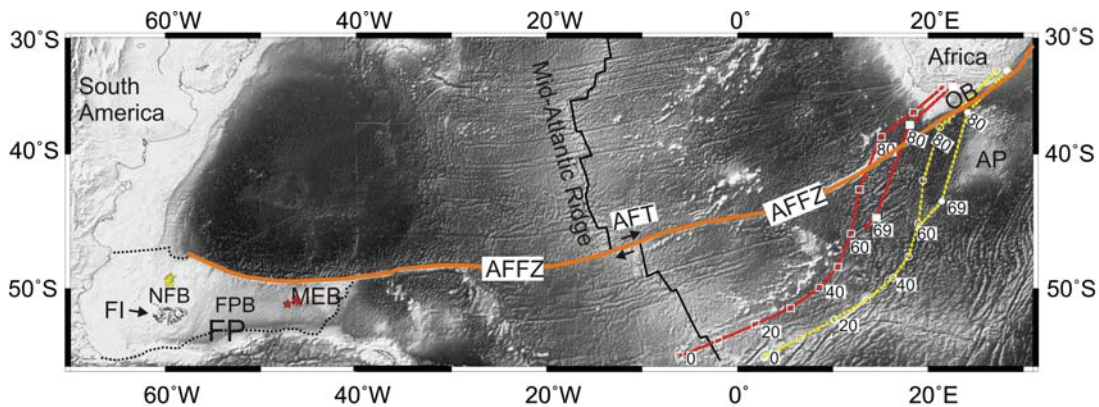


Figure 8-2: Map of the satellite derived bathymetry/topography by Smith and Sandwell [1997] showing the Agulhas-Falkland Fracture Zone (orange line) and bordering continents. The tracks of the Shona (red lines, with filled squares [Martin, 1987], open squares [Hartnady and le Roex, 1985]) and Bouvet (yellow dashed lines, with filled circles [Martin, 1987], with open circles [Hartnady and le Roex, 1985]) hotspots are shown. In the Falkland basins (NFB=North Falkland Basin, FPB=Falkland Plateau Basin) the locations of Deep Sea Drilling Project sites [Jeletzky, 1983; Jones and Plafker, 1977] are marked with red stars and hydrocarbon exploration drill holes with yellow stars [Richards and Hillier, 2000]. AP = Agulhas Plateau, AFT = present-day position of the Agulhas-Falkland Transform, OB = Outeniqua Basin, FP = Falkland Plateau, FI = Falkland Islands, and MEB = Maurice Ewing Bank.

## 8.2 Geological and tectonic background

Southern Africa experienced a 3.8 billion year long geological history of continental accretion and disassembly [Tankard, et al., 1982]. Here, we restrict the review of the relevant geological and tectonic processes to the last ~450 my, starting with the deposition of Cape Fold Belt rocks (CFB) and the Karoo Basin (Figure 8-1). The Cape Supergroup (Figure 8-3) was deposited between 450 and 300 Ma during a series of transgression-regression cycles [Hälbich, 1993; Tankard, et al., 1982]. Between 278 and 215 Ma, these strata were folded by re-activation of Pan-African thrusts to form the CFB [Hälbich, 1993; Hälbich, et al., 1983]. The CFB formed part of a single major fold belt that developed during the Gondwanide Orogeny, along with the Sierra de la Ventana (eastern Argentina) and Pensacola Mountains (East Antarctica) and the Ellsworth Mountains (West Antarctica) [e.g. Vaughan and Pankhurst, 2008]. The cause of

## Dynamic processes of a transform margin

this orogeny is a subject of ongoing debate. While many authors favour flat slab subduction of the proto-Pacific plate beneath Gondwana [e.g. *Lock, 1980*], others find supporting arguments for collision [*Pankhurst, et al., 2006*] or dextral transpressional scenarios [*Johnston, 2000*]. During late Carboniferous and early Jurassic times, the Karoo Supergroup (Figure 8-3, [*Cole, 1992*]) was deposited in the Karoo basin – the foreland basin of the CFB. Sedimentation ended with the extrusion of basaltic lavas [*Cole, 1992*] to form the Karoo Large Igneous Province at  $183 \pm 1$  Ma [*Duncan, et al., 1997*]. This volcanism has been attributed to the Bouvet plume [*Hawkesworth, et al., 1999*], and accompanied the first movements between eastern and western parts of Gondwana [*Eagles and König, 2008*].

In mid-late Jurassic times, rifting processes started to form the horst, graben and half-graben structures of the Outeniqua Basin [*Broad, et al., 2006; McMillan, et al., 1997*]. This basin (Figure 8-3) consists of a complex system of sub-basins separated from each other by faults and basement arches [*Broad, et al., 2006; McMillan, et al., 1997*]. The sub-basins, from west to east, are the Bredasdorp, Infanta, Pletmos, Gamtoos, and Algoa basins and their deep, southern extension the Southern Outeniqua Basin (SOB, Figure 8-3). *Broad, et al. [2006]* divides the sedimentary fill of these basins into syn-rift and drift sequences, related to their development during a phase of active rifting that was followed by passive subsidence following the separation of the Falkland Plateau from the South African margin. The Diaz Marginal Ridge (DMR, Figure 8-3) separates the sedimentary basins from the Agulhas-Falkland Fracture Zone (AFFZ, Figure 8-1 - Figure 8-3), which is formed during right lateral strike-slip motion between South America and Africa in early Cretaceous times. *Ben-Avraham et al. [1993]* and *Thomson [1999]* show how shearing on the fracture zone caused local deformation in neighbouring parts of the Outeniqua Basin.

An episode of increased denudation accompanied Gondwana break-up in southern Africa, and may be related to epeirogenic uplift over an area of increased mantle buoyancy [*Tinker, et al., 2008*]. Another denudation (~uplift) episode took place between 100 and 80 Ma [*Tinker, et al., 2008*]. Both uplift episodes were accompanied by kimberlite emplacement and the formation of Large Igneous Provinces [*Tinker, et al., 2008*]. The latter uplift phase occurred when the Agulhas Plateau Large Igneous Province formed 100-94 m.y. ago [*Gohl and Uenzelmann-Neben, 2001; Parsiegla, et al., 2008; Uenzelmann-Neben, et al., 1999*]. The interplay of uplift, mantle buoyancy, igneous activity, and continental break-up has led to the present-day appearance of southern Africa and its continental margin.

## Dynamic processes of a transform margin

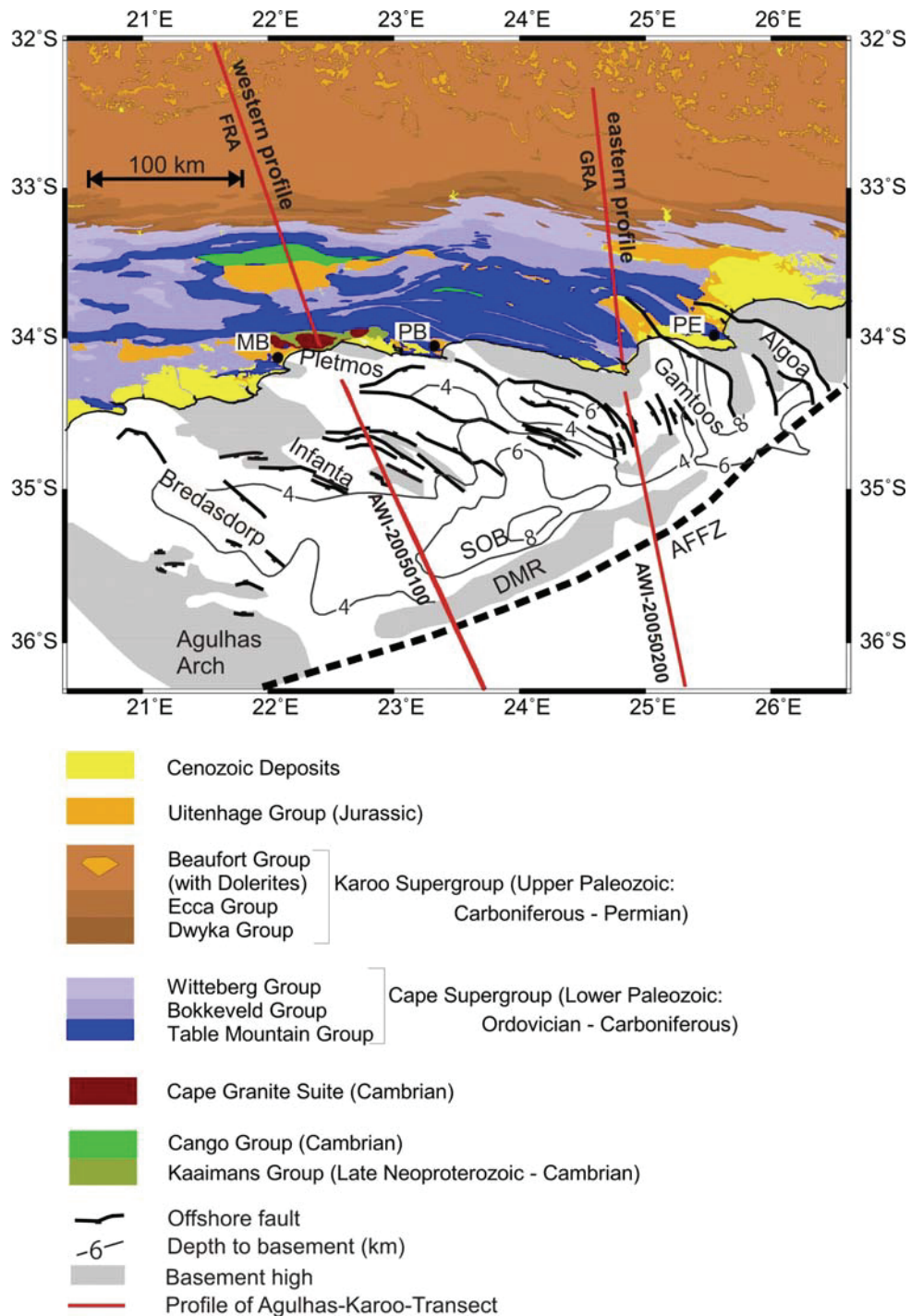


Figure 8-3: Detail map of the onshore geology and structure of the offshore basins. The locations of dominant faults and the depth-to-basement information of the Outeniqua Basin and its sub-basins (Bredasdorp, Infanta, Pletmos, Gamtoos, Alcoa, and Southern Outeniqua Basin) were adopted from PASA [2003]. The onshore geology available from the AEON Africa database [de Wit and Stankiewicz, 2006] was included. FRA/GRA and AWI-20050100/200 are the names of the onshore and offshore sub-profiles of the western and eastern profile, respectively. The dashed line marks the position of the Agulhas-Falkland Fracture Zone (AFFZ). DMR = Diaz Marginal Ridge, MB = Mossel Bay, PB = Plettenberg Bay, PE = Port Elizabeth, and SOB = Southern Outeniqua Basin.

### 8.3 Seismic data acquisition, processing, and modelling

Three types of data sets were acquired along both profiles (Figure 8-1), those from (a) airgun shots recorded by ocean bottom seismometers (OBS) [Parsiegl, *et al.*, 2007; 2008], (b) airgun shots recorded at onshore seismic stations equipped with a GPS synchronised electronic data logger and a three-component seismometer (this study), and (c) land shots (twin explosives of 75 – 125 kg each) recorded with seismic land stations [Stankiewicz, *et al.*, 2007]. Land shots could not be identified in the OBS records. The settings for the two profiles are summarized in Table 8-1. In this study, we present a new combined onshore-offshore model of the eastern profile and compare it with results from the western profile [Stankiewicz, *et al.*, in press-a]. Data examples for the eastern profile are shown in Figure 8-4, and explanations of phase names are given in Table 8-2.

P-wave travel times of airgun shots recorded at land stations, which have not been published before, were identified and added to the data sets of Parsiegl *et al.* [2008] and Stankiewicz *et al.* [2007]. Their data include P-wave travel time information from airgun shots recorded by ocean bottom seismometers and from land shots recorded at seismic land stations. We set pick uncertainties in the range from 40 ms to 150 ms, depending on the signal-to-noise ratio, and used the RAYINVR raytracing and travel-time inversion routine of Zelt and Smith [1992] for modelling. The onshore [Stankiewicz, *et al.*, 2007] and offshore [Parsiegl, *et al.*, 2008] velocity-depth models were combined in a joint model of the velocity-depth structure over the continental margin of southern Africa from the Karoo basin to the Agulhas Plateau (Figure 8-1, Table 8-1). We extended this initial model with the additional data from the airgun shots recorded at land stations. The resulting velocity-depth model of the eastern profile is shown in Figure 8-5. This P-wave velocity-depth model consists of 6 layers, where the crust is represented by four layers (layers 1-4), and the mantle by two layers (layers 5-6). The first layer of the crust (sediments) only exists in the offshore part of the profile. Results from seismic reflection measurements were used to assign the thickness of this layer [Parsiegl, *et al.*, 2008].

The quality of our P-wave velocity-depth model is assessed with the tools of RAYINVR [Zelt and Smith, 1992]. We obtained very good fits between modelled and measured travel times (Figure 8-4). The modelled travel-times of the eastern profile have an overall rms travel-time deviation of 0.141 s and  $\chi^2$  of

## Dynamic processes of a transform margin

1.154 (see Table 8-3 for details of the statistics). Most parts of the velocity-depth model are well constrained (Figure 8-6A). The only poorly constrained velocities are those between 300 and 350 km, where the lower crust lacks good ray coverage. The depth nodes of the model are mostly well resolved (Figure 8-6B) except for small areas with a lower ray coverage.

	Western Profile		Eastern Profile	
	AWI-20050100	FRA	AWI-20050200	GRA
<b>Source description</b>	8 G.Guns™, 1 Bolt airgun $V_{tot}=96$ litres	Twin explosives 75 -125 kg each	8 G.Guns™, 1 Bolt airgun $V_{tot}=96$ litres	Twin explosives 75 -125 kg each
<b>Number of shots</b>	4420	13	4761	13
<b>Average shot spacing (km)</b>	0.15	20	0.15	20
<b>Number (type) of stations</b>	20 (OBS)	48 (3-component seismometer)	27 (OBS)	48 (3-component seismometer)
<b>Length of profile (km)</b>	457	240	663	210
<b>Start of profile</b>	34.24525° S, 22.56826° E	32.01766° S, 21.56335° E	34.39750° S, 24.84840° E	32.32425° S, 24.58266° E
<b>End of profile</b>	37.45232° S, 24.38704° E	34.04344° S, 22.40620° E	40.20290° S, 26.30270° E	34.20247° S, 24.82166° E

Table 8-1: Description of sources, receivers, length and positions of the offshore seismic refraction profiles AWI-20050100 and AWI-20050200 and the onshore seismic refraction profiles FRA and GRA, which are parts of the western and eastern combined onshore-offshore profiles.  $V_{tot}$  is the total volume of the airguns, which were used during the marine experiment.

Name	Type	Origin
P <sub>1</sub>	refracted P-wave	model layer 1
Ps <sub>1</sub> P	reflected P-wave	top of model layer 2
Pg	refracted P-wave	model layer 2, 3, 4
Pc <sub>1</sub> P	reflected P-wave	top of model layer 3
Pc <sub>2</sub> P	reflected P-wave	top of model layer 4
PmP	reflected P-wave	top of model layer 5
Pn	refracted P-wave	model layer 5
Pm <sub>2</sub> P	reflected P-wave	top of model layer 6

Table 8-2: Names of phases identified in the seismic P-wave refraction data are given together with a distinction between refracted and reflected phases and their origin in the crust or mantle.

## Dynamic processes of a transform margin

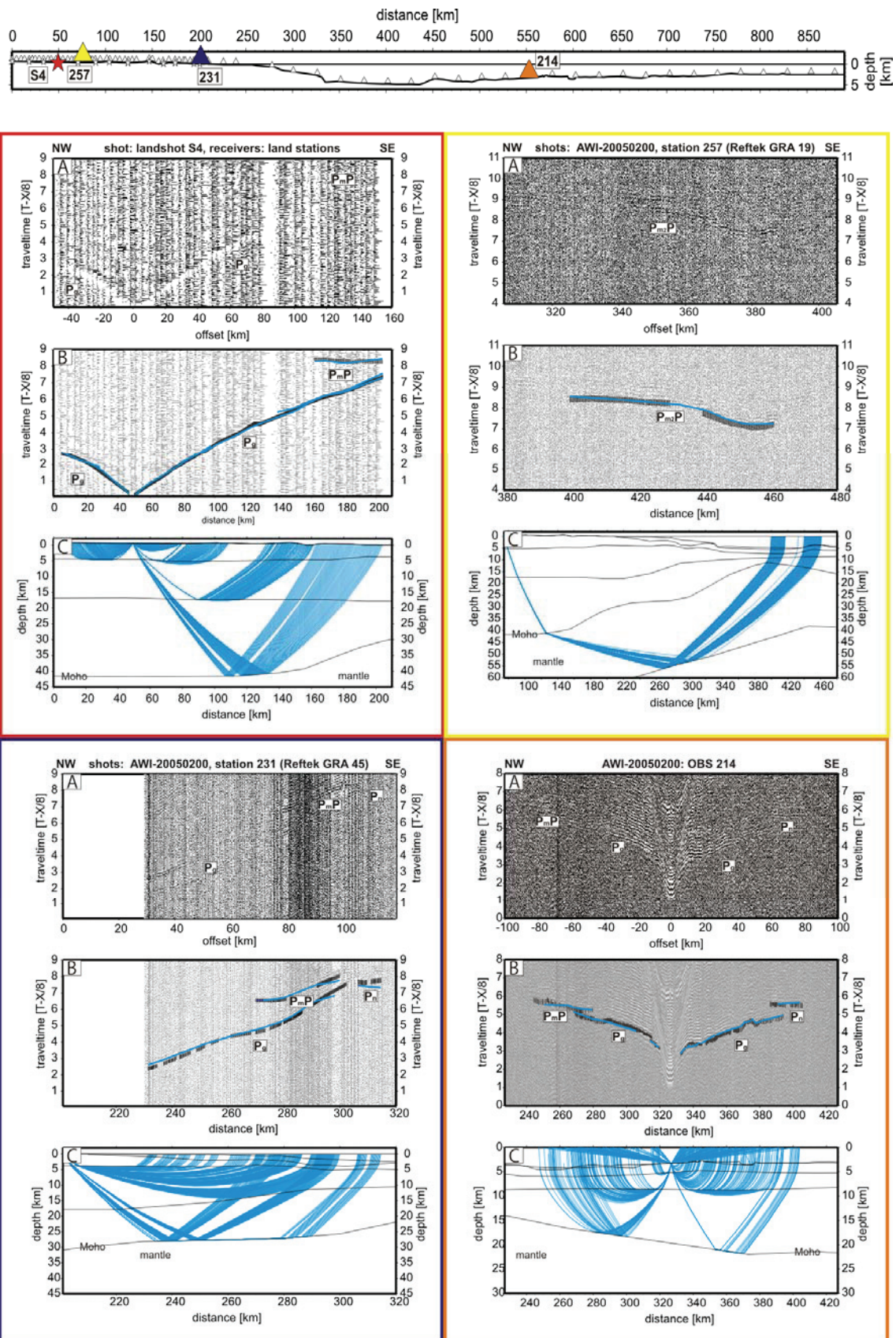


Figure 8-4: Four data examples along the eastern onshore-offshore profile (AWI-200050200-GRA) are shown. The top plate illustrates the positions of stations and land shots on the profile, where triangles mark station locations (land stations and ocean bottom seismometers (OBS))

## Dynamic processes of a transform margin

and stars represent the location of land shots. The three stations and the shot whose data are shown are marked with a larger coloured symbol where its colour corresponds to the colour of the box surrounding each set of illustrations consisting of a plot of the data itself (A), the fits between measured and modelled travel times (B) and the ray-paths through the model (C). Data of station 273 (landshot S4) are shown in the red box, of station 257 (GRA 19) in the yellow box, of station 231 (GRA 45) in the blue box, and of station 214 (OBS) in the orange box. AWI-20050200 is the name of the airgun shot profile and the offshore seismic refraction profile, GRA is the name of the onshore seismic refraction profile.

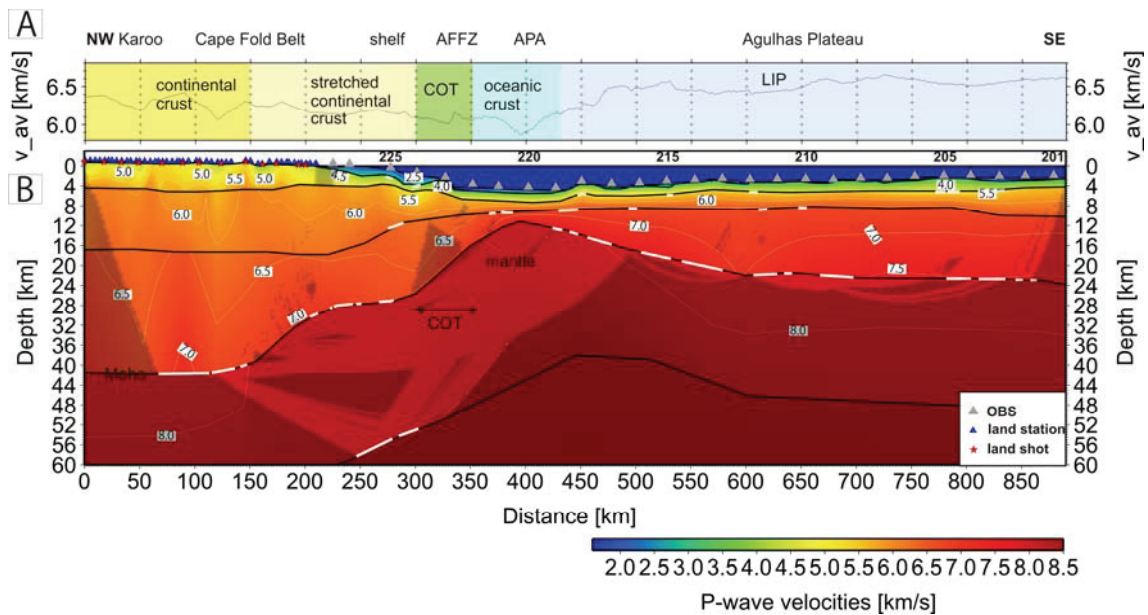


Figure 8-5: A) Average velocities of the crust (without sediments) along the profile with interpretation. B) Seismic P-wave velocity-depth model of the eastern onshore-offshore profile AWI-20050200-GRA. Gray triangles mark OBS positions and numbers over triangles indicate station numbers, blue triangles mark the positions of land stations, and red stars correspond to the positions of shots carried out onshore. Black lines represent model layer boundaries where thick white lines mark positions of reflected phases at these boundaries. Thin white lines are velocity isolines. Annotations on these lines in white boxes are velocities in km/s. Dark shaded areas are not covered by rays. AFFZ = Agulhas-Falkland Fracture Zone and APA = Agulhas Passage, COT = continent-ocean transition zone, and LIP = Large Igneous Province.

Name	Picks	RMS	$\chi^2$
P <sub>1</sub>	56	0.077	1.113
Ps <sub>1</sub> P	29	0.059	0.498
Pg	14720	0.117	0.986
Pc <sub>1</sub> P	66	0.115	0.554
Pc <sub>2</sub> P	131	0.081	0.554
PmP	1995	0.162	1.557
Pn	5224	0.189	1.559
Pm <sub>2</sub> P	293	0.074	0.244
All	22514	0.141	1.154

Table 8-3: Statistics of P-wave travel-time inversion. Number of travel-time picks, the root-mean squared (rms) error of the fitting, and the  $\chi^2$  value of the different phases.

## Dynamic processes of a transform margin

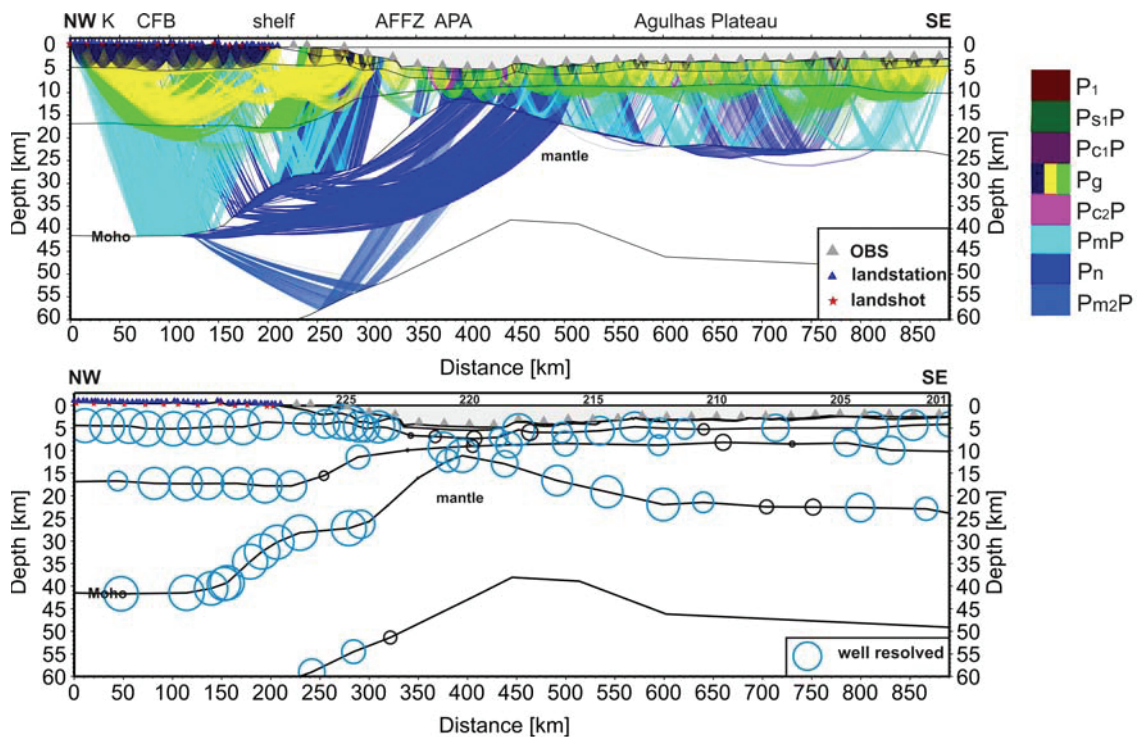


Figure 8-6: Quality control of the eastern profile (AWI-20050200-GRA). Abbreviations are AFFZ = Agulhas-Falkland Fracture Zone, APA = Agulhas Passage, CFB = Cape Fold Belt, K = Karoo. A) Plot of the ray coverage with rays modelling reflected and refracted waves. Different colours represent different phases where the assignment of the colours to the phases can be found in the legend on the right. B) Resolution of depth nodes of the velocity-depth model. Blue circles represent a good resolution. Black circles mark depth nodes with a resolution of less than 0.5. The circle diameter corresponds to the resolution, where circles with the largest diameter have a resolution of 0.95. For the bottom of the first layer 75 percent of the depth nodes in the offshore part of the profile are well resolved (layer one does not exist onshore), but the nodes are too numerous to be clearly arranged, and are therefore not displayed in the figure.

### 8.4 Seismic refraction and wide-angle reflection results and implications

#### 8.4.1 Velocity-depth structure along the eastern profile and comparison with the western profile

The first crustal layer of the P-wave velocity-depth model (Figure 8-5) represents sediments with velocities between 1.7 and 3.4 km/s and a maximum thickness of 1.7 km in the shelf area (230-320 km profile distance). On the Agulhas Plateau (see also Parsieglä *et al.* [2008] for more information on this part of the profile), this sedimentary cover is thin or absent. The three crustal layers beneath the sediments differ in their seismic velocities and thicknesses in the northern part of the profile (0-290 km profile distance) compared to the

## Dynamic processes of a transform margin

southern part (350-890 km profile distance), which change over a 50-60 km wide transition zone centred on the AFFZ. Upper crustal seismic velocities are higher in the north (average 5.5 km/s) than in the south (average 5.0 km/s). A thick (up to 10 km) layer with seismic velocities above 7 km/s is observed in the lower crust of the southern part, while the lower crust in the north is characterized by average seismic velocities of 6.8 km/s.

Crustal thickness (including sediments) varies along the profile from 42 km beneath land, via 28 km in the shelf area and 8 km in the Agulhas Passage, to around 20 km on the Agulhas Plateau. Therefore, we observe distinct relief along the Mohorovičić discontinuity (Moho); between 150 and 200 km profile distance the Moho rises from 41 km to 29 km, and between 320 and 400 km it rises again from 27 to 12 km, before descending to 22 km further south.

The western profile [see also *Stankiewicz, et al., in press-a*] (Figure 8-1, Figure 8-3, Figure 8-5 and Figure 8-7) crosses similar variations. The shelf area, however, is 2.5 times wider than that on the eastern profile. A similar onshore crustal thickness, of 40 km, is observed, albeit with slightly higher seismic velocities (6.4-7.2 km/s) in the lower part of the crust (layer 4), especially at the southward decrease in Moho depth (140-250 km profile distance, 6.4-7.4 km/s) (Figure 8-7). Both profiles exhibit a kink in the Moho starting at about 50 to 70 km inland from the coast and extending over a length of 50 to 60 km with a height difference of ca. 14 km. On both profiles, the transition zone between continental and oceanic crust is centred at the Agulhas-Falkland Fracture Zone with a width of ~50 km [*Parsiegla, et al., 2007* and this study].

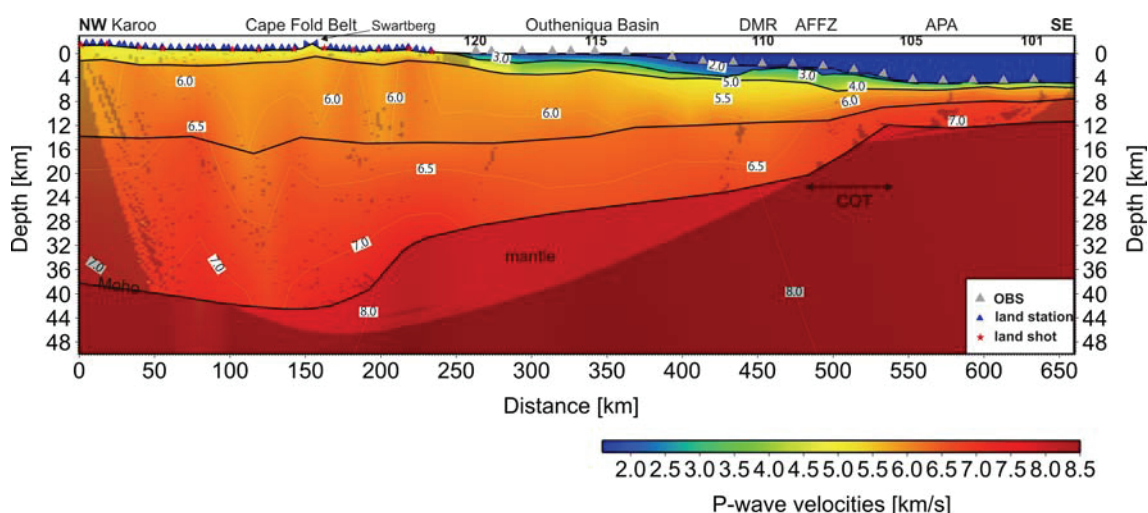


Figure 8-7: Seismic P-wave velocity-depth model of the western onshore-offshore profile AWI-20050100-FRA redrawn after *Stankiewicz et al. [in press-a]*. Gray triangles mark OBS positions and numbers over triangles indicate station numbers, blue triangles mark the positions of land

## Dynamic processes of a transform margin

stations, and red stars correspond to the positions of shots carried out onshore. Black lines represent model layer boundaries. Thin white lines are velocity isolines with annotated velocities in km/s. Dark shaded areas are not covered by rays. AFFZ = Agulhas-Falkland Fracture Zone and APA = Agulhas Passage, and DMR = Diaz Marginal Ridge.

### 8.4.2 Crustal types along the eastern profile

According to the velocity-depth structure and the average velocities of the crystalline crust (Figure 8-5), the profile can be subdivided into four units from north to south. For each unit, the thicknesses given are for the complete crustal column including sediments but, for calculation of the average crustal velocity, the sedimentary layer was removed.

From 0 to 300 km profile distance, the crust is about 42 km thick on the onshore part and about 28 km on the shelf. These thicknesses are within the normal ranges for un-stretched and stretched continental crust [e.g. *Christensen and Mooney*, 1995]. The onset of crustal thinning begins 50 km inland from the coast. Average crustal velocities of 6.29 km/s for the un-stretched onshore part (0-150 km), 6.25 km/s for the stretched onshore part (150-200 km), and 6.15 km/s for the stretched offshore part (200-300 km) fall within the expected range for normal continental crust [*Christensen and Mooney*, 1995]. The similar average (crystalline) crustal velocities for the stretched onshore and offshore continental crust suggest that rocks of the Cape Supergroup underlie the shelf area, consistent with results of drilling into basement highs of the Outeniqua Basin [e.g. *McMillan, et al.*, 1997]. Uppermost crustal velocities of between 4.5 and 5.5 km/s (Figure 8-5) fit well in the velocity range of the lithologically-diverse Cape Supergroup.

The region between 300 and 350 km profile distance (Figure 8-5) is characterized by the Moho's ascent from 25 to 14 km over a distance of 50 km, and an average crustal velocity of 6.07 km/s. The changes in crustal thickness and average crustal velocity across this zone classify it as a continent-ocean transition (COT) zone. Unfortunately, this part of the model is not as well resolved as the remainder, with higher uncertainties in the velocity-structure and geometry. The sub-parallel western profile (Figure 8-7) displays a COT with a similar geometry but which is better constrained [*Parsieglä, et al.*, 2007], suggesting that the COT in the eastern profile is reasonable. The width of this COT (50 km) fits within the known range from other sheared margin COTs (50-80 km; [*Bird*, 2001]).

## Dynamic processes of a transform margin

The crustal thickness in the Agulhas Passage varies between 6 and 10 km (350 to 435 km profile distance). Although this thickness is in the normal range for oceanic crust, the average (crystalline) crustal velocity of 6.04 km/s is at the lower limit of those reported [Mutter and Mutter, 1993; White, et al., 1992]. Oceanic crust near fracture zones can be up to 50 % thinner than normal, usually shows low average crustal velocities, and often lacks a normal oceanic layer 3 [White, et al., 1984; White, et al., 1992]. White et al. [1984] attribute the observed characteristics at fracture zones to modified intrusive/extrusive processes near the transform. Sage et al. [1997] discussed thermal effects of the adjacent continent on crustal formation processes as an explanation for the anomalously thin heterogeneous oceanic crust at the Ivory Coast-Ghana transform margin. Similar processes could provide an explanation for the relatively low average crustal velocities south of the Agulhas-Falkland Fracture Zone. In contrast to the Ivory Coast margin, we do not observe anomalously thin oceanic crust. Having the unique setting of the Agulhas Plateau Large Igneous Province being situated south of the sheared margin, it is possible that the oceanic crust in the Agulhas Passage was originally thinner than it is today and was overprinted during the formation of the plateau e.g. by volcanic flows migrating north of the Agulhas Plateau.

On the Agulhas Plateau (profile distance 435-890 km), the crustal thickness increases again to an average of 20 km, with an average crustal velocity of 6.5 km/s. This significantly higher average crustal velocity is due to the Agulhas Plateau's ~10 km thick high-velocity lower crustal body, which identifies it as a Large Igneous Province [Parsiegla, et al., 2008].

### **8.5 Crustal stretching and tectonic processes along/across the southern African margin**

#### **8.5.1 Calculation of crustal stretching factors**

Based on our crustal velocity-depth models north of 150 km profile distance, where very little or no crustal stretching is expected (Figure 8-5 and Figure 8-7), we assume initial crustal thicknesses before stretching,  $T_c$ , of 43 km for the western profile and 42 km for the eastern profile. The continental crust thins between distances 180 and 520 km on the western profile, most likely due to crustal stretching (Figure 8-7). A significantly smaller part of the eastern profile consists of stretched continental crust (Figure 8-5, 150-340 km profile distance). For both profiles, we measured the (crystalline) crustal

## Dynamic processes of a transform margin

thickness,  $T_s$ , of these stretched regions at 10 km intervals and calculated the stretching factors  $\beta = T_c/T_s$  (Figure 8-8).

Stretching factors increase from north to south along both profiles (Figure 8-8). The lowest stretching factors were observed in the southernmost CFB with average  $\beta$  factors of 1.1 – 1.2. Peak  $\beta$  factors occur next to the AFFZ ( $\beta = 3.2 - 3.3$ ). Stretching factors in the Pletmos and Gamtoos Basins are similar ( $\beta = 1.6$ ), while in the Southern Outeniqua Basin  $\beta = 1.9$ .

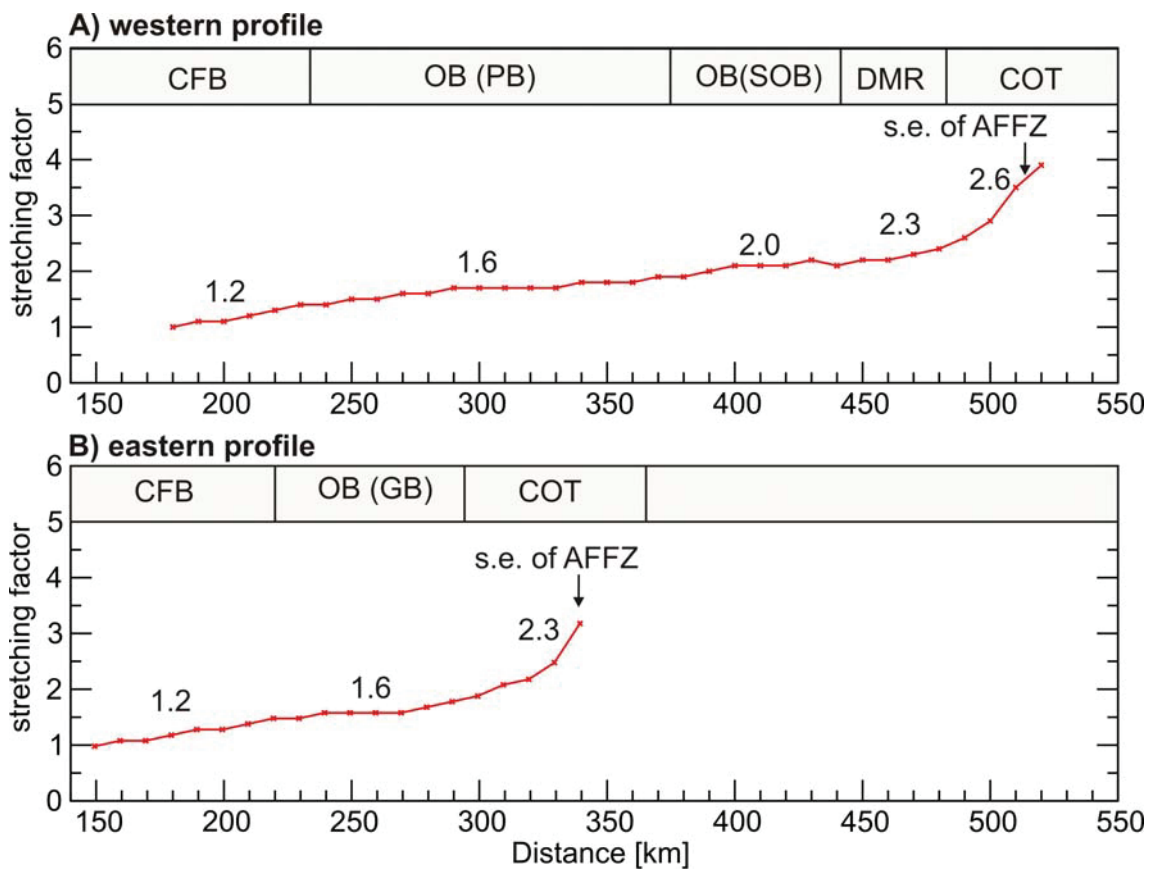


Figure 8-8: Variations of the stretching factor  $\beta$  with profile distance on the western (A) and eastern (B) profile. On top of each diagram the different regions of the profile are labelled. Crosses mark the positions where the stretching factor was calculated. Numbers on top of the curve state average stretching factors for each segment. Abbreviations are CFB = Cape Fold Belt, COT = continent-ocean transition zone, DMR = Diaz Marginal Ridge, GB = Gamtoos Basin, OB = Outeniqua Basin, PB = Pletmos Basin, s.e. of AFFZ = surface expression of Agulhas-Falkland Fracture zone and SOB = Southern Outeniqua Basin.

### 8.5.2 Discussion of the observed stretching factors, their possible implications, and tectonic processes along/across the margin

With a discussion of extension geometries in pure and simple shear regimes, *Jackson* [1987] showed that the accommodation of stretching factors of more than 1.7 is most likely to require more than one set of faults. Thus, the clear step in our calculated Outeniqua Basin stretching factors can be interpreted as reflecting one episode of extension in the northern sub-basins and two episodes in the wider southern basin. Furthermore, it is most economical to assume that one of these episodes affected both the northern and southern basins to achieve a stretching factor of 1.6 (Figure 8-9). To account for the additional stretching in the southern Outeniqua Basin, a  $\beta$  factor of 1.3 has to be added.

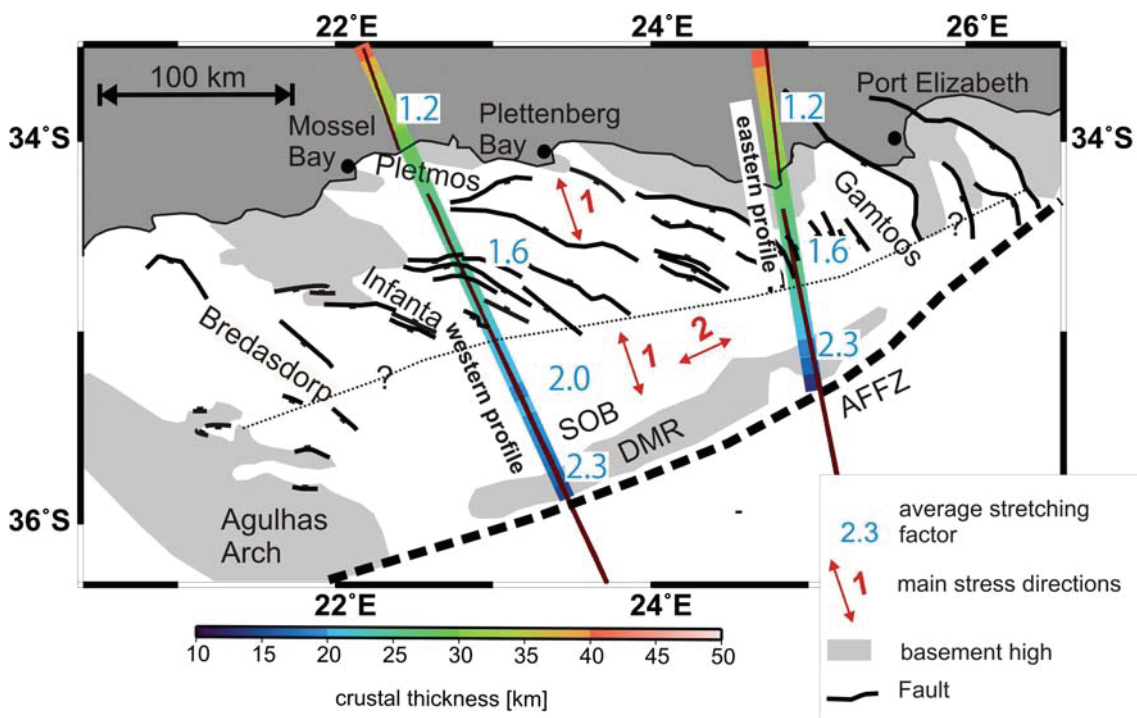


Figure 8-9: Outeniqua Basin with colour-coded crystalline crustal thickness along the profiles and average stretching factors. The subdivision between the area of the Outeniqua Basin which experienced one and the area which was affected by two stretching episodes is marked by a dashed line. The approximate stress directions are shown as red arrows. Arrow 1 shows the direction in Jurassic times and arrow 2 the direction in Cretaceous times. The locations of the main faults and basement highs are adapted from PASA [2003].

Earlier studies based on seismic reflection and well data showed that rifting in the Outeniqua Basin started in middle to late Jurassic times [*Broad, et al.*, 2006; *McMillan, et al.*, 1997]. *McMillan et al.* [1997] suggested that this rifting accompanied the break-up between East Gondwana (Antarctica,

## Dynamic processes of a transform margin

Australia, India) and West Gondwana (South America, Africa) that eventually gave rise sea-floor spreading in the Riiser Larsen and Weddell seas (Figure 8-9., Figure 8-10) [e.g. *Eagles and König, 2008; Jokat, et al., 2003; König and Jokat, 2006*]. From our stretching factors, we infer that this episode resulted in crustal thinning over the whole basin (Figure 8-9) and up to ~50 km inland of the present-day coast (Figure 8-8). The second episode probably accompanied shear motion along the active Agulhas-Falkland transform system, i.e. in early Cretaceous times when the stress direction was sub-parallel to the present-day AFFZ at ~ 136 Ma (Figure 8-9, Figure 8-10). Consistent with this, seismic reflection and well data exhibit an upper Valanginian unconformity (~135 Ma) [Broad, et al., 2006; McMillan, et al., 1997] and McMillan et al. [1997] report evidence for strike-slip faulting in the southern Outeniqua Basin.

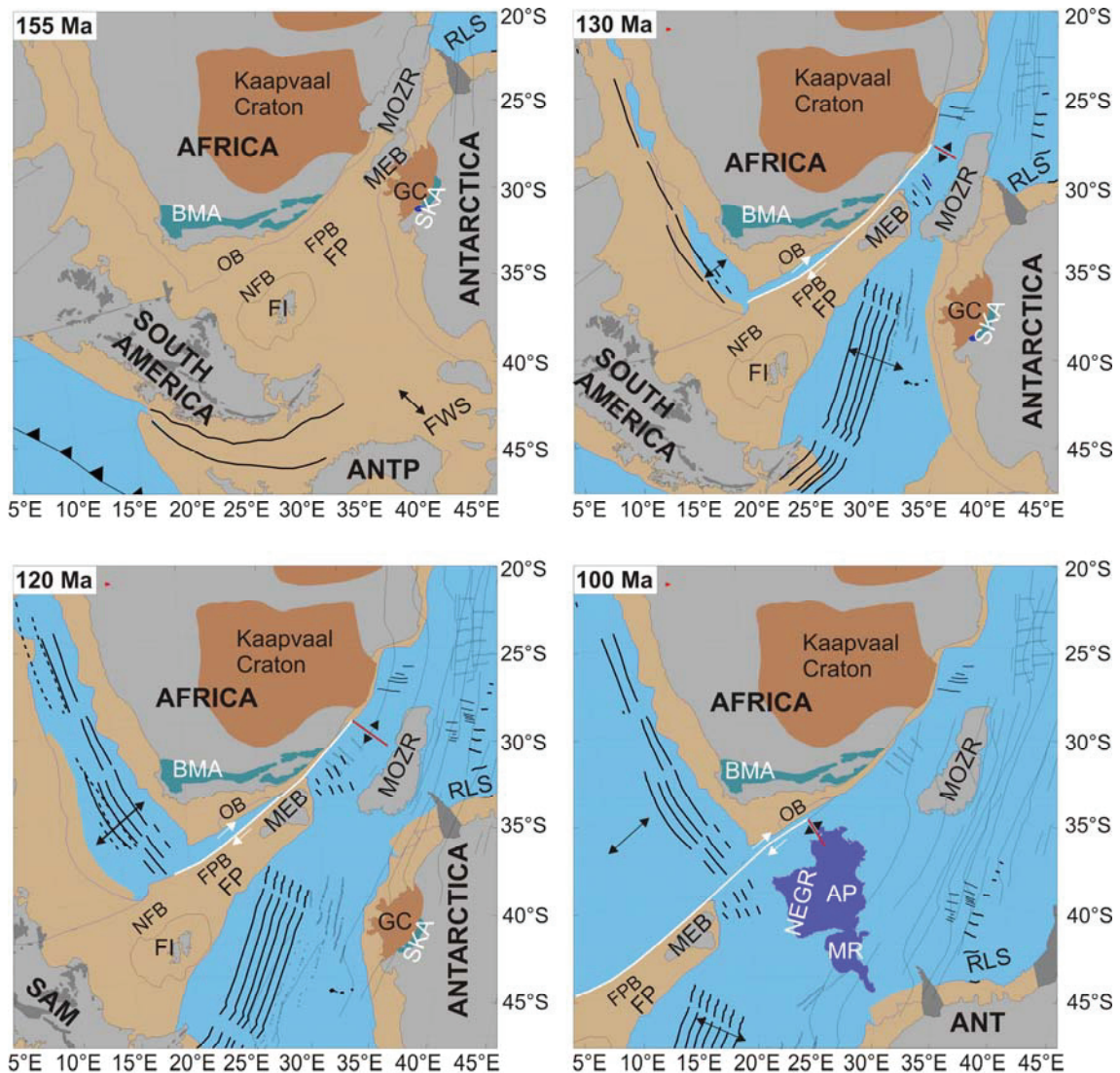


Figure 8-10: Plate-tectonic reconstruction for the main steps of the southern African margin evolution using the rotation poles of König and Jokat [2006]. We use the present-day coordinate system for orientation. The rotations were performed with respect to Africa. Before 155 Ma)

## Dynamic processes of a transform margin

*Africa and South America are still attached to each other. The Gondwana break-up between Africa and Antarctica and the related stress field had possibly caused the onset of the rifting episode in the Outeniqua Basin (OB) and in the sedimentary basins of the Falkland Plateau (FP). 130 Ma) Seafloor spreading takes place in the Weddell Sea, Riiser Larsen Sea (RLS), north of the Maurice Ewing Bank (MEB) and has started in the South Atlantic. Note the position of the spreading ridge northeast of the MEB (red). The shear motion along the Agulhas Falkland Transform started ~136 Ma and actively formed the continental margin in this early drift stage and caused a second pulse of crustal stretching in the Outeniqua Basin, 120 Ma) In the later drift stage transtension along the AFT is still responsible for crustal thinning in the southern parts of the Outeniqua Basin and the Falkland Plateau Basin (FPB). 100 Ma) The Agulhas Plateau (AP) developed together with Maud Rise (MR) and Northeast Georgia Rise (NEGR). The thermal conditions along the margin have changed as hot young oceanic crust slides along old continental crust with the spreading ridge (red) perpendicular to the Outeniqua Basin. ANTP = Antarctic Peninsula, BMA = Beattie magnetic anomaly, FWS = future Weddell Sea, GC=Grunehogna Craton, MOZR = Mozambique Ridge, North Falkland Basin = NFB and SKA = Sverdrupfjella-Kirvanveggen magnetic anomaly.*

The Diaz Marginal Ridge (DMR) forms the southern boundary of the Southern Outeniqua Basin. Suggestions for the time of its formation range from before the first shear motion along the AFFZ [Ben-Avraham, et al., 1997] to contemporaneous with it [McMillan, et al., 1997]. Results from our seismic reflection measurements show that the DMR is buried by 200-250 m of sediments (Figure 8-11). Assuming the stratigraphy of the northern parts of the Outeniqua Basin [Broad, et al., 2006] can be extrapolated onto the DMR, we observe 150 to 200 m of undisturbed Cretaceous sediments over the DMR (Figure 8-11). These sediments are younger than the oldest Cretaceous sediments in the Southern Outeniqua Basin (Figure 8-11). This in turn, places the formation time of the DMR after the initial movement along the Agulhas Falkland Transform. As sedimentation and erosion rates are unknown and any drill hole control is lacking in this region, the formation time of the DMR can only be estimated within a wide time range between 130 and 90 Ma. In this time span, two formation mechanisms are discussed. One possible scenario was described by Parsiegla et al. [2007]. They suggest that the DMR was uplifted from a metasedimentary basin during a transpressional episode along the Agulhas-Falkland Transform. We modelled a similar crustal thickness beneath the DMR as observed beneath the Southern Outeniqua Basin (Figure 8-5, Figure 8-7 and Figure 8-9). Therefore, it is likely that the crust beneath the marginal ridge experienced the same extensional episodes as the Southern Outeniqua Basin. This makes a setting more likely in which the crust of the DMR was first stretched and then uplifted. In this second scenario, the DMR developed when newly formed oceanic crust slid past old continental crust in the continent-ocean shear stage. With this configuration of (hot) oceanic crust and (cold) continental crust opposed across the Agulhas-Falkland Transform, it

## Dynamic processes of a transform margin

is likely that a significant temperature contrast existed across the transform fault during the drift episode, especially when the spreading ridge passed. Therefore we propose that this temperature contrast could have induced a thermal uplift of the DMR. Induced thermal uplift has also been suggested for other sheared margins e.g. the Ivory Coast-Ghana transform margin [Basile, et al., 1993], the Senja Fracture Zone (SW Barents Sea, [Våges, 1997]), and the Demerara Plateau (French Guiana-Northeast Brazil margin, [Greenroyd, et al., 2008]). Numerical simulations of induced thermal uplift were able to model the height, extent and shape of marginal ridges realistically [e.g. Gadd and Scrutton, 1997; Våges, 1997]. The thin continental crust beneath the DMR could be an argument against transpression as a formative mechanism. Due to the lack of drill holes into the DMR, its composition is still unknown. A metasedimentary composition is inferred from low seismic P-wave velocities in the Diaz Marginal Ridge [Parsiegla, et al., 2007] and evidence that Cape Supergroup rocks underlie parts of the Outeniqua Basin was found [McMillan, et al., 1997].

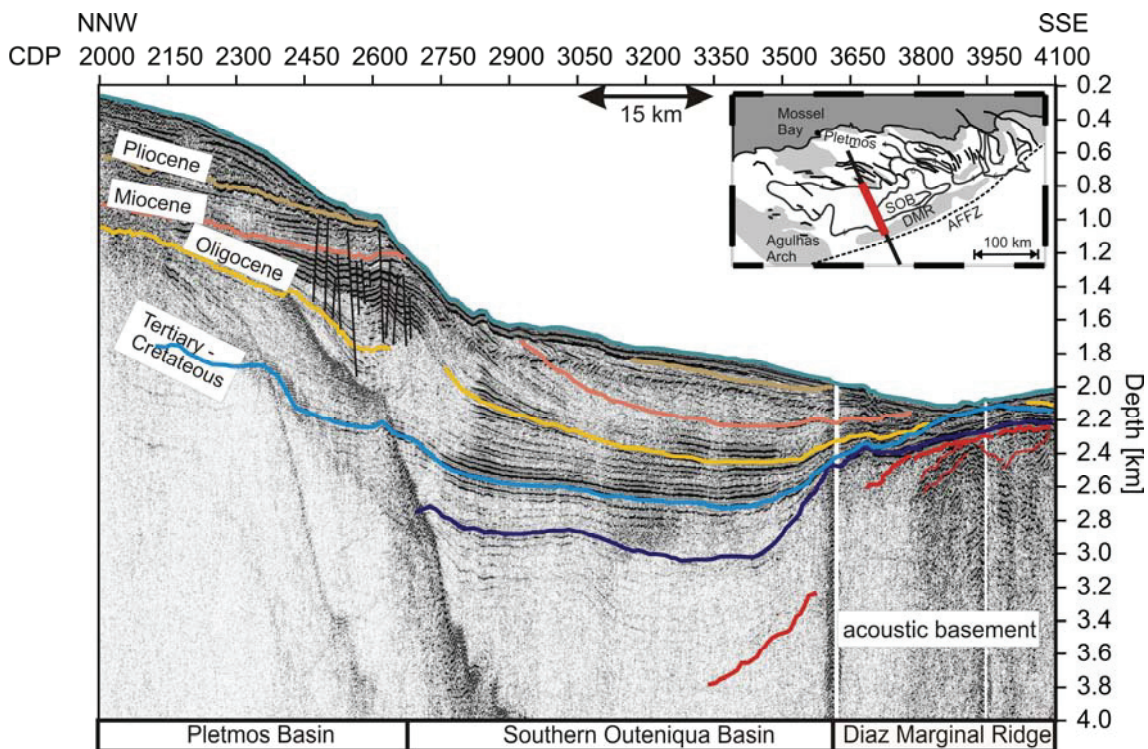


Figure 8-11: Depth migrated seismic reflection section AWI-20050200 (red straight line in the map) which is coincident to refraction line AWI-20050200 (black straight line in the map) and crosses the northern part of the Pletmos Basin, the Southern Outeniqua Basin and the northern part of the Diaz Marginal Ridge [modified after Parsiegla, et al., 2007]. Seismic reflectors are marked with different colours, reflector ages are annotated. Ages are based on the seismostratigraphic model of Broad et al. [2006]. For details on seismic reflection processing see Parsiegla et al. [2007; 2008].

### 8.5.3 Comparison between crustal stretching and formation of the Outeniqua and Falkland basins

During the rifting period (Figure 8-10) of the sheared margin the future Outeniqua Basin was situated opposite the Falkland Plateau [e.g. 1982; *Martin, et al.*, 1981]. Knowledge of the development of the plateau is complicated by the proposed rotation of a Falkland Islands plate [e.g. *Adie*, 1952; *Storey, et al.*, 1999] that dates from 178-121 Ma [*Stone, et al.*, 2008] that may or may not have accompanied extension in its sedimentary basins. Recent plate-tectonic reconstructions that use movements on a Gastre Fault system show the Outeniqua Basin contiguous with the North Falkland Basin [*Jokat, et al.*, 2003; *König and Jokat*, 2006] (Figure 8-10). The rift stage in the North Falkland Basin is constrained to mid-Jurassic times, albeit not tightly [*Richards and Hillier*, 2000] (Figure 8-2), and *McMillan* [1997] suggested the possible presence of pre-Kimmeridgian sediments (> 155 Ma) in the Outeniqua Basin. While this is not inconsistent with recent reconstructions, *von Gosen and Loske's* [2004] field-based study of the Gastre Fault reported no evidence for dextral shear, but for downfaulting. Plate-tectonic reconstructions, which do not incorporate shear motion along the Gastre Fault, showed the Falkland Plateau Basin as a southern extension of the Outeniqua Basin [*Eagles*, 2007; *Martin, et al.*, 1982]. This seems to be supported by dating of the oldest sediments at Deep Sea Drilling Project (DSDP) sites 327A (leg 36), 330 (leg 36) and 511 (leg 71) on the eastern flank of the Falkland Plateau (Figure 8-2) to Kimmeridgian/Oxfordian times [*Jeletzky*, 1983; *Jones and Plafker*, 1977]. As neither the DSDP sites, nor the drill holes in the Outeniqua Basin sampled the oldest rift sediments in the basins, i.e. it is very likely that rifting in these basins started already in mid Jurassic times.

Recent 3-D gravity modelling on the Falkland Plateau revealed a crustal thickness of between 19 and 23 km on the Falkland Plateau Basin [*Kimbell and Richards*, 2008], a range that includes our determination of the crustal thickness beneath the Southern Outeniqua Basin (~21 km; Table 8-4). If we take the same initial crustal thickness of 43 km as proposed for the Outeniqua Basin, it is not surprising that these thicknesses imply stretching factors of between 1.9 and 2.3, similar to those that we have calculated for the Southern Outeniqua Basin (1.8-2.1). Hence, it seems likely that the Falkland Plateau Basin experienced the same two extensional episodes as the southern extent of the Outeniqua Basin

## Dynamic processes of a transform margin

Basin	Average crustal thickness/km	Info based on	Reference
Outeniqua Basin (Pletmos Basin)	27 ± 2	Seismic refraction profiling	This study
Outeniqua Basin (Gamtoos Basin)	26 ± 1	Seismic refraction profiling	This study
Outeniqua Basin (Southern Outeniqua Basin)	21 ± 1	Seismic refraction profiling	This study
Falkland Plateau Basin	19 - 23	3D Gravity modelling	Kimbell and Richards, 2008

Table 8-4: Average crustal thicknesses of the Outeniqua Basin and the Falkland Plateau Basin with standard deviations of the values derived in this study

### 8.6 Geodynamic evolution of the margin

Rifting started to form the Outeniqua and Falkland Plateau Basins in mid-late Jurassic times (Figure 8-10). Shear motion along the Agulhas-Falkland Transform can be considered as the cause of additional stretching in the southern parts of the Outeniqua Basin in early Cretaceous times (Figure 8-10). These two episodes formed a large basin during the break-up of Gondwana and through the early continent-continent shear stage of West Gondwana break-up (Figure 8-10).

Most important for the evolution of the southern African margin from ~136 Ma onwards was the development of the Agulhas-Falkland Transform Fault (and later its remnant structure – the AFFZ). It is not clear whether this transform developed entirely in the Cretaceous [e.g. *Broad, et al.*, 2006] or represents the re-activation of a pre-existing crustal feature [e.g. *Jacobs and Thomas*, 2004]. Our data and drill hole evidence [*McMillan, et al.*, 1997] suggest that the CFB underlies the Outeniqua Basin, raising the question of whether the transform is a re-activated Gondwanide orogenic structure. *Johnston* [2000] showed a model for the formation of the CFB during dextral transpressional processes suggesting that structures suitable for reactivation in a strike-slip mode existed in this region well before early Cretaceous times. However, the azimuths of Johnston's proposed structures are not consistent with the development of an NE-SW directed shear along the intra-continental Agulhas-Falkland Transform about 100 my later. If a pre-existing structure is to be invoked, then, it may be that one has to look back to before the Gondwanide orogeny. *Jacobs and Thomas* [2004] suggested that shear zones may have developed in the region during lateral escape tectonics related to the East African-Antarctic orogen. Another possibility is the re-activation of an old trench-

## Dynamic processes of a transform margin

linked strike-slip fault as a very deep-seated fault type with high preservation and re-activation potential [Woodcock, 1986].

But why was such a large scale transform possible in the first place? We have already looked at the possibility of zones of lithospheric weakness formed during southern Africa's billions of years history of continental accretion and dispersal. Additionally, the sites of original break-up may have been influenced by the presence and action of plumes (e.g. that forming the Karoo Large Igneous Province [e.g. Duncan, et al., 1997; Ernst and Buchan, 2002]). Plume activity possibly weakened the lithosphere enough for the re-activation of pre-existing faults into an intra-continental, and later ridge-offset, transform (Figure 8-10).

The formation of the Diaz Marginal Ridge can be tentatively dated to between 130 and 90 Ma (this study). Either a transpressional episode along the Agulhas-Falkland Transform or a temperature difference across the transform (Figure 8-10) caused its uplift.

At about 100 Ma the spreading ridge was approximately located at the western margin of the present-day Agulhas Plateau. This oceanic plateau has been identified as a Large Igneous Province (LIP) [Gohl and Uenzelmann-Neben, 2001; Uenzelmann-Neben, et al., 1999] (Figure 8-10). The development of this LIP can be related to the location of the Bouvet triple junction on its southwestern edge and the activity of the Bouvet plume [Parsieglä, et al., 2008]. During the ~ 6 million year formation time [Parsieglä, et al., 2008] this massive volcanism had a great impact on crustal generation south of and possibly in the Agulhas Passage. Contemporaneous uplift of southern Africa (100-80 Ma, [e.g. Tinker, et al., 2008]) and the injection of kimberlites (108-74 Ma, [e.g. Kobussen, et al., 2008]) can be interpreted as indications that these mantle processes had an influence even further north.

The beginning of the post-shear phase of the margin, the present state of the southern African continental margin, can be estimated at ~84 Ma. From this time onwards active parts of Agulhas-Falkland Fracture Zone system (i.e. the transform itself) were no longer opposite the African continent but had moved to the west. Spreading ridge jumps in the South Atlantic at about 61-64 Ma [Barker, 1979; Marks and Stock, 2001] and 60-58 Ma [Barker, 1979] caused a significant reduction of the transform offset and led to its present ridge-ridge offset of about 290 km. Neotectonic activity at the Agulhas-Falkland Fracture Zone was identified [Ben-Avraham, 1995; Parsieglä, et al., 2007] and may be

## Dynamic processes of a transform margin

an expression of lithospheric weakness along the Agulhas-Falkland Fracture Zone acting to accommodate the uplift of southern Africa

### 8.7 Conclusions

Two combined land-sea velocity-depth models, derived from seismic refraction/wide-angle reflection data of the Agulhas-Karoo Geoscience Transect, and seismic reflection data were presented in this study. They provide new insights into the crustal structure of the southern African continental transform margin (Figure 8-5, Figure 8-7) and provide conclusions about the nature and timing of the related tectonic/geodynamic processes (Figure 8-10, Table 8-5).

Time	Event
~169 - 155 Ma	- First rifting started to form the Outeniqua and Falkland Plateau Basins
From ~136 Ma	- Start of shear motion along the Agulhas-Falkland Transform - Further crustal stretching in the southern parts of the Outeniqua Basin and the Falkland Plateau Basin - Continent-continent shear stage of the transform margin
~130 - 90 Ma	- Formation of the Diaz Marginal Ridge either due to transpression or thermal uplift (in a short episode within this interval)
~115 - 84 Ma	- Continent-ocean shear stage
~100 - 94 Ma	- Formation of the Agulhas Plateau Large Igneous Province - Uplift of southern Africa - Increased denudation onshore
From ~84 Ma	- Post-shear stage
~64 – 58 Ma	- Two ridge jumps reduced the ridge-ridge offset of the Agulhas-Falkland Transform to its present offset of ~290 km

Table 8-5: Summary of the development of the southern African continental margin from initiation of basin formation to the present-day post-shear stage.

Both profiles cross continental, stretched continental, transitional and oceanic crust. From crustal thickness information of unstretched and stretched continental crust, we calculated crustal stretching factors in the Outeniqua Basin which provide important indications to understand the basin formation. Stretching factors lower than 1.7 are interpreted to be the result of an episode of crustal extension which was attributed to the rift stage of the basin. This was possibly initiated by stresses associated with the break-up between Africa and Antarctica. This episode had influence on the whole Outeniqua Basin and the conjugate Falkland Plateau Basin. A second stretching episode – possibly related to shear motion along the Agulhas Falkland transform system starting in Valanginian times - is hinted at by stretching factors > 1.7 in the southern parts of the Outeniqua Basin and Falkland Plateau Basin.

## Dynamic processes of a transform margin

The crustal velocities in the Diaz Marginal Ridge and its sedimentary cover are used to discuss two models about its formation. A transpressional episode or a temperature difference across the transform may have been responsible for the uplift of the Diaz Marginal Ridge. The theory of a thermal uplift is favoured because similar stretching factors in the Southern Outeniqua Basin and Diaz Marginal Ridge suggest a common stretching history.

As the formation of the Agulhas-Falkland Transform is important for the margin's evolution we discussed if it is a Cretaceous feature or related to older tectonic processes. Even with our new high quality data, the question of whether the Agulhas-Falkland Transform exploited a pre-existing zone of crustal/lithospheric weakness can not be conclusively answered. However, supercontinent amalgamation and dispersal processes together with plume activity in this region provide scenarios which make re-activation more likely than a first formation in the Cretaceous.

### ***Acknowledgements:***

We acknowledge the excellent cooperation of Captain L. Mallon and his crew of RV *Sonne* as well as the AWI geophysics team during cruise SO-182. We are grateful to Ernst Flüh of IFM-GEOMAR for lending us 40 OBS systems. The equipment of the onshore experiments was provided by the Geophysical Instrument Pool of GFZ Potsdam. We thank the seismic and MT field teams as well as the farmers who granted us access to their land. We are grateful to Graeme Eagles who greatly improved this manuscript by invaluable comments on a pre-review version. We thank Jan Grobys and Anthony Tankard for valuable discussions. Thanks to Matthias König for providing access to his plate rotation code and an initial introduction. Many thanks to Maarten de Wit (UCT and Africa Earth Observatory Network) for his support before and during the research visit of N.P. in Cape Town. The *German Academic Exchange Service* (DAAD) funded a research visit of N.P. at the University of Cape Town (South Africa), where parts of the research were carried out. Most figures were generated with GMT [Wessel and Smith, 1998]. The SO-182 cruise (project AISTEK-I) and N.P.'s PhD position were primarily funded by the German *Bundesministerium für Bildung und Forschung* (BMBF) under contract no. 03G0182A. This is AWI contribution no. ??? and *Inkaba ye Africa* contribution no. ???.

## 9 Conclusions and Outlook

### 9.1 Conclusions

In my thesis the structure of the southern African continental margin and the dynamic processes that formed its dominant features were investigated. Shear and transtensional processes along the Agulhas-Falkland Transform Zone caused the sharp transition zone from continental to oceanic crust. Possibly the high temperature gradient across the transform zone resulted in the uplift of the Diaz Marginal Ridge. South of the Agulhas-Falkland Fracture Zone, the interaction of the Bouvet hotspot with the Bouvet triple junction initiated lava flows as well as intrusions of magma that built the Agulhas Plateau.

The first key question addresses the processes which were active during the formation of the marginal structures including the interactions between the strike-slip process and new crustal formation. These topics are covered within chapters 6, 8 and partly in chapter 7. Knowledge of its precise crustal structure is a prerequisite for deriving the processes which formed the margin as it is today. Velocity-depth models derived from seismic refraction modelling revealed a variety of previously unknown features across the margin (e.g. a low-velocity region beneath the Outeniqua Basin) and mapped the continent-ocean transition zone. The Agulhas-Falkland Fracture Zone is located within the continent-ocean transition zone, which stretches over a length of 50 km (chapter 6, 7, 8). This small continent-ocean transition zone and the lacking evidence for break-up related volcanism are distinct differences compared to classic passive rifted margins (chapter 7). The Agulhas-Falkland Fracture Zone was found to have experienced phases of re-activation which caused faults clearly seen in our seismic reflection records. A re-activation did not occur in a strike-slip sense but possibly in a dip-slip manner. In this sense the anomalous elevation of southern Africa (African Superswell) as a result of the African Superplume may have been enhanced by sub-vertical motion on this zone of lithospheric weakness.

In its active shear episode the Agulhas-Falkland Transform had significant influence on the evolution of Africa's southern margin. After the first episode of crustal stretching in the Outeniqua Basin, which started the basin formation in Jurassic times (chapter 8), transtensional processes along the Agulhas-Falkland Transform caused further crustal stretching, which affected

## Conclusions and Outlook

only the southern parts of the basin. It was previously suggested that the Falkland Plateau Basin and the Outeniqua Basin formed a single large basin before the break-up. I showed that crustal stretching factors and crustal thicknesses in both basins are similar. Therefore, it is likely that they experienced the same initial crustal stretching episode during the early break-up of East and West Gondwana, and later transtensionally caused crustal thinning during shear between Africa and the Falkland Plateau. These stretching processes affected the metasediments and crystalline continental crust underlying the Outeniqua Basin. The study showed that there must have been a pre-cursor of the Outeniqua Basin, which existed in the southern extensions of the Cape Fold Belt and whose sedimentary infill experienced metamorphic overprinting. The later history of this pre-break-up metasedimentary basin was possibly tied to the uplift of the Diaz Marginal Ridge during a transpressional episode along the Agulhas-Falkland Fracture Zone or due to thermal uplift triggered by a passing spreading ridge (chapter 6 and 8). Relatively low seismic velocities in the oceanic crust which formed at this spreading ridge near the transform are possibly a result of transform-ridge intersection processes which cause changes in the magmatic supply. It is most likely that the magmatic feeding system was also altered due to the opposition of cold continental crust against newly built hot oceanic crust.

Magmatic processes are also addressed with the second key question, which explored whether the Agulhas Plateau is a Large Igneous Province. I established new evidence for an evolution of the Agulhas Plateau as a Large Igneous Province. Results from seismic reflection measurements and seismic refraction modelling are consistent with the typical structure of an oceanic LIP. They showed the thick volcanic flows on this plateau and a ten kilometre thick high-velocity body which makes up the base of the Agulhas Plateau. The excessive magmatic processes which formed the LIP possibly originated from the interaction of the Bouvet triple junction and Bouvet plume. Plate-tectonic reconstructions placed this event between 100 and 94 Ma. They showed that the Agulhas Plateau was part of an even larger LIP, whose other members were the North East Georgia Rise and the Maud Rise. These three parts were split along the spreading ridges of the Bouvet triple junction causing their present-day location on three different crustal plates.

The characterization of the Agulhas Plateau as a Large Igneous Province led to a study on its possible impact on the paleo-climate during its formation with emphasis on the gas emissions from the extruded lava. I base the analysis solely on geophysical methods as no rock samples were available. The carbon dioxide emissions were surprisingly small and provide therefore most

## Conclusions and Outlook

likely no direct influence on the paleo-climate. As this estimation is the first of its kind for an oceanic LIP, the result may have a significant impact on this debate but drill and dredge samples are necessary to intensify the research by means of geological and geochemical methods.

All four publications constituting this thesis discuss processes in southern Africa which are linked on a larger scale. The initial rifting in the Outeniqua is a result of intra-continental stretching during the early break-up of Gondwana. This supercontinental dispersal was predated by plume activity. As the break-up proceeded, intra-continental stretching started to form the western margin (preceded by plume activity) and dextral strike-slip motion along the Agulhas-Falkland Transform occurred. This transform movement resulted in another stretching episode in the Outeniqua Basin and triggered the formation of the Diaz Marginal Ridge. As seafloor spreading formed new ocean floor south of Africa and the Bouvet plume “arrived” there the Agulhas Plateau formed as a Large Igneous Province.

### **9.2 Outlook**

This thesis solved many of the open questions about southern Africa and its southern continental margin. But answers always pose new questions and some issues need additional data to be fully understood.

I showed that the Agulhas Plateau consists of oceanic crust and is a Large Igneous Province. It is now necessary to drill and dredge the Agulhas Plateau in order to find out whether there is any chemical signature from small-scale continental fragments which could not be resolved, yet. Additionally, these samples could lead to a more precise dating of the LIP emplacement which was derived from a plate-tectonic reconstruction in this study. Environmental issues could be further investigated when eruption periods are dated and in-situ gas content can be measured in these samples.

For a better understanding of the stresses involved in the proposed re-activation of the AFFZ, a numerical modelling of its vertical motion based on rheological parameters would be of great value.

It is possible that the formation of the Agulhas Plateau is causally linked with the development of the Mozambique Ridge and the overthickened crust between them. For an understanding of the magmatic development of this area,

## Conclusions and Outlook

this possible relationship has to be investigated. Such a study has currently been started with a paper in preparation where I serve as a co-author.

## References

### 10 References

Adie, R. J. (1952), The position of the Falkland islands in a reconstruction of Gondwanaland, *Geol. Mag.*, 89, 401-410.

Allen, P. A. and Allen, J. R. (1990), *Basin Analysis, Principles & Applications*, Reprinted 1992, 53-91, Blackwell Scientific Publications, Oxford

Allen, R. B., and B. E. Tucholke (1981), Petrology and implications of continental rocks from the Agulhas Plateau, southwest Indian Ocean, *Geology*, 9, 463-468.

Anderson, D. L. (1982), Hotspots, polar wander, Mesozoic convection and the geoid, *Nature*, 297, 391-393.

Barker, P. F. (1979), The history of ridge-crest offset at the Falkland-Agulhas Fracture Zone from a small-circle geophysical profile, *Geophys. J. R. astr. Soc.*, 59, 131 - 145.

Barnett, W., Armstrong, R and de Wit, M.J. (1997), Stratigraphy of the upper Neoproterozoic Kango and lower Paleozoic Table Mountain groups of the Cape fold belt revisited. *S. Afr. J. Geol.*, 100, 237-250.

Basile, C., J. Mascle, M. Popoff, J. P. Bouillin, and G. Mascle (1993), The Ivory Coast-Ghana transform margin: a marginal ridge structure deduced from seismic data, *Tectonophys.*, 222, 1-19.

Bauer, K., S. Neben, B. Schreckenberger, R. Emmermann, K. Hinz, N. Fechner, K. Gohl, A. Schulze, R. B. Trumbull, and K. Weber (2000), Deep crustal structure of the Namibia continental margin as derived from integrated geophysical studies, *J. Geophys. Res.*, 105, 25,829-825,853.

Beattie, J.C. (1909), Report of a magnetic survey of South Africa. Royal Society of London Publication, Cambridge University Press, London.

## References

- Ben-Avraham, Z. (1995), Neotectonic activity offshore southeast Africa and its implications, *S. Afr. J. Geol.*, 98, 202-207.
- Ben-Avraham, Z., C. J. H. Hartnady, and K. A. Kitchin (1997), Structure and tectonics of the Agulhas-Falkland fracture zone, *Tectonophys.*, 282, 83-98.
- Ben-Avraham, Z., C. J. H. Hartnady, and A. P. le Roex (1995), Neotectonic activity on continental fragments in the Southwest Indian Ocean: Agulhas Plateau and Mozambique Ridge, *J. Geophys. Res.*, 100, 6199-6211.
- Ben-Avraham, Z., C. J. H. Hartnady, and J. A. Malan (1993), Early tectonic extension between the Agulhas Bank and the Falkland Plateau due to the rotation of the Lafonia microplate, *Earth Planet. Sci. Lett.*, 117, 43-58.
- Bird, D. (2001), Shear margins: Continent-ocean transform and fracture zone boundaries, *The Leading Edge*, 150-159.
- Branch, T., Ritter, O., Weckmann, U., Sachsenhofer, R.F. and Schilling, F. (2007), The Whitehill Formation – a high conductivity marker horizon in the Karoo Basin. *S. Afr. J. Geol.*, 110 (2/3), 465-476
- Broad, D. S., E. H. A. Jungslager, I. R. McLachlan, and J. Roux (2006), Geology of the offshore Mesozoic basins, in *The Geology of South Africa*, edited by M. R. Johnson, et al., 553-571, Geological Society of South Africa/Council for Geoscience, Pretoria.
- Broquet, C.A.M. (1992), The sedimentary record of the Cape Supergroup: a review. In: *Inversion Tectonics of the Cape Fold Belt, Karoo and Cretaceous Basins of Southern Africa*, 159-183, edited by de Wit, M.J. and Ransome, I.G.D., Balkema, Rotterdam.
- Burke, K., and T. H. Torsvik (2004), Derivation of Large Igneous Provinces of the past 200 million years from long-term heterogeneities in the deep mantle, *Earth Planet. Sci. Lett.*, 227, 531-538.

## References

- Caldeira, K., and M. R. Rampino (1990), Carbon dioxide emissions from Deccan volcanism and K/T boundary greenhouse effect, *Geophys. Res. Lett.*, *17*, 1299-1302.
- Catuneanu, O., Hancox, P.J. and Rubidge, B.S. (1998), Reciprocal flexural behaviour and contrasting stratigraphies: a new basin development model for the Karoo retroarc foreland system, South Africa, *Basin Res.*, *10*, 417-439.
- Charvis, P., M. Recq, S. Operto, and D. Bretort (1995), Deep structure of the northern Kerguelen Plateau and hotspot-related activity, *Geophys. J. Int.*, *122*, 899-924.
- Christensen, N. I., and W. Mooney (1995), Seismic velocity structure and composition of the continental crust: A global view, *J. Geophys. Res.*, *100*, 9761-9788.
- Christensen, U. (1998), Fixed hotspots gone with the wind, *Nature*, *391*, 739-740.
- Class, C., and A. P. le Roex (2006), Continental material in the shallow oceanic mantle - How does it get there?, *Geology*, *34*, 129-132.
- Cloetingh, S., Lankreijer, A., de Wit, M.J. and Martinez, I. (1992). Subsidence history analyses and forward modelling of the Cape and Karoo Supergroups. In: *Inversion tectonics of the Cape Fold Belt, Karoo and Cretaceous basins of Southern Africa*, 239-248, edited by de Wit, M.J and Ransome, I.G.D., Balkema, Rotterdam.
- Coffin, M. F., R. A. Duncan, O. Eldholm, J. G. Fitton, F. A. Frey, H. C. Larsen, J. J. Mahoney, A. D. Saunders, R. Schlich, and P. J. Wallace (2006), Large Igneous Provinces and Scientific Ocean Drilling, *Oceanography*, *19*, 150-160.
- Coffin, M. F., and O. Eldholm (1994), Large igneous provinces: crustal structure, dimensions, and external consequences, *Rev. Geophys.*, *32*, 1-36.

## References

Cole, D. J. (1992), Evolution and development of the Karoo Basin, in *Inversion Tectonics of the Cape Fold Belt, Karoo and Cretaceous Basins of Southern Africa*, edited by M. de Wit and I. G. D. Ransome, Balkema, Rotterdam.

Dalziel, I. W. D. (2007), The Ellsworth Mountains: Critical and Enduringly Enigmatic, in *Antarctica: A Keystone in a Changing World*, edited by A. K. Cooper and C. R. Raymond, pp. 5; doi:10.3133/of2007-1047.srp3004, USGS Open-File Report 2007-1047, Short Research Paper 004.

Dalziel, I. W. D., L. A. Lawver, and J. B. Murphy (2000), Plumes, orogenesis, and supercontinental fragmentation, *Earth Planet. Sci. Lett.*, 178, 1-11.

de Beer, J. H., J. S. V. van Zijl, and v. Gough (1982), The Southern Cape Conductivity Belt (South Africa): its composition, origin and tectonic significance, *Tectonophys.*, 83, 205-225.

de Beer, J.H. and Gough, D.I. (1980), Conductive structures in southernmost Africa: A magnetometer array study. *Geophys. J. R. Astr. Soc.*, 63, 479-495.

de Beer, J. H., Van Zyl, J. S. V. and Bahnemann, F. K. (1974), Plate tectonic origin for the Cape Fold Belt? *Nature*, 252, 675-676.

de Wit, M. J. (1992), The Cape Fold Belt: A Challenge for an integrated approach to inversion tectonics. In: *Inversion Tectonics of the Cape Fold Belt, Karoo and Cretaceous Basins of Southern Africa*, 3-12, edited by de Wit, M.J. and Ransome, I.G.D., Balkema, Rotterdam.

de Wit, M. J. (2007), The Kalahari Epeirogeny and climate change: differentiating cause and effect from core to space. *S. Afr. J. Geol.*, 110 (2/3), 367-392.

de Wit, M., and B. Horsfield (2006), Inkaba yeAfrica Project Surveys Sector of Earth from Core to Space. *EOS Trans. AGU*, 87, 113-117.

## References

- de Wit, M., and I. G. D. Ransome (1992), Regional inversion tectonics along the southern margin of Gondwana, in *Inversion tectonics of the Cape Fold Belt, Karoo and Cretaceous basins of southern Africa*, edited by M. de Wit and I. G. D. Ransome, 15-21, Balkema, Rotterdam.
- de Wit, M. J., and J. Stankiewicz (2006), Changes in Surface Water Supply Across with Predicted Climate Change, *Science*, 311, 1917-1921.
- Dewey, J. F., R. E. Holdsworth, and R. A. Strachan (1998), Transpression and transtension zones, in *Continental Transpressional and Transtensional Tectonics*, edited by R. E. Holdsworth, et al., 1-14, Geological Society, London, Special Publications.
- Dewey, J. F., Robb, L. and van Schalkwyk, L. (2006), Did Bushmanland extensionally unroof Namaqualand. *Precambrian Res.*, 150, 173-182.
- Dingle, R. V., W. G. Siesser, and A. R. Newton (1983), *Mesozoic and Tertiary geology of southern Africa*, A.A. Balkema, Rotterdam.
- Duncan, R. A., P. R. Hooper, J. Rehacek, J. S. Marsh, and A. R. Duncan (1997), The timing and duration of the Karoo igneous event, southern Gondwana, *J. Geophys. Res.*, 102, 18127-18138.
- Durrheim, R.J. (1987), Seismic reflection and refraction studies of the deep structure of the Agulhas Bank. *Geophys. J. R. Astr. Soc.*, 89, 395-398.
- Durrheim, R. J. and W. D. Mooney (1994), Evolution of the Precambrian lithosphere: Seismological and geochemical constraints. *J. Geophys. Res.*, 99(B8), 15,359–15,374.
- Eagles, G. (2007), New Angles on South Atlantic Opening, *Geophys. J. Int.*, 168, 353-361, doi:310.1111/j.1365-1246X.2006.03206.x.
- Eagles, G., and M. König (2008), A model of plate kinematics in Gondwana breakup, *Geophys. J. Int.*, 173, 703-717, doi:710.1111/j.1365-1246X.2008.03753.x.

## References

- Eglington, B.M. (2006), Evolution of the Namaqua-Natal Belt, southern Africa – A geochronological and isotope geochemical review. *J. Afr. Earth Sci.*, *46*, 93-111.
- Eglington, B.M. and Armstrong, R.A. (2003), Geochronological and isotopic constraints on the Mesoproterozoic Namaqua-Natal Belt: evidence from deep borehole intersections in South Africa. *Precambrian Res.*, *125*, 179-189.
- Eldholm, O., and M. F. Coffin (2000), Large Igneous Provinces and Plate Tectonics, *Geophys. Mon.*, *121*, 309-326.
- Eldholm, O., and K. Grue (1994), North Atlantic volcanic margins: Dimensions and production rates, *J. Geophys. Res.*, *99*, 2955-2968.
- Eldholm, O., and E. Thomas (1993), Environmental impact of volcanic margin formation, *Earth Planet. Sci. Lett.*, *117*, 319-329.
- Ernst, R. E., and K. L. Buchan (2002), Maximum size and distribution in time and space of mantle plumes: evidence from large igneous provinces, *J. Geodyn.*, *34*, 309-342.
- Fouche, J., Bate, K.J. and van der Merwe, R. (1992), Plate tectonic setting of the Mesozoic Basins, southern offshore, South Africa: A review. In: *Inversion Tectonics of the Cape Fold Belt, Karoo and Cretaceous Basins of Southern Africa*, 27-32, edited by de Wit, M.J and Ransome, I.G.D.), Balkema, Rotterdam.
- Fowler, C. M. R. (1990), The oceanic lithosphere, in *The solid Earth*, edited, p. 286.
- Furlong, K. P., and W. D. Hugo (1989), Geometry and evolution of the San Andreas Fault Zone in northern California, *J. Geophys. Res.*, *94*, 3100-3110.
- Gadd, S. A., and R. A. Scrutton (1997), An integrated thermomechanical model for transform continental margin evolution, *Geo-Mar. Lett.*, *17*, 21-30.

## References

- Gernigon, L., Ringenbach, J-C., Planke, S. and Le Gall, B. (2004), Deep structures and breakup along volcanic rifted margins: insights from integrated studies along the outer Vøring Basin (Norway). *Mar. Pet. Geol.*, 21, 363–372.
- Gladczenko, T. P., M. F. Coffin, and O. Eldholm (1997a), Crustal structure of the Ontong Java Plateau: Modeling new gravity and existing seismic data, *J. Geophys. Res.*, 102, 7111-722,729.
- Gladczenko, T. P., K. Hinz, O. Eldholm, H. Meyer, S. Neben, and J. Skogseid (1997b), South Atlantic volcanic margins, *J. Geol. Soc., London*, 154, 465-470.
- Goergen, J. E., J. Lin, and H. J. B. Dick (2001), Evidence from gravity anomalies for interactions of the Marion and Bouvet hotspots with the Southwest Indian Ridge: effects of transform offsets, *Earth Planet. Sci. Lett.*, 187, 283-300.
- Gohl, K., and G. Uenzelmann-Neben (2001), The crustal role of the Agulhas Plateau, southwest Indian Ocean: evidence from seismic profiling, *Geophys. J. Int.*, 144, 632-646.
- Gough, D.I. (1973), Possible linear plume under southernmost Africa. *Nat. Phys. Sci.*, 245, 93-94.
- Gough, D.I., de Beer, J.H. and Van Zyl, J.S.V. (1973), A magnetometer array study in southern Africa. *Geophys. J. R. Astr. Soc.*, 34, 421-433.
- Gray, D. R., D. A. Foster, J. G. Meert, B. D. Goscombe, R. Armstrong, R. A. J. Trouw, and C. W. Passchier (2008), A Damara orogen perspective on the assembly of southwestern Gondwana, *Geophys. Soc., London, Spec. Pub.*, 294, 257-278.
- Green, R.W.E. and Durrheim, R.J. (1990), A Seismic Refraction Investigation of the Namaqualand Metamorphic Complex, *South Africa. J. Geophys. Res.*, 95(B12), 19,927-19,932.

## References

- Greenroyd, C. J., C. Pierce, M. Rodger, A. B. Watts, and R. W. Hobbs (2008), Demerara Plateau - the structure and evolution of a transform passive margin, *Geophys. J. Int.*, 172, 549-564.
- Hälbich, I. W. (1993). The Cape Fold Belt – Agulhas Bank Transect across the Gondwana Suture in Southern Africa. *AGU Spec. Pub.*, 202, 18pp.
- Hälbich, I. W., F. J. Fitch, and J. A. Miller (1983), Dating the Cape orogeny, *Spec. Pub. Geol. Soc. S. Afr.*, 12, 149-164.
- Hälbich, I. W. (1983), A tectogenesis of the Cape Fold Belt (CFB). In: *Geodynamics of the Cape Fold Belt*, 165-175, edited by Söhnge, A.P.G. and Hälbich, I. W., *Spec. Pub. Geol. Soc. S. Afr.*
- Hartnady, C. J. H., and A. P. le Roex (1985), Southern Ocean hotspot tracks and the Cenozoic absolute motion of the African, Antarctic, and South American plates, *Earth Planet. Sci. Lett.*, 75, 245-257.
- Harvey, J. D., de Wit, M. J., Stankiewicz, J. and Doucoure, C.M. (2001), Structural variations of the crust in the Southwestern Cape, deduced from seismic receiver functions. *S. Afr. J. Geol.*, 104, 231-242.
- Hawkesworth, C., S. Kelly, S. Turner, A. Le Roex, and B. Storey (1999), Mantle processes during Gondwana break-up and dispersal, *J. Afr. Earth Sci.*, 28, 239-261.
- Hirsch, K. K., K. Bauer, and M. Scheck-Wenderoth (2008), Deep structure of the western South African passive margin - Results of a combined approach of seismic, gravity and isostatic investigations, *Tectonophys.*
- Jackson, J. A. (1987), Active normal faulting and crustal extension, *Geol. Soc., London, Spec. Pub.*, 28, 3-17, doi:10.1144/GSL.SP.1987.1028.1101.1102.
- Jacobs, J., and R. J. Thomas (2004), Himalayan-type of indenter-escape tectonics model for the southern part of the late Neoproterozoic-early Paleozoic East African-Antarctic orogen, *Geology*, 32, 721-724.

## References

- Jacobs, J. and R. J. Thomas (1994), Oblique collision at 1.1 Ga along the southern margin of the Kaapvaal continent, SE Africa. *Geol. Rundsch.*, 83, 322-333
- Jacobs, J., Thomas, R. J. and Weber, K., (1993), Accretion and indentation tectonics at the southern edge of the Kaapvaal craton during the Kibaran (Grenville) orogeny. *Geology*, 21, 203-206.
- Jeletzky, J. A. (1983), Macroinvertebrate palaeontology, biochronology and palaeoenvironments of Lower Cretaceous and Upper Jurassic rocks, Deep Sea Drilling Hole 511, Eastern Falkland Plateau, in *Initial Reports DSDP*, edited by J. H. Blakeslee and M. Lee, 951-975.
- Johnston, S. T. (2000), The Cape Fold Belt and Syntaxis and the rotated Falkland Islands: dextral transpressional tectonics along the southwest margin of Gondwana, *J. Afr. Earth Sci.*, 31, 51-63.
- Jokat, W., T. Boebel, M. König, and U. Meyer (2003), Timing and geometry of early Gondwana breakup, *J. Geophys. Res.*, 108, doi: 10.1029/2002JB001802.
- Jones, D. L., and G. Plafker (1977), Mesozoic megafossils from DSDP Hole 327A and Site 330 on the Eastern Falkland Plateau, in *Initial Reports DSDP*, edited by P. F. Barker and I. W. D. Dalziel, 845-856.
- Kastens, K. A. (1987), A Compendium of Causes and Effects of Processes at Transform Faults and Fracture Zones, *Rev. Geophys.*, 25, 1554-1562.
- Kerr, A. C. (2005), Oceanic LIPs: The Kiss of Death, *Elements*, 3, 289-292.
- Kimbell, G. S., and P. C. Richards (2008), The three-dimensional lithospheric structure of the Falkland Plateau region based on gravity modelling, *J. Geol. Soc.*, 165, 795-806.
- Kobussen, A. F., W. L. Griffin, S. Y. O'Reilly, and S. R. Shee (2008), Ghosts of lithospheres past: Imaging an evolving lithosphere mantle in southern Africa, *Geology*, 36, 515-518.

## References

- König, M., and W. Jokat (2006), The Mesozoic breakup of the Weddell Sea, *J. Geophys. Res.*, *111*, doi:10.1029/2005JB004035.
- Li, C., and R. D. Van der Hilst (2008), A new global model for P wave speed variations in the Earth's mantle, *Geochem. Geophys. Geosyst.*, *9*, doi:10.1029/2007GC001806.
- Lindeque, A. S., Ryberg, T., Stankiewicz, J., Weber, M. and de Wit, M. J. (2007). Deep Crustal Seismic Reflection Experiment Across the Southern Karoo Basin, South Africa. *S. Afr. J. Geol.*, *110* (2/3), 419-438.
- Lithgow-Bertelloni, C., and P. G. Silver (1998), Dynamic topography, late driving forces and the African superswell, *Nature*, *395*, 269-271.
- Lock, B. E. (1980), Flat-plate subduction and the Cape Fold Belt of South Africa, *Geology*, *8*, 35-39.
- Lorenzo, J. M. (1997), Sheared continent-ocean margins: an overview, *Geo-Mar. Lett.*, *17*, 1-3.
- Mahoney, J. J., and M. F. Coffin (1997), *Large Igneous Provinces - Continental, Oceanic, and Planetary Flood Volcanism*, 438 pp., Geophysical Monograph, Washington.
- Marks, K. M., and J. M. Stock (2001), Evolution of the Malvinas Plate South of Africa, *Mar. Geophys. Res.*, *22*, 289-302.
- Marks, K. M., and A. A. Tikku (2001), Cretaceous reconstructions of East Antarctica, Africa and Madagascar, *Earth Planet. Sci. Lett.*, *186*, 479-495.
- Martin, A. K. (1987), Plate reorganisations around Southern Africa, hot spots and extinctions, *Tectonophys.*, *142*, 309-316.
- Martin, A. K., S. W. Goodlad, C. J. H. Hartnady, and A. du Plessis (1982), Cretaceous palaeopositions of the Falkland Plateau relative to southern Africa using Mesozoic seafloor spreading anomalies, *Geophys. J. R. astr. Soc.*, *71*, 567-579.

## References

- Martin, A. K., and C. J. H. Hartnady (1986), Plate tectonic development of the south west Indian Ocean: A revised reconstruction of East Antarctica and Africa, *J. Geophys. Res.*, *91*, 4767-4786.
- Martin, A. K., C. J. H. Hartnady, and S. W. Goodland (1981), A revised fit of South America and South Central Africa, *Earth Planet. Sci. Lett.*, *75*, 293-305.
- Maus, S., H. Lühr, M. Rother, K. Hemant, G. Balasis, P. Ritter, and C. Stolle (2007), Fifth-generation lithospheric magnetic field model from CHAMP satellite measurements, *Geochem. Geophys. Geosyst.*, *8*, doi:10.1029/2006GC001521.
- McCourt, S., Armstrong, R. A., Grantham, G. H. and Thomas, R. J. (2006), Geology and evolution of the Natal Belt, South Africa. *J. Afr. Earth Sci.*, *46*, 71-92
- McKenzie, D. (1978), Some remarks on the development of sedimentary basins, *Earth Planet. Sci. Lett.*, *40*, 25-32.
- McMillan, I. K., G. I. Brink, D. S. Broad, and J. J. Maier (1997), Late Mesozoic Basins Off the South Coast of South Africa, in *African Basins*, edited by R.C.Selley, pp. 319-376, Elsevier Science Amsterdam.
- Meert, J. G., and R. van der Voo (1996), The assembly of Gondwana 800-550 Ma, *J. Geodyn.*, *23*, 223-235.
- Menzies, M.A., Klemperer, S.L., Ebinger, C.J., Baker, J. (2002), Characteristics of volcanic rifted margins. In: *Volcanic Rifted Margins*, 1-14, edited by Menzies, M.A., Klemperer, S.L., Ebinger, C.J. and Baker, J., *GSA Special Paper* 362.
- Montinelli, R., G. Nolet, F. A. Dahlen, and G. Masters (2006), A catalogue of deep mantle plumes: New results from finite-frequency tomography, *Geochem. Geophys. Geosyst.*, *7*, doi:10.1029/2006GC001248.
- Morgan, W. J. (1971), Convection Plumes in the Lower Mantle, *Nature*, *230*, 42-43.

## References

- Mutter, C. Z., and J. C. Mutter (1993), Variations in thickness of layer 3 dominate oceanic crustal structure, *Earth Planet. Sci. Lett.*, *117*, 295-317.
- Nair, S.K., Gao, S.S., Liu, K.H. and Silver, P.G. (2006) Southern Africa crustal evolution and composition: constraints from receiver function studies. *J. Geophys. Res.*, *111*, B02304, doi: 10.1029/2005JB003802.
- Neal, C. R., J. J. Mahoney, L. W. Kroenke, A. R. Duncan, and M. G. Petterson (1997), The Ontong Java Plateau, in *Large Igneous Provinces - Continental, Oceanic, and Planetary Flood Volcanism*, edited by J. J. Mahoney and M. F. Coffin, Geophys. Mon., Washington.
- Newton, A.R. (1992), Thrusting on the northern margin of the Cape Fold Belt, near Laingsburg. In: *Inversion Tectonics of the Cape Fold Belt, Karoo and Cretaceous Basins of Southern Africa*, 193-196, edited by de Wit, M.J and Ransome, I.G.D., Balkema, Rotterdam.
- Nguuri, T.K., Gore, J., James, D.E., Webb, S.J., Wright, C, Zengeni, T.G. and Gwavava, O. (2001), Crustal structure beneath southern Africa and its implications for the formation and evolution of the Kaapvaal and Zimbabwe cratons. *Geophys. Res. Lett.*, *28*, 2501-2504.
- Ni, S., and D. Helmberger (2003), Seismological constraints on the South African superplume; could be oldest distinct structure on earth, *Earth Planet. Sci. Lett.*, *206*, 119-131.
- Nyblade, A. A., and W. S. Robinson (1994), The African Superswell, *Geophys. Res. Lett.*, *21*, 765-768.
- Nyblade, A. A., and N. H. Sleep (2003), Long lasting epeirogenic uplift from mantle plumes and the origin of the Southern African Plateau, *Geochem. Geophys. Geosyst.*, *4*, doi:10.1029/2003GC000573.
- Oguti, J. (1964), Geomagnetic anomaly around the continental shelf margin southern offshore of Africa. *J. Geomag. Geoelec.*, *16*, 65-57.

## References

- O'Reilly, S. Y. (2001), Journey beneath southern Africa, *Nature*, 412, 777-780.
- Operto, S., and P. Charvis (1996), Deep structure of the southern Kerguelen Plateau (southern Indian Ocean) from ocean bottom seismometer wide-angle seismic data, *J. Geophys. Res.*, 101, 25,077-025,103.
- Pankhurst, R. J., C. W. Rapela, C. M. Fanning, and M. Márquez (2006), Gondwanide continental collision and the origin of Patagonia, *Earth-Sci. Rev.*, 76, 235-257.
- Parsiegla, N., K. Gohl, and G. Uenzelmann-Neben (2007), Deep crustal structure of the sheared South African continental margin: first results of the Agulhas-Karoo Geoscience Transect  
*S. Afr. J. Geol.*, 110, 393-406.
- Parsiegla, N., K. Gohl, and G. Uenzelmann-Neben (2008), The Agulhas Plateau: Structure and Evolution of a Large Igneous Province, *Geophys. J. Int.*, 174, 336-350, doi: 310.1111.j.1365-1246X.2008.03808.x.
- Parsons, B., and D. McKenzie (1978), Mantle convection and the thermal structure of plates, *J. Geophys. Res.*, 83, 4485-4496.
- PASA (2003), South African Exploration Opportunities, South African Agency for Promotion of Petroleum Exploration and Exploitation, Parow, Cape Town.
- Paton, D.A., Macdonald, D.I.M. and Underhill, J.R. (2006), Applicability of thin or thick skinned structural models in a region of multiple inversion episodes; southern South Africa. *J. Struct. Geol.*, 28, 1933-1947.
- Pitts, B., Maher, M., de Beer, J.H. and Gough, D.I. (1992), Interpretation of magnetic, gravity and magnetotelluric data across the Cape Fold Belt and Karoo Basin. In: *Inversion Tectonics of the Cape Fold Belt, Karoo and Cretaceous Basins of Southern Africa*, 33-45, edited by de Wit, M.J and Ransome, I.G.D., Balkema, Rotterdam.

## References

- Pe'eri, S., S. Wdowinski, A. Shtibelman, and N. Bechor (2002), Current plate motion across the Dead Sea Fault from three years of continuous GPS monitoring, *Geophys. Res. Lett.*, *29*, doi: 10.1029/2001GL013879.
- Quesnel, Y., Weckmann, U., Ritter, O., Stankiewicz, J., Lesur, V., Manda, M., Langlais, B., Sotin, C., Galdeano, A. (2008), Local Modelling of the Beattie Magnetic Anomaly in South Africa. *Tectonophys.*, under review.
- Rabinowitz, P.D. and LaBrecque, J. (1979), The Mesozoic South Atlantic Ocean and Evolution of Its Continental Margins. *J. Geophys. Res.*, *84*, B11, 5973-6002.
- Raith, J.G., Cornell, D.H., Frimmel, H.E. and de Beer, C.H. (2003), New insights into the geology of the Namaqua tectonic province, South Africa, from ion probe dating of detrital and metamorphic zircons. *J. Geol.*, *111*, 347-366.
- Richards, P. C., R. W. Gatliff, M. F. Quinn, P. Williamson, and N. G. T. Fannin (1996), The geological evolution of the Falkland Islands continental shelf, *Weddell Sea Tectonics and Gondwana Break-up*, *Geol. Soc. London Spec. Pub.*, *108*, 105-128.
- Richards, P. C., and B. V. Hillier (2000), Post-Drilling Analysis of the North Falkland Basin - Part 1: Tectono-Stratigraphic Framework, *J. Pet. Geol.*, *23*, 253-272.
- Robb, L.J., Armstrong, R.A. and Waters, D.J. (1999), The history of granulite-facies metamorphism and crustal growth from single zircon U-Pb geochronology: Namaqualand, South Africa. *J. Petro.*, *40*, 1747–1770.
- Ryberg, T., Weber, M., Garfunkel, Z. and Bartov, Y. (2007), The shallow velocity structure across the Dead Sea Transform fault, Arava Valley, from seismic data. *J. Geophys. Res.*, *112*, B08307, doi:10.1029/2006JB004563.

## References

- Sage, F., B. Pontoise, J. Mascle, and C. Basile (1997), Structure of oceanic crust adjacent to a transform margin segment: the Côte d'Ivoire-Ghana transform margin, *Geo-Mar. Lett.*, *17*, 31-39.
- Sager, W. W., J. Kim, A. Klaus, M. Nakanishi, and L. M. Khankishieva (1999), Bathymetry of Shatsky Rise, northwest Pacific Ocean: Implications for oceanic plateau formation at a triple junction, *J. Geophys. Res.*, *104*, 7557-7576.
- Saunders, A. D. (2005), Large Igneous Provinces: Origin and Environmental Consequences, *Elements*, *1*, 259-263.
- Schmitz, M.D. and Bowring, S.A. (2004), Lower crustal granulite formation during Mesoproterozoic Namaqua-Natal collisional orogenesis, southern Africa. *S. Afr. J. Geol.*, *107*, 261-284.
- Schön, J. (1983), *Petrophysik*, Ferdinand Encke Verlag, Stuttgart.
- Scrutton, R.A. and du Plessis, A. (1973), Possible Marginal Fracture Ridge south of South Africa, *Nature*, *242*, 180-182.
- Scrutton, R. A. (1976), Crustal Structure at the Continental Margin South of South Africa, *Geophys. J. R. astr. Soc.*, 601-623.
- Scrutton, R. A. (1979), On sheared passive continental margins, *Tectonophys.*, *59*, 293-305.
- Self, S., T. Thordarson, and M. Widdowson (2005), Gas Fluxes from Flood Basalt Eruptions, *Elements*, *1*, 283-287.
- Simmons, N. A., A. M. Forte, and S. P. Grand (2007), Thermochemical structure and dynamics of the African superplume, *Geophys. Res. Lett.*, *34*, doi: 10.1029/2006GL028009.
- Skelton, P. (2003), Fluctuating sea-level, in *The Cretaceous World*, edited by P. Skelton, pp. 67-83, Cambridge University Press, Cambridge.
- Smith, W. H. F., and D. T. Sandwell (1997), Global seafloor topography from satellite altimetry and ship depth soundings, *Science*, *277*, 1957-1962.

## References

- Stankiewicz, J., N. Parsieglia, T. Ryberg, K. Gohl, U. Weckmann, R. Trumbull, and M. Weber (in press-a), Crustal Structure of the Southern Margin of the African Continent: Results from Geophysical Experiments, *J. Geophys. Res.*
- Stankiewicz, J., T. Ryberg, A. Schulze, A. Lindeque, M. H. Weber, and M. J. de Wit (2007), Results from Wide-Angle Seismic Refraction Lines in the Southern Cape, *S. Afr. J. Geol.*, *110*, 407-418.
- Stankiewicz, J., T. Ryberg, A. Schulze, A. Lindeque, M. H. Weber, and M. J. de Wit (in press-b), Results from Wide-Angle Seismic Refraction Lines in the Southern Cape, *S. Afr. J. Geol.*
- Stone, P., P. C. Richards, G. S. Kimbell, R. P. Esser, and D. Reeves (2008), Cretaceous dykes discovered in the Falkland Islands: implications for regional tectonics in the South Atlantic, *J. Geol. Soc.*, *165* 1-4.
- Storey, B. C. (1995), The role of mantle plumes in continental break-up: case histories from Gondwanaland, *Nature*, *377*, 301-308.
- Storey, B. C., M. L. Curtis, J. K. Ferris, M. A. Hunter, and R. A. Livermore (1999), Reconstruction and break-out model for the Falkland Islands within Gondwana, *J. Afr. Earth Sci.*, *28*, 153-163.
- Su, W. J., R. L. Woodward, and A. M. Dziemonski (1994), Degree 12 model of shear velocity heterogeneity in the mantle, *J. Geophys. Res.*, *99*, 6945-6980.
- Talwani, M. and Eldholm, O. (1973), The boundary between continental and oceanic basement at the margin of rifted continents. *Nature*, *241*, 325-330.
- Tankard, A. J., M. P. A. Jackson, K. A. Eriksson, D. K. Hobday, D. R. Hunter, and W. E. L. Minter (1982), *Crustal Evolution of Southern Africa*, 523 pp., Springer-Verlag, New York.
- Thomson, K. (1999), Role of the continental break-up, mantle plume development and fault activation in the evolution of the Gamtoos Basin, South Africa, *Mar. Pet. Geol.*, *16*, 409-429.

## References

- Tinker, J., M. de Wit, and R. Brown (2008), Mesozoic exhumation of the southern Cape, South Africa, quantified using apatite fission track thermochronology, *Tectonophys.*, doi:10.1016/j.tecto.2007.1010.1009.
- Trumbull, R.B., Sobolev, S.V. and Bauer, K. (2002), Petrophysical modelling of high seismic velocity crust at the Namibian volcanic margin. In: Menzies, M.A., Klemperer, S.L., Ebinger, C.J. and Baker, J. (Eds.) *Volcanic Rifted Margins GSA Special Paper 362*, 221-230.
- Trumbull, R.B., Reid, D.L., De Beer, C.H. and Romer, R.L. (2007). Magmatism and continental breakup at the west margin of southern Africa: A geochemical comparison of dolerite dikes from NW Namibia and the Western Cape. *S. Afr. J. Geol.*, 110 (2/3), 477-502.
- Tucholke, B. E., R. E. Houtz, and D. M. Barrett (1981), Continental Crust Beneath the Agulhas Plateau, Southwest Indian Ocean, *J. Geophys. Res.*, 86, 3791-3806.
- Uenzelmann-Neben, G. (Ed.) (2005), *Southeastern Atlantic and southwestern Indian Ocean: reconstruction of sedimentary and tectonic development since the Cretaceous, AISTEK I: Agulhas Transect*, 1-73.
- Uenzelmann-Neben, G., and K. Gohl (2004), The Agulhas Ridge, South Atlantic: the peculiar structure of a fracture zone, *Mar. Geophys. Res.*, 25, 305 - 319.
- Uenzelmann-Neben, G., K. Gohl, Ehrhardt, A., and M. Seargent (1999), Agulhas Plateau, SW Indian Ocean: New Evidence for Excessive Volcanism, *Geophys. Res. Lett.*, 26, 1941-1944.
- Uenzelmann-Neben, G., Schlüter, P., Weigelt, E. (in press), Cenozoic oceanic circulation in the South African gateway: indications from seismic stratigraphy, *S. Afr. J. Geol.*

## References

- Våges, E. (1997), Uplift at thermo-mechanical coupled ocean-continent transforms: Modeled at the Senja Fracture Zone, southwestern Barents Sea, *Geo-Mar. Lett.*, *17*, 100-109.
- Vaughan, A. P. M., and R. J. Pankhurst (2008), Tectonic overview of the West Gondwana margin, *Gondwana* *13*, 150-162.
- Vidale, J.E. (1988), Finite-difference calculation of travel times. *Bull. Seismol. Soc. Am.*, *78*(6), 2062-2076.
- von Gosen, W., and W. Loske (2004), Tectonic history of the Calcatapul Formation, Chubut province, Argentina, and the "Gastre fault system", *Journal of S. Am. Earth Sci.*, *18*, 73-88.
- Voss, M., and W. Jokat (2007), Continent-ocean transition and voluminous magmatic underplating derived from P-wave velocity modelling of the East Greenland continental margin, *Geophys. J. Int.*, *170*, 580-604.
- Weckmann, U., Ritter, O., Jung, A., Branch, T. and de Wit, M.J. (2007a), Magnetotelluric measurements across the Beattie magnetic anomaly and the Southern Cape Conductive Belt, South Africa. *J. Geophys. Res.*, *112*, B05416, doi:10.1029/2005JB003975.
- Weckmann, U., Jung, A., Branch, T. and Ritter, O. (2007b). Comparison of electrical conductivity structures and 2D magnetic modelling along two profiles crossing the Beattie Magnetic Anomaly, South Africa. *S. Afr. J. Geol.*, *110* (2/3), 449-464.
- Wessel, P., and W. H. F. Smith (1998), New, improved version of generic mapping tools released, *EOS Trans. AGU*, *79*, 579.
- White, R. S., R. S. Detrick, M. C. Sinha, and M. H. Cormier (1984), Anomalous seismic crustal structure of oceanic fracture zones, *Geophys. J. R. astr. Soc.*, *79*, 779-798.

## References

- White, R. S., D. McKenzie, and R. K. O'Nions (1992), Oceanic Crustal Thickness From Seismic Measurements and Rare Earth Element Inversions, *J. Geophys. Res.*, 97, 19683-19715.
- Wignall, P. B. (2001), Large igneous provinces and mass extinctions, *Earth-Sci. Rev.*, 53, 1-33.
- Wignall, P. B. (2005), The Link between Large Igneous Province Eruptions and Mass Extinctions, *Elements*, 1, 293-297.
- Woodcock, N. H. (1986), The role of strike-slip fault systems at plate boundaries, *Phil. Trans. Roy. Soc. London, A* 317, 13-29.
- Yilmaz, Ö. (Ed.) (2001), *Seismic data analysis: processing, inversion, and interpretation of seismic data*, 1000 pp., Society of Exploration Geophysics, Tulsa.
- Zelt, C. A. and P. J. Barton (1998), Three-dimensional seismic refraction tomography: A comparison of two methods applied to data from the Faeroe Basin. *J. Geophys. Res.*, 103(B4), 7187-7210.
- Zelt, C. A., and D. A. Forsyth (1994), Modeling wide-angle seismic data for crustal structure: Southeastern Grenville Province, *J. Geophys. Res.*, 99, 11,687-611,704.
- Zelt, C. A., and R. B. Smith (1992), Seismic travelttime inversion for 2-D crustal velocity structure *Geophys. J. Int.*, 108, 16-34.
- Zelt, C.A., and D. J. White (1995), Crustal structure and tectonics of the southeastern Canadian Cordillera, *J. Geophys. Res.*, 100, 24255-24273.



## 11 Acknowledgements

During my PhD thesis I experienced a great support from many people. I would like to thank:

Prof. Dr. Heinz Miller for the support, efficiency-improving suggestions and for reviewing my thesis.

Prof. Dr. Katrin Huhn for interesting discussions, helpful suggestions and for reviewing this thesis.

Dr. Karsten Gohl for supervising my work, for discussions and for the encouragement to be proactive. Thank you for the opportunity to take part in three scientific cruises and for giving me more and more responsibility each time.

Dr. Gabriele Uenzelmann-Neben for co-supervising my work, for the opportunity to take part in the Sonne cruise to collect my data, for answering my seismic-reflection questions, and for being a source of motivation (by “caring and provoking” as Jan stated it).

Dr. Wilfried Jokat for improving my abilities to express and hold my views in a very enjoyable way.

Dr. Max Voss, Dr. Jan Grobys and Dr. Mechita Schmidt-Aursch for sharing their seismic refraction knowledge.

Dr. Matthias König answering questions on plate tectonics, providing a very handy program code for plate rotations and for interesting discussions.

Dr. Graeme Eagles for having answers when they are needed, for providing an innovative view on plate tectonics, for fruitful discussions, for reading and improving two of my manuscripts and sharing a coffee break.

Dr. Jacek Stankiewicz for a pleasant research co-operation which led to two joint publications.

Morelia Urlaub and Kristina Meier for doing excellent “HIWI”-jobs.

## Acknowledgements

Prof. Dr. Maarten de Wit for being a great host at the University of Cape Town, for insightful discussions and for taking me to the Cape Fold Belt.

David Long and Ansa Lindeque for making me feel at home during my research visit in Cape Town.

Daniela Berger, Birte-Marie Ehlers, Dr. Wilfried Jokat, Dr. Jan Grobys, Dr. Karsten Gohl, Dr. Wolfram Geißler, Dr. Graeme Eagles, Dr. Matthias König, Dr. Philip Schlüter, Dr. Mechita Schmidt-Aursch, Dr. Gabriele Uenzelmann-Neben, Dr. Max Voss, and Dr. Estella Weigelt for “interdisciplinary” exchange and discussions, for being great colleagues, and for creating the fantastic working atmosphere in the Geophysics group at AWI.

The BMBF and the AWI, the DAAD, and the DFG for funding.

Jan Grobys for sustaining work discussions at the kitchen table, for making me laugh and in love.

My parents for their love and support.

## 12 Erklärung

Hiermit versichere ich, dass ich

- die Arbeit ohne fremde Hilfe angefertigt habe
- keine anderen als die von mir angegebenen Quellen und Hilfsmittel verwendet habe
- die den benutzen Werken wörtlich und inhaltlich entnommen Stellen als solche kenntlich gemacht habe.